ADSORPTION MEDIA FOR THE REMOVAL OF PHOSPHORUS IN SUBSURFACE DRAINAGE FOR MICHIGAN CORN FIELDS

By

Jessica Kathleen Hauda

A THESIS

Submitted to
Michigan State University
in partial fulfillment of the requirements
for the degree of

Biosystems Engineering – Master of Science

2020

ABSTRACT

ADSORPTION MEDIA FOR THE REMOVAL OF PHOSPHORUS IN SUBSURFACE DRAINAGE FOR MICHIGAN CORN FIELDS

By

Jessica Kathleen Hauda

Phosphorus is a valuable, non-renewable resource in agriculture promoting crop growth. and is used in the global food chain, mainly as fertilizer. Soluble phosphorus plays a part in the eutrophication in freshwater environments, which impacts tourism, human health, environmental safety, and property values. Phosphorus loss from agricultural land is also a loss of investment that went into keeping it on the soil, and its addition into water bodies can increase costs to manage the affected area(s).

This research entails selecting the phosphorus adsorption media best suited for removing phosphorus from subsurface drainage in Michigan farms. Selected adsorption media from the literature includes engineered nanomaterials, biochar, and natural materials. These media were evaluated with typical subsurface drainage phosphorus concentrations using batch adsorption and column experiments to verify if the media worked in this application. Both the steel furnace slag (SFS) and PO4Sponge removed soluble reactive phosphorus from 0.500 to below 0.05 mg/L in column experiments at an empty bed contact time of 5-minutes The SFS was the most cost-effective option based on a case-study and generalized analysis. The most expensive option was the use of PO4Sponge media to remove phosphorus, then regenerating it at the manufacturer.

ACKNOWLEDGEMENTS

Thank you to the Michigan Corn Growers Association for funding this project so I could achieve this goal, I am extremely grateful. Thank you to my faculty adviser, Dr. Steven Safferman, for taking the time to train, advise, and teach me incredible things from 2017 -2020. Thank you Dr. Ghane & Dr. Harrigan for serving on my committee and bringing new perspectives into my research. Thank you to MetaMateria Technologies for your expertise on and supply of PO4Sponge media. Thank you to Ed Weinburg at ESSRE Consulting & Nick Backman at Purolite for your expertise on and supply of the FerrIXA33E and HIX(Zr)-Nano media. Thank you Thiramet (Dream) Sotthiyapai, Kiran Lantrip, Megan Curtin, Brynn Chesney, Corrine Zeeff and Emily Dettloff for all your dedication and hard work done year-round to grow this project from inception to its current state. Thank you, Jason Piwarski and Dr. Ehsan Ghane, for collecting and sharing site-specific information and samples that were used in this project. Thank you Dr. Christopher Saffron and Zhongyu Zhang for allowing us to use your laboratory equipment and for your expertise concerning the biochar adsorption media. Thank you, Phil Hill, for your assistance with modifying the biochar reactor lid in your shop. Thank you, Younsuk Dong, for being the first graduate student I worked with, for teaching me how to use Hach Kits, and for making sure our lab was safe to work in. Thank you Umesh Adhikari for helping me sample during finals week and for teaching me how to prepare biosolids. Thank you, Merit Laboratories, for analyzing subsurface drainage for my project. Thank you, Barb DeLong, for helping me with timesheets, stipends, packages, sharing interesting stories at lunch events, and for answering all my questions about the biosystems engineering program. Thank you, Emily Williams, for letting me test your hoverboard in the upstairs hallway of Farrall Hall before giving it to your kids. Thank you, Jamie Lynn, for being a great conversationalist when I came into the office. Thank you to my friends and family – for emotional support, good company in the lab, and for cheering me on this whole time. Thank you to Joe, the janitor in Farrall Hall, for being the only other working individual in the building after 12 AM. Thank you to my parents, Karen and William Hauda, for your support and advice on this journey while I was away from home. Lastly, thank you to the Farrall Hall cockroaches for keeping me alert and on my toes when I was working in the lab late enough for y'all to come out and spook me.

I do not thank the leeches.

TABLE OF CONTENTS

LIST OF TABLES	. viii
LIST OF FIGURES	X
KEY TO ABBREVIATIONS	xvii
Chapter 1: Introduction	1
Chapter 2: Objectives	4
Chapter 3: Literature Review	
3.1. Agricultural Subsurface Tile Drains and Soluble Phosphorus Losses	
3.2. Factors Impacting Phosphorus Transport into Subsurface Tile Drains	
3.3. Subsurface Drainage Characteristics	
3.4. Eutrophication	
3.5. The Chemistry Governing Phosphorus Adsorption Media	
3.6. Column and Batch Adsorption Experiments	
3.6.1. Column Experiments	
3.6.1.1. Concepts and Theory	
3.6.1.2. Experimental Design	
3.6.2.1. Concepts and Theory	
3.6.2.2. Experimental Design	
3.6.3 The Relationship between Batch Adsorption and Column Experiments	
3.7. Types of Phosphorus Adsorption Media	
Chapter 4: Methods	25
4.1. Factors for Optimal Media Performance and Use in Agricultural Subsurface Tile Drain	ıs 25
4.2. Biochar Creation & Media Preparation for Batch Adsorption and Column experiments	. 26
4.3. Creation and Testing of Synthetic and Real Subsurface Drainage Water	
4.3.1. Site-Specific Information for Real Subsurface Drainage Water Collection	
4.3.2. Formulation of the Synthetic Subsurface drainage Water	
4.4. Batch Adsorption experiments	
4.5. Column Experiments	
4.6. Analytical Methods	38
Chapter 5: Results & Discussion	
5.1 Phosphorus Adsorption Media	. 41

	5.1.1. PO4Sponge Generation 1	. 42
	5.1.2. PO4Sponge Generation 2	. 43
	5.1.3. FerrIXA33E	. 44
	5.1.4. HIX(Zr)-Nano	. 45
	5.1.5. Ferrous Sulfate Modified Biochar	. 45
	5.1.6. Calcium-Magnesium Modified Biochar	. 46
	5.1.7. Blast Furnace Slag	. 47
	5.1.8. Steel Furnace Slag	. 48
5.	2. Batch Adsorption Experiments	. 49
	5.2.1. PO4Sponge Generation 1	. 50
	5.2.2. PO4Sponge Generation 2	. 50
	5.2.3. FerrIXA33E	. 51
	5.2.4. HIX(Zr)-Nano	. 51
	5.2.5. Ferrous Sulfate Modified Biochar	. 51
	5.2.6. Calcium-Magnesium Modified Biochar	. 52
	5.2.7. Blast Furnace Slag	. 53
	5.2.8. Steel Furnace Slag	. 53
	5.2.9. Selection of Media for Column experiments	. 54
5.	3. Column experiments	
	5.3.1. Phase 1a: Fresh PO4Sponge Generation 1 and FerriXA33E media with RSD and SS	SD
	at an EBCT of 30-minutes and target initial TP concentration of 0.200 mg TP/L	
	5.3.2. Phase 1b: Used PO4Sponge and FerriXA33E media with SSD at an EBCT of 60-	
	minutes	. 57
	5.3.3. Phase 1c: Used PO4Sponge Generation 1 and FerrIXA33E media with RSD at an	
	EBCT of 60-minutes	. 57
	5.3.4. Phase 1d: Used PO4Sponge Generation 1 and FerriXA33E media with SSD at an	
	EBCT of 60-minutes and initial SRP concentration of 1.00 mg SRP/L	
	5.3.5. Phase 2a: Fresh PO4Sponge and SFS with SSD at an EBCT of 5-minutes and initia	
	SRP concentration of 0.500 mg SRP/L	. 59
	5.3.6. Phase 2b: Used PO4Sponge Generation 1 and SFS with SSD at an EBCT of 10-	
	minutes and initial concentration of 0.500 mg SRP/L	. 60
	5.3.7. Phase 2c: Used PO4Sponge Generation 1 and SFS with SSD at an EBCT of 20-	
	· · · · · · · · · · · · · · · · · · ·	. 60
	5.3.8. Phase 2d: Used PO4Sponge Generation 1 and SFS with SSD at an EBCT of 20-	
	minutes and initial concentration of 2.00 mg SRP/L	. 60
	5.3.9. Phase 2e: Used PO4Sponge Generation 1 and SFS with SSD at an EBCT of 60-	
	minutes and initial concentration of 2.00 mg SRP/L	. 61
	5.3.10. Phase 3 – Replication of Phase 2a: Fresh PO4Sponge Generation 1 and SFS with	
	SSD at an EBCT of 5-minutes and initial concentration of 0.500 mg SRP/L	
_	5.3.11. Selection of Media for Feasibility Studies	
5.	4. Economic Analysis	
	5.4.1. Media Performance in Batch Adsorption and/or Column experiments	
	5.4.2. Capital and Operational Costs	
	5.4.3. Media Implementation in Tile Drains	
	5.4.4. Further Analysis on Media Feasibility	.73

Chapter 6: Conclusions and Future Research	
APPENDICES	80
APPENDIX A – Supplemental Material	
APPENDIX B – Batch adsorption experiments	
APPENDIX C – Column experiments	
APPENDIX D – Sample Calculations	
REFERENCES	

LIST OF TABLES

Table 1: Percentages of water-soluble phosphate in several common fertilizers [29]
Table 2: Subsurface drainage ion composition based on literature
Table 3: Concentrations of soluble reactive or soluble, and total phosphorus in subsurface drainage
Table 4: Different types of natural, waste, and nano-engineered P adsorption media
Table 5: Laboratory production of biochar P sorption media
Table 6: Summary of ion analyses for the three samples (dated) of real subsurface drainage water from Site BN in Michigan
Table 7: Concentration of each chemical compound in synthetic subsurface drainage water based off the testing results for the real subsurface drainage water (this table assumes that there was no phosphorus in the water used to make this formulation)
Table 8: Phosphorus test kits for use with the DR6000 and with the ranges of phosphorus or phosphate the kits can measure
Table 9: Average percent relative range replicates used in batch adsorption and column experiments
Table 10: Average percent recovery for standards used in batch adsorption and column experiments
Table 11: Summary table of media options used in this research
Table 12: Summary of all column study phases and their characteristics
Table 13: Cost estimates for the PO4Sponge Generation 1 media and SFS
Table 14: "Site BN" tile drain data for drainage flow rate and SRP ranges
Table 15: The maximum and minimum calculated empty bed contact times for the PO4Sponge and steel furnace slag based on daily flow rates from "Site BN" data
Table 16: The maximum and minimum calculated hydraulic retention times for the PO4Sponge and steel furnace slag based on daily flow rates from "Site BN" data

Table 17: Rough cost estimates for scenario A over a 15-year period	70
Table 18: Rough cost estimates for scenario B over a 15-year period	71
Table 19: Rough cost estimates for scenario C over a 15-year period	71
Table 20: Calculated percent difference in the annual cost per acre for scenarios A, B, and C	72
Table 21: Results from the calculations comparing total annual cost to the mass of SRP requirement	_
Table 22: Ferrous sulfate biochar solution preparation	84
Table 23: Calcium-magnesium biochar MgCl ₂ solution preparation	86
Table 24: Calcium-magnesium biochar CaCl ₂ solution preparation	86
Table 25: When and which jars should be taken out together based on the batch adsorption experiment type and the corresponding placement configurations	91
Table 26: Summary of column phases and influent conditions for each column	101
Table 27: Column study phase 3 information for the PO4Sponge and steel furnace slag	137
Table 28: Summary of bulk density and capacity calculations for the PO4Sponge and steel furnace slag	138
Table 29: Summary of calculations used to determine the mass and volume of PO4Sponge an steel furnace slag required to treat 1.66 kg of SRP assuming breakthrough capacity	
Table 30: Costs of the PO4PSonge and SFS contactors	141
Table 31: The cost of the media contactor, labor, and installation	142
Table 32: Vacuum truck costs, transport information, and fees for recycling center	149
Table 33: Cost of Scenario A for 15-years	152
Table 34: Cost of Scenario B for 15-years	152
Table 35: Cost of Scenario C for 15-years	153

LIST OF FIGURES

Figure 1: (a) Schematic describing chemical forms of P: $TP = total\ P$, $PP = particulate\ P$, Partic. $OrgP = organic\ P$ associated with particulates, Partic. $InorgP = inorganic\ P$ associated with particulates, $TDP = total\ dissolved\ P$, $Ortho\ P = inorganic\ P$, and $SOP = soluble\ organic\ P$ (b) Schematic describing measured forms of P: $TP = total\ P$ on an unfiltered sample (TP can be determined by digestion and molybdate reaction or by ICP spectroscopy, which may include P not measured by digestion), $TSP = total\ soluble\ P$ on a filtered (0.45 μ m) sample, $PP = TP$ associated with the particulate captured on a 0.45 μ m filter, $SRP = soluble\ molybdate$ -reactive P of filtered sample, and $SUP = soluble\ molybdate$ -unreactive P of filtered sample. Figure from [9].
Figure 2: Diagram of an agricultural subsurface drainage system
Figure 3: Side view of a subsurface tile drain and visual depiction of how phosphorus enters the subsurface drainage
Figure 4: Visual depiction of when breakthrough concentration and media exhaustion are reached for a media [77]
Figure 5: A downflow column experiencing exhaustion from top to bottom [77]
Figure 6: A upflow column experiencing exhaustion from bottom to top [77]
Figure 7: The relationship between batch adsorption and column experiments for the partial design of a pilot/full-scale treatment system
Figure 8: The outside of the F62700 Furnace used to pyrolyze the both the ferrous sulfate and the calcium-magnesium biochar
Figure 9: (Left) the snorkel fitted on top of the F62700 furnace; (Right) the interior top side of the F62700 furnace where the snorkel is located
Figure 10: (Left) The rupture disc; (Right) the reactor vessel with the lid attached
Figure 11: The reactor vessel with eight outer holes for bolts
Figure 12: Jars placed in the shaker

Figure 13: Laboratory column
Figure 14: Diagram of adsorption media columns connected to the influent and effluent 110-gallon tanks
Figure 15: The PO4Sponge nano-engineered phosphorus adsorption media monolith (left) and crushed monolith granules (right) [76]
Figure 16: The second version of the PO4Sponge phosphorus adsorption media
Figure 17: The FerrIXA33E phosphorus adsorption media
Figure 18: The HIX(Zr)-Nano phosphorus adsorption media
Figure 19: Ferrous sulfate biochar after pyrolysis
Figure 20: Calcium-magnesium biochar after pyrolysis and sieving
Figure 21: The blast furnace slag after being wet-sieved dried in an oven & a zoomed in view of the media
Figure 22: Hardened steel furnace slag media after the end of column study phase 2e
Figure 23: Relationship between the SRP loaded onto the PO4Sponge vs. SFS
Figure 24: The media flow diagram for scenarios A, B, and C
Figure 25: Graphical representation of Table 21
Figure 26: First set of results from the commercial laboratory ion analyses of RSD collected from "Site BN"
Figure 27: Second set of results from the commercial laboratory ion analyses of RSD collected from "Site BN"
Figure 28: Third set of results from the commercial laboratory ion analyses of RSD collected from "Site BN"

Figure 29: Diagram of a standard batch adsorption study (non-24-hour batch adsorption study) 88
Figure 30: The placement configuration for jars in a standard batch adsorption study (non-24-hour batch adsorption study)
Figure 31: Diagram of the standard 24-hour batch adsorption study
Figure 32: The placement configuration for jars in a standard 24-hour batch adsorption study 89
Figure 33: Diagram of a dual 24-hour batch adsorption study
Figure 34: The placement configuration for jars in a dual 24-hour batch adsorption study 90
Figure 35: Mixing the magnesium sulfate and calcium sulfate chemical compounds turned the water a milky white color
Figure 36: There was no recorded data for total phosphorus during the batch adsorption experiments for PO4Sponge generation 1, PO4Sponge generation 2, FerrIXA33E, and HIX(Zr)-Nano
Figure 37: Soluble phosphorus data recorded during the batch adsorption experiments for PO4Sponge generation 1, PO4Sponge generation 2, FerrIXA33E, and HIX(Zr)-Nano96
Figure 38: Soluble reactive phosphorus data recorded during the batch adsorption experiments for PO4Sponge generation 1, PO4Sponge generation 2, FerrIXA33E, and HIX(Zr)-Nano 97
Figure 39: Total phosphorus data recorded during the batch adsorption experiments for the ferrous sulfate biochar, calcium-magnesium biochar, blast furnace slag, and steel furnace slag. 97
Figure 40: Soluble phosphorus data recorded during the batch adsorption experiments for the ferrous sulfate biochar, calcium-magnesium biochar, blast furnace slag, and steel furnace slag. 98
Figure 41: Soluble reactive phosphorus data recorded during the batch adsorption experiments for the ferrous sulfate biochar, calcium-magnesium biochar, blast furnace slag, and steel furnace slag
Figure 42: The original 5-gallon bucket method used for column experiments 100

Figure 43: The improved 110-gallon tank method used for column experiments	100
Figure 44: Phase 1a column with the PO4Sponge monolith media receiving SSD	103
Figure 45: Phase 1a column "b" with the PO4Sponge granular media receiving RSD (day 0	
Figure 46: Phase 1a control column with no media receiving SSD	104
Figure 47: Phase 1a column "a" with the PO4Sponge granular media receiving SSD	104
Figure 48: Phase 1a column "b" with the PO4Sponge granular media receiving SSD instead RSD (day 71-124)	
Figure 49: Phase 1a column with the FerrIXA33E media receiving SSD	105
Figure 50: Phase 1b column with the PO4Sponge monolith media receiving SSD	106
Figure 51: Phase 1b control column with no media receiving SSD	106
Figure 52: Phase 1b column "a" with the PO4Sponge granular media receiving SSD	107
Figure 53: Phase 1b column "b" with the PO4Sponge granular media receiving SSD	107
Figure 54: Phase 1b column with the FerrIXA33E media receiving SSD	108
Figure 55: Phase 1b column with the PO4Sponge monolith media receiving SSD	109
Figure 56: Phase 1b control column with no media receiving SSD	109
Figure 57: Phase 1b column "a" with the PO4Sponge granular media receiving SSD	110
Figure 58: Phase 1b column "b" with the PO4Sponge granular media receiving SSD	110
Figure 59: Phase 1b column with the FerrIXA33E media receiving SSD	111
Figure 60: Phase 1c column with the PO4Sponge monolith media receiving RSD	112

Figure 61: Phase 1c control column with no media receiving RSD	112
Figure 62: Phase 1c column "a" with the PO4Sponge granular media receiving RSD	113
Figure 63: Phase 1c column "b" with the PO4Sponge granular media receiving RSD	113
Figure 64: Phase 1c column with the FerrIXA33E media receiving RSD	114
Figure 65: Phase 1c column with the PO4Sponge monolith media receiving RSD	115
Figure 66: Phase 1c control column with no media receiving RSD	115
Figure 67: Phase 1c column "a" with the PO4Sponge granular media receiving RSD	116
Figure 68: Phase 1c column "b" with the PO4Sponge granular media receiving RSD	116
Figure 69: Phase 1c column with the FerrIXA33E media receiving RSD	117
Figure 70: Phase 1d column with the PO4Sponge monolith media receiving SSD	118
Figure 71: Phase 1d control column with no media receiving SSD	118
Figure 72: Phase 1d column "a" with the PO4Sponge granular media receiving SSD	119
Figure 73: Phase 1d column "b" with the PO4Sponge granular media receiving SSD	119
Figure 74: Phase 1d column with the FerrIXA33E media receiving SSD	120
Figure 75: Phase 1d column with the PO4Sponge monolith media receiving SSD	121
Figure 76: Phase 1d control column with no media receiving SSD	121
Figure 77: Phase 1d column "a" with the PO4Sponge granular media receiving SSD	122
Figure 78: Phase 1d column "b" with the PO4Sponge granular media receiving SSD	122

Figure 79: Phase	ld column with the Fe	rrIXA33E media red	ceiving SSD	123
Figure 80: Phase 2	2a column with the PC	04Spnge granular m	edia receiving SSD	124
Figure 81: Phase 2	2a column with the ste	eel furnace slag med	ia receiving SSD	124
Figure 82: Phase 2	2a column with the PC	04Spnge granular m	edia receiving SSD	125
Figure 83: Phase 2	2a column with the ste	el furnace slag med	ia receiving SSD	125
Figure 84: Phase 2	2b column with the PC	04Spnge granular m	edia receiving SSD	126
Figure 85: Phase 2	2b column with the ste	eel furnace slag med	ia receiving SSD	126
Figure 86: Phase 2	2b column with the PC	04Spnge granular m	edia receiving SSD	127
Figure 87: Phase 2	2b column with the ste	eel furnace slag med	ia receiving SSD	127
Figure 88: Phase 2	2c column with the PC	04Spnge granular m	edia receiving SSD	128
Figure 89: Phase 2	2c column with the ste	el furnace slag med	ia receiving SSD	128
Figure 90: Phase 2	2c column with the PC	04Spnge granular m	edia receiving SSD	129
Figure 91: Phase 2	2c column with the ste	el furnace slag med	ia receiving SSD	129
Figure 92: Phase 2	2d column with the PC	04Spnge granular m	edia receiving SSD	130
Figure 93: Phase 2	2d column with the ste	eel furnace slag med	ia receiving SSD	130
Figure 94: Phase 2	2d column with the PC	04Spnge granular m	edia receiving SSD	131
Figure 95: Phase 2	2d column with the ste	eel furnace slag med	ia receiving SSD	131
Figure 96: Phase 2	2e column with the PC	04Spnge granular m	edia receiving SSD	132

Figure 97: Phase 2e column with the steel furnace slag media receiving SSD	132
Figure 98: Phase 3 column with the PO4Spnge granular media receiving SSD	133
Figure 99: Phase 3 column with the steel furnace slag media receiving SSD	133
Figure 100: Phase 3 column with the PO4Spnge granular media receiving SSD	134
Figure 101: Phase 3 column with the steel furnace slag media receiving SSD	134
Figure 102: U-Ship calculator (https://www.uship.com/shipping-calculator.aspx) cost to ship contactor for the PO4Sponge and SFS	
Figure 103: Uship.com cost estimates for shipping PO4Sponge (Left) from manufacturer to farm; (right) from farm to manufacturer	145

KEY TO ABBREVIATIONS

Abbreviation Full Word

BAE Batch adsorption experiments

BFS Blast furnace slag

DI Deionized

HRT Hydraulic retention time

P Phosphorus

PP Particulate phosphorus

RSD Real subsurface drainage

SFS Steel furnace slag

SP Soluble phosphorus

SRP Soluble reactive phosphorus

SSD Synthetic subsurface drainage

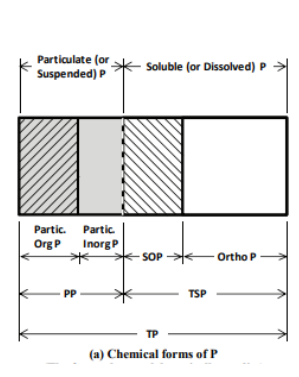
TP Total phosphorus

Chapter 1: Introduction

Phosphorus (P), the 11th most abundant element, is a non-renewable resource required for nearly all plant growth [1, 2]. About 90% of P is used in the global food chain, mainly as fertilizer [3, 4]. The practice of phosphate fertilization has been implemented since the end of World War II and it is estimated that P reserves will be depleted in 50 to 100 years at its current consumption rate [3, 5].

Total P (TP) can be classified as particulate or soluble (See Figure 1). Soluble P (SP), also known as dissolved P, is the P that remains in a solution after water is filtered to remove particulate P (PP), so only the dissolved P remains. SP is 95% bioavailable to algae [6], meaning that SP is easily utilized as a substrate, and this puts nutrient-rich water bodies at risk for eutrophication. PP can be filtered out of a solution, and this particulate matter includes living and dead plankton, P precipitates, and P adsorbed to particulate matter [7]. PP is about 30% bioavailable to algae [6]. The particulates containing P settle to the bottom of lakes and streams, making the P less available to algae [6].

Additionally, SP is typically found in aqueous environments as phosphate and can be further classified as inorganic and organic P. Inorganic phosphates are not bound to organic material and includes orthophosphates and polyphosphates. Orthophosphate is also known as "reactive P" and is the form of phosphate utilized by plants. Polyphosphates are strong complexing agents for metal ions commonly found in detergents and can convert into orthophosphate [7, 8]. Organic phosphates are bonded to plant or animal tissues and can be found in excreta, pesticides containing phosphates, and can be formed from orthophosphates after going through a biological process [7, 8]. Figure 1 visualizes a summary of chemical and measured forms of P [9].



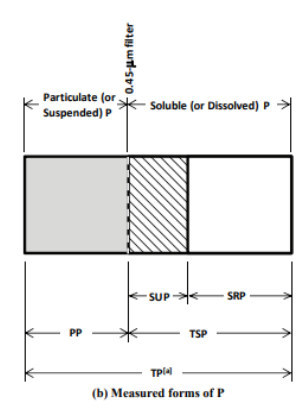


Figure 1: (a) Schematic describing chemical forms of P: $TP = total\ P$, $PP = particulate\ P$, Partic. OrgP = organic P associated with particulates, Partic. InorgP = inorganic P associated with particulates, $TDP = total\ dissolved\ P$, Ortho $P = inorganic\ P$, and $SOP = soluble\ organic\ P$ (b) Schematic describing measured forms of P: $TP = total\ P$ on an unfiltered sample (TP can be determined by digestion and molybdate reaction or by ICP spectroscopy, which may include P not measured by digestion), $TSP = total\ soluble\ P$ on a filtered (0.45 μ m) sample, PP = TP associated with the particulate captured on a 0.45 μ m filter, $SRP = soluble\ molybdate$ -reactive P of filtered sample, and $SUP = soluble\ molybdate$ -unreactive P of filtered sample. Figure from [9].

P losses from agricultural land is a loss of investment that went into keeping the P in the soil as a nutrient for crop growth. Manure and fertilizers containing P are the main contributors to non-point source pollution into freshwater bodies [10]. SP is mobilized by flow, such as subsurface drainage or surface runoff, and its release from agricultural systems into freshwater environments contributes to eutrophication[11]. Eutrophication affects tourism, human health, environmental safety, and property values [3]. Consequences of eutrophication include the growth of harmful algal blooms, higher frequency of hypoxia events, poisonous seafood, losses to aquaculture enterprises, long-term ecosystem changes, and loss of biodiversity [12, 13]. In one case, agricultural runoff partially caused the eutrophication of Lake Erie, leaving upwards of a \$100-million annual impact on Ohio's economy [14-16].

P adsorption media has been proposed to capture SP at the source of agricultural subsurface drainage to prevent downstream environmental impacts. Figure 2 shows a diagram of

agricultural subsurface drainage, and Figure 3 shows how SP makes its way into subsurface drainage, and ultimately, freshwater bodies.

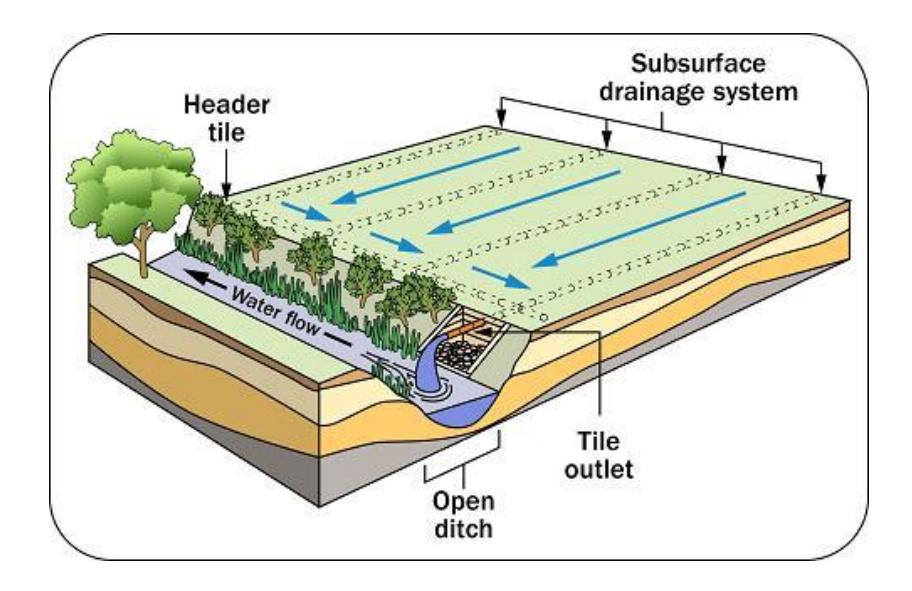


Figure 2: Diagram of an agricultural subsurface drainage system

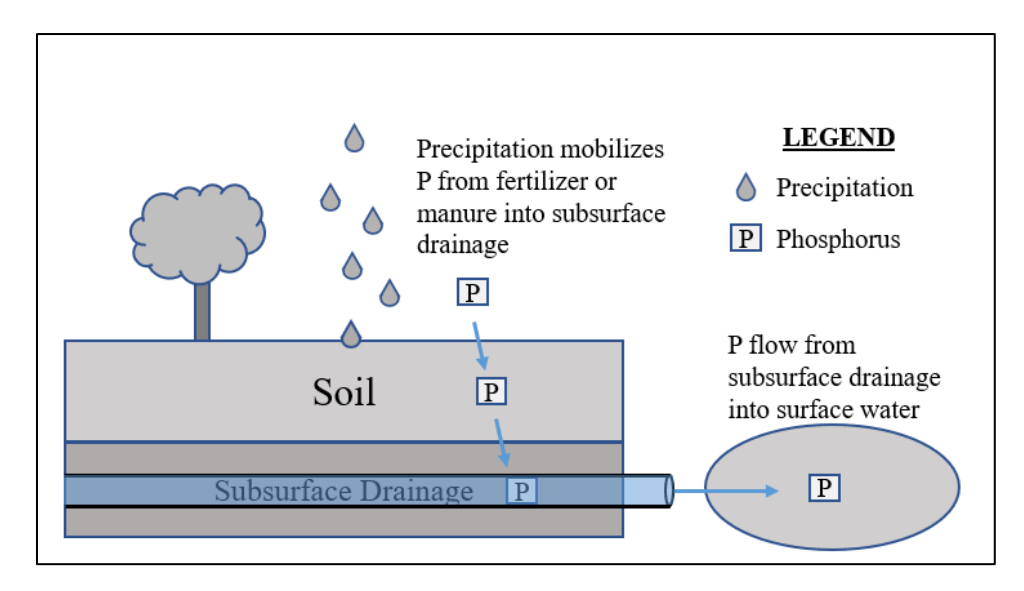


Figure 3: Side view of a subsurface tile drain and visual depiction of how phosphorus enters the subsurface drainage

Chapter 2: Objectives

The goal of this research was to improve water quality by removing P from agricultural subsurface drainage. The main objective of this research is to determine the P adsorption media option best suited for managing and removing SP in subsurface tile drains to reduce the SP input from subsurface drainage into surface waters. This was achieved using the following tasks:

- Select media options from literature with known and well-demonstrated removal in subsurface drainage and in other applications.
- 2. Formulate synthetic subsurface drainage (SSD) for laboratory use by analyzing real subsurface drainage (RSD) from a study site.
- Conduct batch adsorption experiments to determine if the selected adsorption media can remove SP from the SSD.
 - a. Eliminate media options from further consideration if there was poor SP removal from the SSD, if the media was not commercially available, or if the media was not cost effective.
- 4. Run column experiments to estimate SP removal and media capacity under different conditions and to gather data on media options to use in an economic analysis.
- Conduct an economic analysis to determine if site specific conditions change the media option best suited for removing SP from subsurface drainage.

Chapter 3: Literature Review

This chapter discusses agricultural subsurface tile drains and their relationship to SP losses, subsurface drainage characteristics, eutrophication, types of P adsorption media and regeneration, the chemistry governing P adsorption media, batch adsorption experiments, and column reactor experiments.

3.1. Agricultural Subsurface Tile Drains and Soluble Phosphorus Losses

Approximately 18 to 28 million hectares of cropland in the Midwest region of the U.S. have implemented the use of subsurface tile drains [17]. Subsurface tile drains are a collection of perforated tubes placed 2 to 4 feet below the surface that allow water to seep in and drain away [18]. A properly designed subsurface drainage system will remove excess water from the root zone 24 to 48 hours after a heavy rain [19]. The subsurface tile drain outlet is the common destination for multiple tubes and should be 3 to 5 feet underground [20]. This outlet utilizes gravity to discharge the subsurface drainage into water bodies, streams, constructed open ditches, or large underground drainage mains [20].

By lowering the water table in the soil below the crop's root zone, subsurface tile drains improve soil aeration, reduces compaction since drier soils are less prone to compaction than wet soils, reduces surface erosion and surface runoff, allows soils to warm up faster in the spring so planting can occur earlier in the growing season, and allows crop roots to grow deeper to improve access to water and nutrients in the soil [17, 19]. Subsurface tile drains also control the concentration of salts and toxic trace chemicals that can be harmful if in excess in the root zone [21].

However, subsurface tile drains can pose negative changes to the surrounding area such as an increase in soluble nutrient concentrations and a reduction in wetland area due to alterations in

the water table [19]. It was reported that subsurface drainage contributed up to 41% and 58% of cumulative total and dissolved P loads, respectively [22].

3.2. Factors Impacting Phosphorus Transport into Subsurface Tile Drains

There is a positive correlation between subsurface tile drain outlets connected to bodies of water and the amount of P present in those water bodies [17, 23]. P transport to subsurface tile drains depends on the following factors: soil type, land-management practices, such as tillage, season, and precipitation [17, 24]. Soils are categorized into a hydrologic soil group based on drainage and texture [25].

- Soil group A (sand, sandy loam, and loamy sand) are very well-drained and highly permeable.
- Soil group B (silt loam, loam) has good drainage.
- Soil group C (sandy clay loam) has fair drainage.
- Soil group D (clay loam, silty clay loam, sandy clay, silty clay, clay) has poor drainage.

Clay content is one of the governing factors in soil P sorption capacity. Clay particles carry a negative charge, attracting positively-charged aluminum and iron oxides [26]. These positively charged aluminum and iron oxides then attract negatively charged phosphate ions. Additional factors contributing to P sorption are the soil pH, concentration of metal oxides, and the soils history of manure and fertilizer applications.

Multiple manure and fertilizer applications to cropland builds up soil P levels in surface soils [27]. Manure contains approximately 70% soluble P, which is easily lost through leaching and surface runoff [28]. Fertilizer SP (as P₂O₅) ranges from 82% to 100%, and this is further described by Table 1.

Table 1: Percentages of water-soluble phosphate in several common fertilizers [29]

Fertilizer	Available P ₂ O ₅	Available PO ₄ ³⁻	Water Soluble
	(g/kg)	(g/kg) *	P_2O_5
Superphosphate (OSP)	200	268	85%
Concentrated Superphosphate	450	602	85%
(CSP)			
Monoammonium Phosphate	480	642	82%
(MAP)			
Diammonium Phosphate (DAP)	460	616	90%
Ammonium Polyphosphate	340	455	100%
(APP)			

^{*}Converted P₂O₅ to PO₄³- by dividing by 0.7473 [30]

Manure is a main contributor to non-point source pollution in freshwater bodies near areas used for concentrated animal feeding operations (CAFOs) [31]. Bouwman et al. (2013) found that fertilizer application introduces more P into soils used for cropland, but manure releases more P into the soil than fertilizer globally due to CAFOs [32]. Sharpley & Moyer (2002) found that dairy manure, poultry manure, and swine slurry contained 2,030, 7,430, and 6,035 mg/kg manure [33]. Compared to the Table 1, manure contains a larger capacity of P than fertilizers.

Tilling, the mechanical agitation of the soil, removes established macropores, turns over organic matter buried in deeper soil, breaks up compacted soil to plant seeds, and increases oxygen availability to plant roots [34]. Macropores are the spaces left by plant burrowing their roots in the soil worms, and soil cracking [27]. The frequency of soil tilling is determined by specific field conditions and management requirements [35]. No tillage, also called "No-till", reduces soil erosion, conserves soil moisture, and reduces water runoff [35]. However, no-till encourages the generation of macropores in the soil. Macropores are believed to be one of the key contributing factors in soluble nutrients reaching surface water from subsurface-drained fields by offering preferential flow pathways [27, 36-40]. Even with best management practices, such as testing soil P before adding additional fertilizer/manure, macropores create the preferential flow

pathway into surface waters. In summary, tillage can prevent macroporosity in the soil, but it can also increase erosion and surface runoff, which can still load P into surface waters.

Cover crops are used to improve soil health and water availability, control pests and diseases, manage erosion, and reduce PP losses from erosion, runoff, and leaching through the soil. Cover crops can help P conservation by up-taking and storing nutrients for the primary crop. Maltais-Landry and Frossard (2015) found that a wheat cover crop residue took up 20% to 40% of P in the soil and about 8% to 22% of the uptaken soil P could be recovered [41]. Kleinman et al. (2005) found that a cover crop reduced 36% of the TP runoff from an agricultural field [41, 42]. However, the freezing and thawing of cover crops may increase the release of SP. This has been shown for ryegrass [43-45], alfalfa [46] and winter wheat [46].

At warmer temperatures, increased melting or rain events can increase the amount of soluble P going into subsurface tile drains because there is an increased amount of water infiltrating the soil and flowing through macropores. SP can leave the soil layer if the water passes through the soil too quickly for the equilibrium adsorption of P by minerals such as iron, aluminum and calcium [47]. Frozen soil can also contribute additional SP into surface waters because frozen water within soil pores reduce or block other water from infiltrating, increasing surface runoff [25, 48]. Soil degradation, the decline in soil quality, can also cause P release in soils. Increases in temperature will speed up the breakdown of soil organic matter, which increases the amount of soil available nutrients [49].

3.3. Subsurface Drainage Characteristics

Subsurface drainage composition can vary from field to field due to different soil types, land management practices, geology, hydrology, and climate [21]. Both surface runoff and subsurface drainage can be contaminated with nutrients, such as P and nitrogen, and agricultural chemicals

from pesticides and fertilizer [22]. However, subsurface drainage contains more soluble components such as SP, nitrogenous species, mineral salts, and soluble pesticides [21]. Salt accumulation occurs in subsurface drainage due to the salinity within the soil solution and this adds cations and anions to the subsurface drainage such as sodium, calcium, magnesium, potassium, bicarbonate, sulphate, chloride, and nitrate [21]. Iron, manganese, molybdenum, and zinc are also found in subsurface drainage in low concentrations as trace elements [21]. Table 2 and Table 3 below summarize the ions and P concentrations typically found in subsurface drainage. Note that higher concentrations of P in subsurface drainage are most likely due to manure application instead of fertilizer application since manure contains a larger capacity of P on a mass basis.

Table 2: Subsurface drainage ion composition based on literature

Chemical/ion	Stone & Krishnappan (1997) [50]	Zimmerman (2017) [51]	Average
Mg^{2+}	21.40 mg/L*	27 mg/L***	24.20 mg/L
Na ⁺	7.40 mg/L*	3 mg/L***	5.2 mg/L
Ca^{2+}	106 mg/L*	92 mg/L***	99 mg/L
Cl ⁻	12.30 mg/L*	9 mg/L***	10.65 mg/L
K^+	0.73 mg/L*	N/A	0.73 mg/L
Si	4.98 mg/L*	N/A	4.98 mg/L
SO_4^{2-}	20.90 mg/L*	2 mg/L***	11.45 mg/L
NO_3^-	N/A	42 mg/L***	42 mg/L
Bicarbonate/HCO ₃ -	305 mg/L*	358 mg/L***	331.5 mg/L
рН	7.69 to 8.49**	N/A	8.09

^{*}From Table 2: Chemistry of River and Tile Drain Water

Table 3: Concentrations of soluble reactive or soluble, and total phosphorus in subsurface drainage

Source	Total Phosphorus	Soluble Phosphorus	Soluble Reactive Phosphorus
[17]	0.010 to 0.560 mg P/L	N/A	<0.005* to 0.447 mg P/L
[52]	0.640 mg P/L	N/A	0.05 mg P/L
[53]	N/A	0.080 to 0.200 mg P/L	N/A

^{**}From Table 3: Water Chemistry During Deposition Experiments

^{***}From Table 4; values from "Corn in continuous annual rotation (CC)"

Table 3 (cont'd)

[23]	0.100 to 0.230 mg/L	N/A	0.07 to 0.190 mg/L
[54]	0.007 to 0.182 mg PO4-P/L	0 to 0.038 mg PO4-P/L	N/A
[55]	0.012 to 0.124 mg total P/L	N/A	N/A
[56]	0.230 mg PO4-P/L**	N/A	0.08 mg PO4-P/L**
[27]	N/A	1.11 to 4.69 mg SP/L	N/A
[57]	N/A	N/A	0.330 to 0.590 mg SRP/L
Average	0.190 mg/L	1.22 mg/L	0.220 mg/L

^{*}This concentration is below the detection limit

3.4. Eutrophication

Eutrophication is defined as the increase in biological productivity due to an increase in nutrient availability, or the nutrient over-enrichment of water bodies [58]. Eutrophication impacts freshwater and costal environments by stimulating the growth of phytoplankton that thrive on sunlight and limiting nutrients such as P and nitrogen. Large populations of phytoplankton species occupying surface waters is known as an "algal bloom". Algal blooms typically occur in warmer water temperatures seen in the spring and can last until the Fall [59]. These algal blooms decompose via oxidative decomposition, meaning that microorganisms consume dissolved oxygen in the water to break down and utilize organic matter. As a result, the decomposition of large algal blooms can result in hypoxic, or dead zones, where the dissolved oxygen concentration falls below 2 mg O₂/L [60]. Hypoxic zones can last between hours and decades depending on how quickly the water body is oxygenated again by steams, plants, or other methods [61].

Algal blooms can contain bacteria harmful to human and environmental health. Cyanobacteria, also known as blue-green algae, are a gram-negative photosynthetic bacteria and type of phytoplankton that releases harmful toxins into the aquatic environment. Toxin types include hepatotoxins, cytotoxic and genotoxic alkaloids, alkaloid neurotoxins (anatoxin-a, anatoxin a(S),

^{**}The mean values across 39 tile-drained fields

and saxitoxins), lipopolysaccharide, neurotoxic amino acids, and dermatotoxins [62]. Hepatotoxins are toxins that damage the liver and, in acute doses, can cause liver cancer and/or blood to accumulate in the liver causing hypovolemic shock [63]. One type of cytotoxin, a genotoxic alkaloid called cylindrospermopsin, can alter the double-helix structure of DNA and hinder mammalian protein translation [64-66]. Alkaloid neurotoxins can cause paralysis and death due to the paralysis of the muscles regulating breathing [63, 67] and respiratory arrest [63]. Cyanobacteria possess lipopolysaccharide in cell walls, which can cause gastrointestinal upset to mammals if indigested [65]. Lipopolysaccharide supports other harmful heterotrophic bacteria, such as *Vibrio cholerae*, and this can enable the transfer of waterborne diseases, such as Cholera [68]. Neurotoxic amino acids can result in neurodegenerative diseases such as Alzheimer and amyotrophic lateral sclerosis (ALS) [69]. Dermatotoxins can act as tumor promotors in mammals [70].

There are long-term environmental impacts resulting from eutrophication. Harmful algal blooms can suppress primary producers, which leads to problematic changes in the food web and food chain. These blooms can also inflict diseases on native species in the environment where the bloom occurs, leading to impaired community structures, habitat loss, and an eventual loss in biodiversity [12].

The effects of eutrophication are observed worldwide, but the Great Lakes Basin has received increasing attention over the last decade. In 2014, warm temperatures and increased agricultural runoff caused an algal bloom coating approximately 620 square miles of Lake Erie, shutting down the drinking water supply in Toledo, Ohio for three days [71, 72]. The Great Lakes Basin provides 20% of the world's freshwater and 84% of the surface water in North America [12]. An initiative led by the Environmental Protection Agency (EPA), called the Great Lakes Restoration

Initiative document (GLRI), aims to "protect and restore the largest system of fresh surface water in the world". The three focus areas are to reduce nutrient loads from agricultural watersheds, reduce untreated stormwater runoff, and improve effectiveness of non-point source control and refine management efforts [73]. The US EPA dictates that the SP concentration should not exceed (1) 0.05 mg PO4-P/L in any stream at the point where it enters any lake or reservoir, (2) 0.025 mg PO4-P/L within a lake or reservoir, or (3) 0.100 mg PO4-P/L fir waste streams or wastewater not discharged directly to lakes or impoundments [74]. Since the initiative's inception, more than one million pounds of P runoff have been reduced from farmlands. The GLRI's goal is to have a 2,800,000 pound reduction of P by 2024 through conservation practices implemented in the Great Lakes watershed [73].

3.5. The Chemistry Governing Phosphorus Adsorption Media

Adsorption is the transfer of solutes in their liquid phase, adsorbates, onto a solid adsorbent material, also known as media [75]. Phosphate (PO₄³⁻), also known as orthophosphate, is a negatively charged ion found in aqueous solutions. Positively charged ions (cations) such as iron, magnesium, and calcium, and aluminum will interact with the phosphate ion through physical sorption or chemisorption processes [76]. Van der Waal interactions, a physical sorption process, can occur when the electrostatic charges of the absorbent attract the partial charges of the adsorbate [76]. Chemisorption is stronger than physical sorption processes and is a process where an available sorption site forms a chemical bond with the adsorbate [76]. Adsorption occurs in four or more steps: (1) bulk solution transport, (2) film diffusion transport, (3) pore and surface transport, and (4) adsorption or sorption [77].

Competing ions, ions in addition to the target adsorbate, that also have affinity to the adsorption media will compete for adsorption sites on the media, which can decrease the adsorption

capacity for the target adsorbate [77]. The impact of competing ions on capacity depends on the ion's adsorptive affinities, relative concentrations, and molecule size [77]. For SP removal in agricultural subsurface drainage and wastewater treatment, Na+, K+, Ca2+, Mg2+, Cl-, and SO42 are competing ions that compete with phosphate (PO₄³⁻) [78, 79]. One example of competing ions reducing SP adsorption capacity was demonstrated by Pan et al. (2009), who observed a 67% decrease in SP adsorption from a DI water solution containing added orthophosphate nano-engineered adsorption media (Hydrated Ferric Oxides) was in the presence sulfate anions [79].

If the adsorbate does not desorb back into the bulk solution via equilibrium, regeneration can alter the pH of the solution to precipitate the adsorbate back into the solution. Regeneration is the process of stripping ions off the adsorption media using a pH of 10 or higher, and for the regeneration of phosphate this is induced by a divalent or trivalent metal ion such as magnesium, calcium, aluminum, or iron. [75]. This is advantageous because (1) the media can be returned to the treatment site with additional open adsorption sites, and (2) the precipitated phosphate could be further modified into a value-added product. Aluminum and iron are used to precipitate P in wastewater treatment, but the use of calcium and magnesium precipitation produces P-enriched products that can be implemented as fertilizer [75]. For example, Sengupta & Pandit (2011) used sodium chloride and sodium hydroxide to remove phosphate ions off a hydrated ferric oxide (HFO) adsorption media, then calcium or magnesium salt to precipitate phosphate out as a solid phase fertilizer byproduct [80].

3.6. Column and Batch Adsorption Experiments

3.6.1. Column Experiments

3.6.1.1. Concepts and Theory

Column experiments were conducted to estimate SP removal and media capacity under different conditions and to gather data on media options to use in an economic analysis. Column experiments predict the performance of pilot or full-scale systems. The relationship between the column experiments and pilot/full-scale systems relies on an adsorption media's breakthrough capacity [77]. Breakthrough capacity is the amount of adsorbate per mass of adsorbent required to reach breakthrough concentration [77]. Breakthrough concentration is the maximum allowable effluent concentration leaving the system, and this concentration is typically driven by policies such as governmental regulations. A similar concept to breakthrough capacity is exhaustion. Exhaustion occurs for an adsorbent when the adsorbate concentration in the effluent is 95% of the adsorbate concentration in the influent, indicating that the adsorbent is filled up with, or saturated with adsorbate [77]. Breakthrough capacity is not the same as adsorbent exhaustion. Figure 4 graphically represents the times when breakthrough concentration and media exhaustion occur.

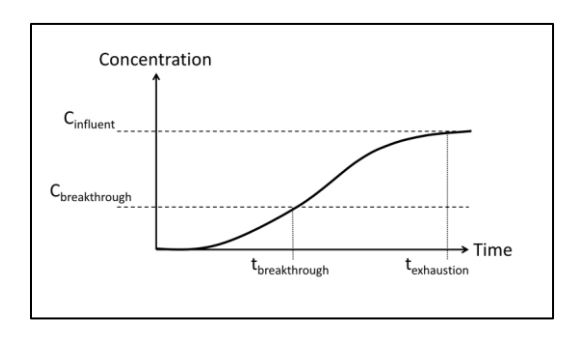


Figure 4: Visual depiction of when breakthrough concentration and media exhaustion are reached for a media [77]

In this research, it was desired to achieve the lowest possible effluent concentration with any given media/adsorbent under subsurface drainage conditions. Thus, media exhaustion, also

called media saturation, occurs when the maximum amount of adsorbate (P) adsorbed to the adsorbent (the media) under subsurface drainage conditions. When this occurs, it was said that the media was saturated under those conditions. Even if the maximum adsorption capacity is not achieved, the media may need to be regenerated or replaced when breakthrough capacity is reached. If media is at breakthrough capacity for an extended time, the media can have decreased adsorptive power, allowing equilibrium between the media and bulk solution to desorb the adsorbate back into the bulk solution. This is most likely to occur when the media's adsorbate concentration is higher than the adsorbate concentration in the bulk solution.

Two main conditions govern a media's breakthrough capacity: (1) empty bed contact time and (2) influent concentration of adsorbate. Empty bed contact time (EBCT) is the length of time a volume of solution is in contact with a volume of adsorption media as it flows through a treatment system [81]. The calculation for EBCT is shown in equation 1 below [77].

$$EBCT = V_b/Q \tag{1}$$

Where EBCT = empty bed contact time, min

 V_b = volume of contactor occupied by the media, mL

O = volumetric flow rate, mL/min

Decreasing the flow rate or increasing the volume of media will increase the EBCT because it increases the amount of time required to move the solution volume through the media. Increasing the EBCT is advantageous because this increases the time window for an adsorption processes to occur, which increases the probability of adsorbate removal by the adsorption media [82]. When scaling up laboratory data to a field or pilot study, it is important to use the same media particle size. Equation 2 below shows how the EBCT is used in the relationship between large- and small-scale columns with respect to particle size. Section 3.6.3. further explains how these concepts in can partially design a treatment system.

$$\frac{EBCT_{SC}}{EBCT_{LC}} = \left(\frac{d_{SC}}{d_{LC}}\right)^{2-x} = \frac{t_{SC}}{t_{LC}} \tag{2}$$

Where $EBCT_{SC}$ = empty bed contact time for the small-scale column, min

 $EBCT_{LC}$ = empty bed contact time for the large-scale column, min

V = volume of media in the column, mL

Q = flow rate of solution through the volume of media, mL/min

 d_{SC} = diameter of particle in small-scale column, mm

 d_{LC} = diameter of particle in large-scale column, mm

 t_{SC} = time in small-scale column, min

 t_{LC} = time in large-scale column, min

x = takes on a value of 0 or 1 for constant or proportional diffusivity, respectively

In addition to EBCT, the hydraulic retention time (HRT) measures the amount of time required for solution to flow through a system [83]. Following the method by Hua et al. (2018), the HRT accounts for the porosity of the media when it is in a packed bed or column [83]. The porosity of the media is important because the water can only pass through the pore spaces within a packed bed of media. Equation 3 below shows the calculation for HRT [83], and equation 4 shows the calculation for porosity. Note that "particle density" is the same as "relative density" and "specific gravity" [84].

$$HRT = \frac{V * \xi}{Q} \tag{3}$$

Where V = volume of the treatment system, mL

 ξ = porosity

Q = flow rate going through the column, mL/min

$$Porosity (\xi) = 1 - \frac{Bulk \ Density}{Particle \ Density}$$
 (4)

3.6.1.2. Experimental Design

Two column flow configurations exist: (1) downflow and (2) upflow. Downflow columns receive influent on at the top and effluent leaves through the bottom, creating an adsorptive front that moves from top to bottom. The adsorptive front is the active adsorption surface area contacting and treating the influent flow [77]. This adsorptive front will move as it becomes saturated, allowing a less saturated area on the media to continue treating influent flow. The media in the column can act as a filter for particulate matter in the influent as it flows down and through the media in the column, but clogging can occur. Clogging is undesirable because slower flow through the column can decrease media performance. Backwashing, the act of changing the flow direction from bottom to top, can mitigate the clogging, but can also destroy the adsorptive front [77]. Figure 5 shows how media is exhausted in a downflow column.

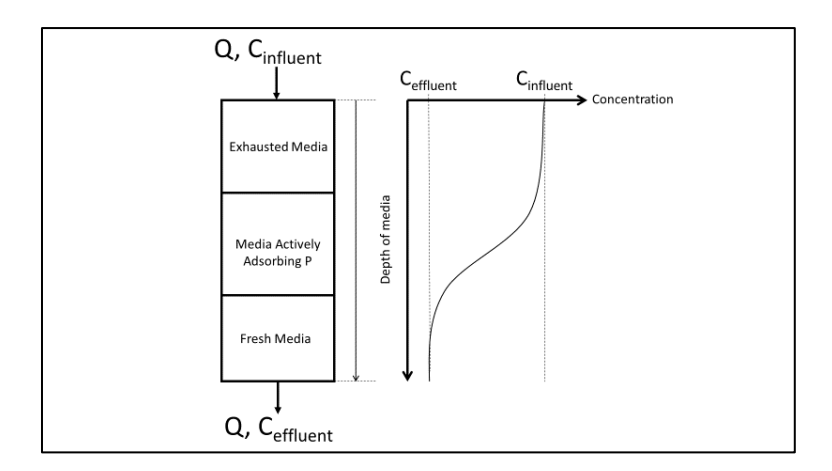


Figure 5: A downflow column experiencing exhaustion from top to bottom [77]

Upflow columns receive influent at the bottom and effluent leaves at the top, creating an adsorptive front that moves bottom to top. Upflow columns allows more control over the EBCT of the column compared to downflow columns because there is less chance of preferential flow or short circuiting, where the solution bypasses the media inside the column and is not properly

treated. Clogging is not a concern for upflow columns [77]. Figure 6 shows how media is exhausted in a downflow column.

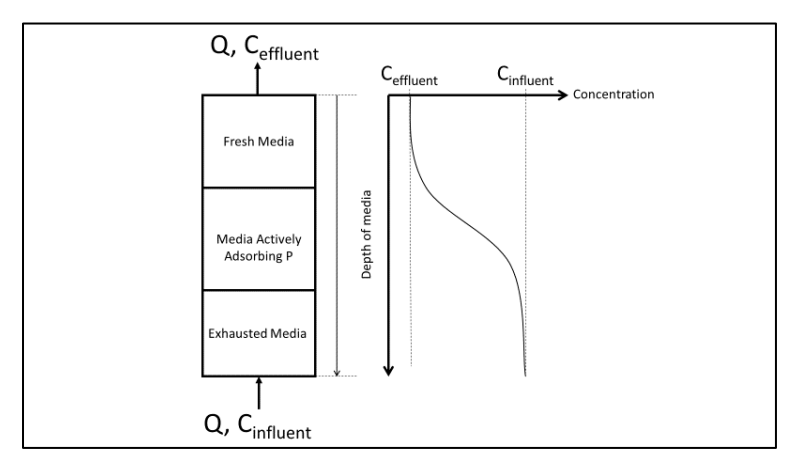


Figure 6: A upflow column experiencing exhaustion from bottom to top [77]

3.6.2. Batch Adsorption Experiments

3.6.2.1. Concepts and Theory

In this research, batch adsorption experiments (BAEs) were a precursor to the column experiments to eliminate media options unable to remove SP under subsurface drainage conditions. BAEs utilize various amounts of media in a fixed volume of liquid at a fixed initial concentration of adsorbate [77]. The amount of adsorbate onto the media, the theoretical media capacity, is calculated as the difference between the initial and final concentration of adsorbent after the set amount of time. The equation to calculate the theoretical media capacity is shown below in equation 5 [77].

$$q_e = -\frac{V}{M}(c_0 - c_e) \tag{5}$$

Where

 q_e = theoretical adsorption capacity, mg adsorbate/g media

M = mass of media, g

V =volume of liquid in the reactor, L

 c_0 =initial solution concentration of adsorbate, mg/L

 c_e = final solution concentration of adsorbate after a set time, mg/L

The duration of the BAEs were limited to 24 hours because it is critical for the media to remove SP within 24 hours, especially for storm flows where large amounts of P can exit the subsurface tile drain. The term "theoretical adsorption capacity" is used because the BAEs are less representative of realistic media performance compared to column experiments. This is explained further in section 3.6.3., which explains how these concepts in can partially design a treatment system.

3.6.2.2. Experimental Design

The experimental design for a BAE includes media immersed in a holding container filled with a solution containing a certain initial concentration. After a certain elapsed time, the sample is tested to determine the concentration removed by the media after that time. For example, one study used 20 g of either gravel, blast furnace slag, or fly ash in 40 mL of solution with P concentration of 5, 10, 20, 50, and 100 mg P/L at 25°C at 1500 rotations per minute (RPM) then tested the concentration after 24 and 30 hours [85]. Another study used 20 g of slag in a 500 mL Erlenmeyer flask with a slag to solution ratio of 1:25, an initial concentration of 30 mg PO4-P/L, and under shaker conditions of 25°C and 120 RPM [86]. A third study used 0.5 g of slag in a 50 mL centrifuge tube containing 25 mL of solution with an initial phosphate concentration of 500 mg/L, then it was tested multiple times between 5-minutes to 24-hours [87].

In addition to the media amount, initial concentration, and shaker conditions, the holding container components cannot interact with the media or the solution. Section II in the US EPA document titled "Specification and Guidance for Contaminant-Free Sample Containers" details the specifications caps, liners, packaging materials, and bottles must meet to be considered a contaminant-free sample container [88].

3.6.3 The Relationship between Batch Adsorption and Column Experiments

The optimal media amount for a given application is determined through literature or done experimentally using batch adsorption and column studies. BAEs provide a theoretical adsorption capacity for the media by immersing media in a target initial concentration of adsorbate. The term "theoretical adsorption capacity" is used because (1) BAEs cannot estimate capacity using EBCT since there is no flow condition, and (2) the media is often free-floating within the BAE container, thus, it behaves differently than a packed volume of media within a column. Additional information on BAEs is located at the end of this section.

BAEs are beneficial to conduct before column experiments because the theoretical adsorption capacity can calculate the desired EBCT if the flow rate for the given application is already known. To elaborate, knowing the concentration of adsorbate requiring treatment (the influent concentration minus the desired effluent, or breakthrough concentration; mg adsorbate/L), theoretical adsorption capacity (mg adsorbate/g media), and flow rate for the application (L/d) can determine media amount per day required to treat the influent concentration to breakthrough concentration (g media/d). Then, multiplying this amount by the time the media is required to treat the influent solution yields the amount of media needed over the course of the treatment period (g media). This information can be used to obtain capital and shipping costs (\$/g media), and the volume of media (L) when the media amount is divided by its bulk density (g/cm³).

Finally, the volume of the media can be used to (1) select the appropriate contactor to hold the media in the treatment system and (2) calculate the EBCT (days) when the volume of media (L) is divided by the known flow rate (L/d) of influent. The EBCT for the application can then be applied to a column experiment to estimate a more accurate adsorption capacity for the media for

the given application. After conducting column experiments to obtain a more accurate adsorption capacity, the above process can be repeated to partially design a pilot or full-scale system for this application. Figure 7 below visualizes the partial design process in a flow diagram.

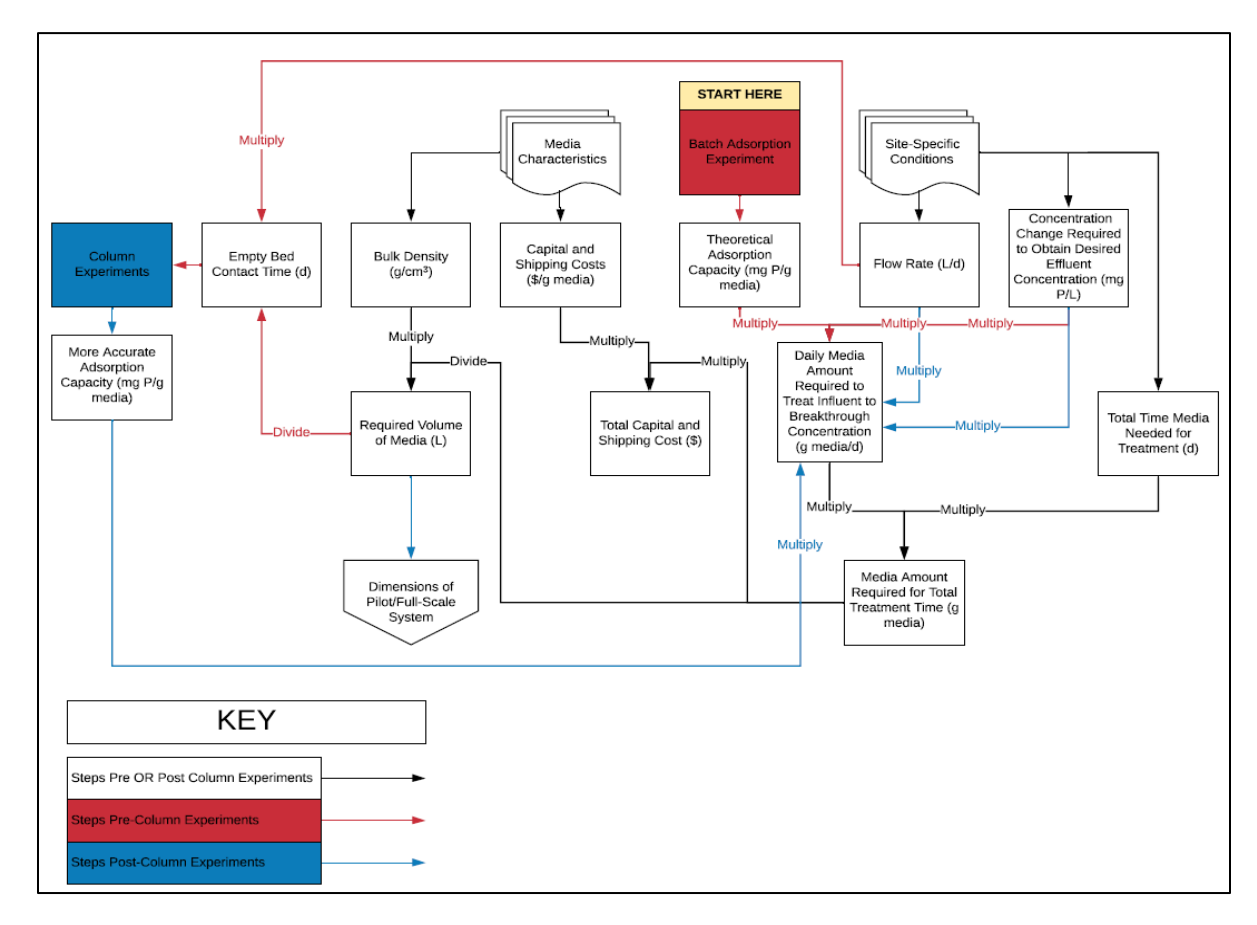


Figure 7: The relationship between batch adsorption and column experiments for the partial design of a pilot/full-scale treatment system

3.7. Types of Phosphorus Adsorption Media

Adsorption media removes constituents in a solution via the liquid-solid interface where the constituent is adsorbed to the adsorbent at an available adsorption site [77]. There are different kinds of P adsorption media that have different performance kinetics and P adsorption capacities. The adsorption media types focused on in this research are natural, waste, and nano-engineered media.

Natural material-based P adsorption media are materials found naturally in the environment that attract phosphate ions. Natural materials include zeolite, limestone, and natural soils. Waste material-based P adsorption media are materials that are byproducts, or waste, from other processes that contain positively charged ions to attract the phosphate ions. Included are slags from metal processing plants, fly ash, and water treatment residuals. One advantage with using waste materials as adsorption media is that it has a lower capital cost than nano-engineered media. However, it is unknown from a life cycle perspective if one is more cost effective than the other for removing SP from subsurface drainage.

Nano-engineered media are chemically modified to produce a large surface area and high concentrations of positively charged ions and/or nanoparticles, which are typically metal oxides. These modifications increase the number of adsorption sites on the media, enhancing the media's overall adsorption capacity, and are done for biochar, hybrid ion exchange resins, and ceramic nano-engineered media [79, 89-93]. Biochar is pyrolyzed material modified to contain a high amount of positively charged ions, usually metal oxides, to attract negatively charged phosphate ions [89, 90, 94, 95].

Ion exchange resins, or nanoscale inorganic particles (NIPs), are produced by copolymerizing styrene and divinylbenzene and can be manufactured to have high selectivity for the desired chemical constituent [77]. Styrene acts as the backbone, or matrix of the resin, and divinylbenzene cross links polymers to make the resin insoluble [77]. Ion exchange relies on electrostatic forces to remove the target ion from a solution and replace it with an ion from the media [76].

Ceramic media contains a porous structure bonded with metal oxides to capture the target ion from the solution [76]. A ceramic material with an large interconnected porosity, such as ceramic

foam, is loaded with metal oxide nanocrystals to adsorb the target ion [76]. The large interconnected porosity provides a high surface area for adsorption and can allow water to pass through at low pressures [76]. One challenge with ceramic nanomaterials is that the active surfaces, the surface and interconnected pores, are easily clogged and difficult to contact, which can make water flow through more difficult [76]. Table 4 highlights different types of natural, waste, and nano-engineered adsorption media.

Table 4: Different types of natural, waste, and nano-engineered P adsorption media

		Adsoration	Initial P		
Name	Type	Adsorption Capacity	Concentration	Water Type	Reference
Limestone	N	0.68 mg P/kg	40 mg P/L	DI water w/ added potassium phosphate	[96]
PO4Sponge	NE	80,000 mg P/kg	>5 mg P/L	Wastewater, agricultural	[97]
r o lopolige	1,2	50,000 mg P/kg	< 2 mg P/L	runoff	[27]
FerrIXA33E	NE	2,300 mg P/kg	0.260 mg P/L	Wastewater	[98]
Zeolite	N	0.46 mg P/kg	40 mg P/L	DI water w/ added potassium phosphate	[96]
Serpentinite	N	1.37 mg P/kg	20 mg P/L	DI water w/ added potassium phosphate	[99]
Natural Soils	N	6.3 to 501.0 mg P/kg	3.3 mg PO4- P/L	DI water w/ added potassium phosphate	[100]
Dolomite	N	0.052 g P/kg	60 mg PO4- P/L	DI water w/ added potassium phosphate	[101]
Banana Straw Biochar	NE	3,115 mg P/kg	250 mg TP/L	DI water w/ added potassium phosphate	[95]
Electric Arc Furnace Slag	W	2.51 mg P/kg	20 mg P/L	DI water w/ added potassium phosphate	[99]
Fly Ash	W	0.86 mg P/kg	40 mg P/L	DI water w/ added potassium phosphate	[96]
Blast Furnace Slag	W	0.006 mg P/kg	0.180 mg PO4/L	DI water w/ added potassium phosphate	[102]
Filtralite P TM	NE	2.5 g P/kg	0.480 mg PO4-P/L	DI water w/ added potassium phosphate	[103]

Table 4 (cont'd)

D-201	NE	1,220 mg P/kg	10 mg PO4- P/L	DI water w/ added potassium phosphate	[79]
HFO-201	NE	17,800 mg P/kg	10 mg PO4- P/L	DI water w/ added potassium phosphate	[79]
Fe-EDA- SAMMS (FE(III)- immobilized porous silica)	NE	43.3 mg P/g	18.53 PO4/L	DI water w/ added potassium phosphate	[93]

N=Natural; W=Waste; NE=Nano-Engineered Media

Chapter 4: Methods

This chapter discusses the methods used to select media options, create synthetic subsurface drainage, operate batch adsorption and column experiments, and analytical methods to test TP, SP, and SRP throughout the research.

4.1. Factors for Optimal Media Performance and Use in Agricultural Subsurface Tile Drains

For this application, media was first selected based on performance in other applications to see if there was qualitative potential for this application. Then it was evaluated on the following factors:

- Cost
- Structural stability
- Likely commercial availability

Structural stability of the media includes its ability to stay in place during peak flow, no degradation of the media during freezing and thawing cycles, and no degradation of the media under long periods of saturation. The ability for the media to stay in place during peak subsurface drainage flow is determined by hydraulic conductivity, media physical characteristics, and its treatment system structure. Hydraulic conductivity is the rate of water passing through the media due to the media's porosity. A large hydraulic conductivity is preferred because less pressure will allow solution to flow through the media. However, prolonged saturation of the media due could soften the media's structure and make it more likely to break off at a high flow rate. Cold temperatures within the soil layer could initiate cracks in the media. Surface area plays a vital role in determining how much P is captured during contact with the drainage. A smoother surface from media degradation decreases the surface area and, thus, decreases the overall performance of the media.

4.2. Biochar Creation & Media Preparation for Batch Adsorption and Column experiments

There were two types of biochar used in this research: ferrous sulfate modified biochar and calcium-magnesium modified biochar. The manufacturing steps for both modified biochar types are in Appendix A.2.1. Table 5 contains a summary of the manufacturing steps used to produce the modified biochar media.

Table 5: Laboratory production of biochar P sorption media

Biochar	Pyrolysis	Pyrolysis	Base	Chemicals	Soaking	Literature
Type	Temperature	Time	Material	Used	Criterion	Source
Ferrous	400°C	2 hours	Corn	FeSO ₄	40 <i>g</i> of	[94]
Sulfate			Stover		material per 1 L of 1 mol/L	
					solution	
Calcium	600°C	3 hours	Corn Cob	MgCl ₂ and	Mass to	[90]
-				CaCl ₂	volume ratio	
Magnesi					is 1:3 for each	
um					soak in both 5	
					mol/L MgCl ₂	
					and 5 mol/L	
					CaCl ₂	
					solutions	

The reactor vessel was comprised of the vessel body (Figure 11) and the lid (Figure 10). The reactor vessel body was approximately 10 cm (4.0 inches) tall with an inner diameter of 8.9 cm (3.3 inches) and outer diameter of 13 cm (5.0 inches). Both the reactor vessel body and lid had eight holes around the circumference that functioned as locations for the nuts and bolts that held the body and lid together. The reactor vessel lid had three additional openings in the center of the lid for the thermocouple, nitrogen gas inlet, and gaseous products outlet. A FisherbrandTM Wide-From porcelain crucible (catalog no. FB965M) was placed into the center of the reactor vessel body holding a specified mass of feedstock. To prevent the possibility of an explosion if there was a large pressure build-up, a rupture disc (Figure 10) was placed between the reactor vessels contents and the interior side of the reactor vessel lid.

A Type F62700 Furnace manufactured by Barnstead Thermolyne (Figure 8 and Figure 9) held the reactor vessel to make the biochar. The furnace had an opening in the top called the "snorkel" to allow small pipes to enter the interior of the furnace to connect with the reactor vessel. The snorkel allowed the gaseous products, such as carbon dioxide and methane [104], to escape the reactor vessel during pyrolysis and into the lab ventilation apparatus above the furnace (Figure 9). This is a vital part of biochar production because if the gaseous products were unable to escape, the increased pressure in the reactor vessel that could potentially result in an explosion.

A type-K thermocouple was used to measure the inside temperature of the reactor vessel. Typically, the furnace was run at a temperature slightly above the target temperature inside the reactor vessel to ensure that the feedstock was heated correctly. The furnace was set to 450 °C or 650 °C to reach an internal temperature of 400 °C or 600 °C inside the reactor vessel for the ferrous sulfate or calcium-magnesium biochar, respectively. This thermocouple was inserted into the largest of the three openings on the reactor vessel lid and was tightened down with a screw. To the feedstock anaerobic during pyrolysis, one of the smaller reactor vessel lid openings was connected to a nitrogen gas inlet supplying nitrogen gas from an Airgas tank, and the other smaller opening was connected to a gaseous products outlet to release the oxygen and any gaseous products produced during pyrolysis. For both of the modified biochar types, the flow of nitrogen gas was kept at 1 mL/min for one hour before the furnace was turned on, and at 1 mL/min once the furnace was turned on and when the internal temperature of the reactor vessel was above 200 °C. After reacting, and the temperature of the reactor vessel was below 200 °C, the nitrogen gas inlet and gaseous products outlet were removed and rinsed with acetone to clean. These procedures were based on laboratory experience.



Figure 8: The outside of the F62700 Furnace used to pyrolyze the both the ferrous sulfate and the calcium-magnesium biochar



Figure 9: (Left) the snorkel fitted on top of the F62700 furnace; (Right) the interior top side of the F62700 furnace where the snorkel is located



Figure 10: (Left) The rupture disc; (Right) the reactor vessel with the lid attached



Figure 11: The reactor vessel with eight outer holes for bolts

4.3. Creation and Testing of Synthetic and Real Subsurface Drainage Water

4.3.1. Site-Specific Information for Real Subsurface Drainage Water Collection

This research utilized real subsurface drainage (RSD) and synthetic subsurface drainage (SSD) for the batch adsorption and column experiments. RSD was collected from "Site BN", a Michigan field with an existing subsurface tile drain that was installed in 2004 or 2005. The exact location and details of the farm were asked to be private in this thesis, but a summary of Site BN's field data was permitted. Samples for ion analyses were collected from the tile drain outlet located in the northern area of a field-testing site that drains 14.9 acres. The tile drain outlet is circular in shape and has a diameter of 10 inches. Lateral spacing between the tile drains is 33 feet. The lateral depth is 2.3 feet, and there is a 0.1% grade. The farmer plants a corn and soybean rotation with wheat as the cover crop in the winter. Variable dry rate fertilizer is applied in the spring. Data collected for RSD from Site BN from January 2019 to August 2019 was made available for this research. The data provided for this research was preliminary data, and there were discrepancies in data when temperatures were cold enough to freeze the autosampler onsite, when the snowmelt or rainfall was very large, or when the water level in the drainage ditch around the tile drain outlet was too high to take samples.

4.3.2. Formulation of the Synthetic Subsurface drainage Water

Three samples of RSD collected from "Site BN" were sent to Merit Laboratories, a commercial laboratory in East Lansing, MI, to perform analyses to determine significant ions and their concentrations. Table 6 contains the average and individual ion concentrations for the RSD samples, and the raw PDF files containing this data are in Appendix A.1. The average TP concentration of the three RSD samples was 0.200 mg/L. The desired P concentration range for the SSD was determined by the RSD testing and literature P concentrations from Table 3. The

SSD formulation is in Table 7. It is important to note that this formulation only represents the subsurface drainage collected from "Site BN" and is not representative of all subsurface drainage.

An Excel spreadsheet was set up to automatically calculate the amounts of each chemical compound in Table 7 based on the desired volume of synthetic subsurface drainage water. This spreadsheet also takes the initial P concentration of the tap and/or DI water into account to ensure an accurate amount of potassium phosphate is added to obtain the target P concentration. A sample calculation is in Appendix D.1. to demonstrate how to calculate the target amount of potassium phosphate, in grams, for the desired P concentration in the SSD.

For BAEs, a volume of 1 L of SSD was required. For the column experiments, a 110-gallon tank was used to hold 100-gallons of influent SSD for the column experiments. For QAQC purposes, the measured amounts of each chemical compound were within $\pm 10\%$ of the target value for that chemical compound before adding it to the mixture. After the SSD was formulated, two samples were taken and the P concentration was measured to ensure that it was within $\pm 10\%$ of the target concentration.

Table 6: Summary of ion analyses for the three samples (dated) of real subsurface drainage water from Site BN in Michigan

Chemical	Formula	Molar mass	Measured subsurface drainage water concentration (mg/L) or [mmol/L]				
		(g/mol)	8/30/2018	Average			
Sulfate SO ₄ ² -	SO ₄ ²⁻	96.06	(251)	(138)	(123)	(170.67)	
Surrate	304	90.00	[2.613]	[1.437]	[1.280]	[1.777]	
Chloride	Cl ⁻	35.45	(14)	(14)	(15)	(14.33)	
Cilioride			[0.395]	[0.395]	[0.423]	[0.404]	
Nitrate-N	NO ₃ -N	62.01	(7.5)	(7.1)	(9.8)	(8.13)	
Muale-IN	1103-11	02.01	[0.121]	[0.114]	[0.158]	[0.131]	
Ciliaa	SiO-	60.00	(14)	(14.5)	(14)	(14.17)	
Silica	SiO ₂	60.09	[0.233]	[0.241]	[0.233]	[0.236]	

Table 6 (cont'd)

Calcium	Ca ²⁺	40.08	(206)	(180)	(171)	(185.67)
Calcium	Ca	40.08	[5.140]	[4.491]	[4.266]	[4.632]
Magnesium	Mg ²⁺	24.30	(50.9)	(39.6)	(40.4)	(43.63)
	Mig		[2.095]	[1.630]	[0.663]	[1.796]
Datasaina	K ⁺	39.10	Under range	(3.49)	(2.91)	(3.20) **
Potassium	K	39.10	*	[0.089]	[0.074]	[0.082]
Codium	Na ⁺	22.99	(15.2)	(11.1)	(13.7)	(13.33)
Sodium	l Na		[0.661]	[0.483]	[0.596]	[0.580]
Avg. Daily Flow (m ³ /d)		30.97	6.69	0.13	0.04	2.29

^{*}Under range for potassium was classified as < 2.5 mg/L

The 110-gallon tanks and batch adsorption jars and lids used for the column and BAEs, respectively, were scrubbed and rinsed before use with P free soap (Liquinox) and DI and tap water. Tap water was used to rinse off the soap, and DI water was used as a final rinse. Table 7 lists the target amounts of chemical compounds, in grams, to create the target amount of SSD for column and BAEs.

Table 7: Concentration of each chemical compound in synthetic subsurface drainage water based off the testing results for the real subsurface drainage water (this table assumes that there was no phosphorus in the water used to make this formulation)

Chemical	Formula	Molar Mass (g/mol)	Target SSD Concentration (mg/L)				
Chemicai	Formula	Wiolai Wiass (g/illoi)	0.200	0.500	1.00	2.00	
Potassium	KCl	74.5513	5.62	4.90	3.69	1.29	
Chloride							
Magnesium	MgSO ₄	120.37	106.93	106.93	106.93	106.03	
Sulfate	MgSO ₄	120.37	100.93	100.93	100.93	106.93	
Calcium	CoCO	126 124	120.93	120.02	120.02	120.93	
Sulfate	CaSO ₄	136.134	120.93	120.93	120.93	120.93	
Sodium	NaNO	94 0047	40.25	49.35	40.25	49.35	
Nitrate	NaNO ₃	84.9947	49.35	49.33	49.35	49.33	
Sodium	NaCl	58.44	10.22	19.79	20.72	22.62	
Chloride	NaCi	38.44	19.22	19.79	20.73	22.62	
Silicon	Si(OH) ₄	(0.00	14.17	14.17	14.17	14.17	
Hydroxide	or H ₄ SiO ₄	60.09	14.17	14.17	14.17	14.17	
Potassium	II VDO	126.00	0.00	2.20	4.20	9.70	
Phosphate	H_2KPO_4	136.09	0.88	2.20	4.39	8.79	

^{**}The under-range value for potassium was not accounted in the average value for potassium

4.4. Batch Adsorption experiments

BAEs were important for this research to determine if the media could remove SP at low initial P concentrations and to compare media performance in similar conditions. Materials used in the BAEs were selected from the literature to ensure no P would adsorb to the materials and impact the final experimental results. It was important to use a jar and lid to uncapable of absorbing P in addition to the P adsorption media because that could make it more difficult to determine how much P was adsorbed by the adsorption media alone.

Nine glass jars with lids meeting the contaminant-free sample container guidelines mentioned in section 3.6.2.2. (Thermo Scientific; catalog no. 05-719-281B) were placed on an orbital shaker (Lab Companion SI-300R) shown in Figure 12.



Figure 12: Jars placed in the shaker

Jars containing media were labeled with "test (T)", and jars with no media were labeled with "control (C)". Control jars contain only SSD, RSD, or DI water and are used to determine the changes in the solution when no media is present. Three unique methods were created to collect data in the BAEs.

- 1. The "standard" method measured the change in P concentration multiple times at & between 0 and 24 hours using one amount of media immersed in either SSD, RSD, or DI water. This method determines if P removal changes for one amount of media over time.
- 2. The "standard 24 hour" method measured the change in P concentration at 0 & 24 hours using multiple amounts of media immersed in either SSD, RSD, or DI water. This method determines if P removal changes for different amounts of media.
- 3. The "dual 24 hour" method measured the change in P concentration at 0 & 24 hours using one or multiple media amounts immersed in SSD and multiple media amounts immersed in DI water containing added P as potassium phosphate. This method compares P removal between SSD containing ions, and DI water only containing phosphate to determine if other ions impact P removal.

Each BAE method has a specific procedure to accurately measure data.

- 1. For the standard method, there are five test jars and four control jars. The test and control jars are sampled in pairs except for the fifth test jar, which can be sampled alone or as a replicate jar for the fourth test jar.
- 2. For the standard 24-hour batch adsorption study type, there are eight test jars and one control jar. All jars are removed and sampled at the same time.
- 3. For the dual 24-hour batch adsorption study type, there are seven test jars and two control jars, one for the SSD and one for the DI water with added P. All jars are

To prepare the test and control jars, the initial P concentration of the SSD, RSD, or DI water was tested within an hour of the start time of the BAE. After the initial SRP concentration is determined, the theoretical P adsorption capacities of the desired media were used to calculate the amount of media required to theoretically adsorb 100% of the initial SRP concentration. This

media amount was then decreased to less than the calculated amount. This was done to ensure that there was enough P to measure in the solution at the end of the BAE. The media amount is calculated by using equation 6 below.

$$Media\ amount = \frac{(V)(c_0)(a)}{2} \tag{6}$$

Where V = volume of solution, L

 c_0 = initial concentration, mg/L

a = theoretical media adsorption capacity, mg P/g media

The amount of media in each jar was within ±10% of the target amount. After adding 1 L of SSD, RSD, or DI water, all media was added to all jars simultaneously. Then each jar was placed in the shaker at a constant temperature of 25°C and 120 RPM for up to 24 hours, an experimental method adapted from Blanco et al. (2016) [86]. The maximum attainable shaker speed was 120 RPM when operated under the weight of nine occupied jars.

At the end of the adsorption period, each jar was inverted 10 times before taking 30 mL of sample from the jar. A Hach brand filter holder (product #: 246800) was used with 25 mm diameter and 1.0 micrometers pore size glass microfiber filter (product #: 2551452) to filter samples for the SP and SRP tests. The filtered sample should be tested in duplicate (n=2). The difference between the initial and final concentration minus the concentration removed by the control is the amount of P the P adsorption media adsorbed under the tested conditions.

4.5. Column Experiments

Column experiments were done to estimate SP removal and media capacity under different conditions and to gather data on media options to use in an economic analysis. Columns were constructed of PVC pipe with an inner diameter of 3.8 cm (1.5 inches) and a length of 31 cm (12 inches). Columns were secured to a pegboard backwall using zip ties at the top and at the base.

Each column had a hose barb fitting (1/4" ID x 1/4" MIP) in the center of the PVC pipe end cap, and another hose barb fitting (1/8" ID x 1/4" MIP) roughly 1" from the top of the column. A picture and diagram of a laboratory column are shown in

Figure 13.

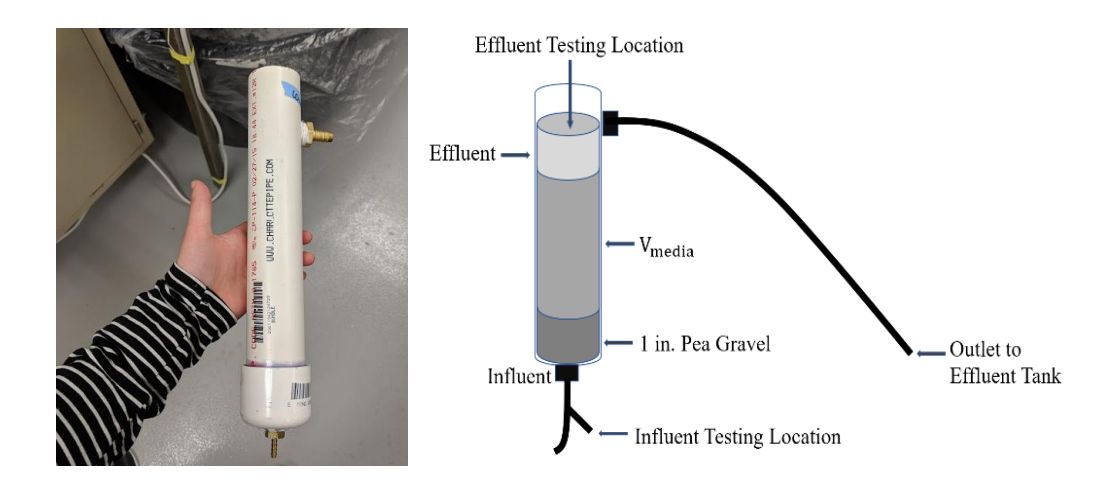


Figure 13: Laboratory column

Influent samples were collected from the tubing at the very bottom of the column to eliminate error associated with concentration changes within the influent storage container and tubing. Effluent samples were collected from the headspace of the column after the solution passed through the entire bed of media. Effluent samples should not be sampled at the end of the plastic tubing connected to the top hose barb because there could be a build-up biofilm along the tube that can interfere with the testing results. Influent feed was pumped using Cole-Parmer brand pumps (model no. 7553-70, 7554-80, or 7553-71) through the bottom of the column and the effluent exited through a fitting near the top into an effluent collection tank. There was one premanufactured column of PO4Sponge media that came from MetaMateria that could only do downwards flow, but all manufactured columns were upwards flow. Figure 14 shows all components of the column experimental setup.

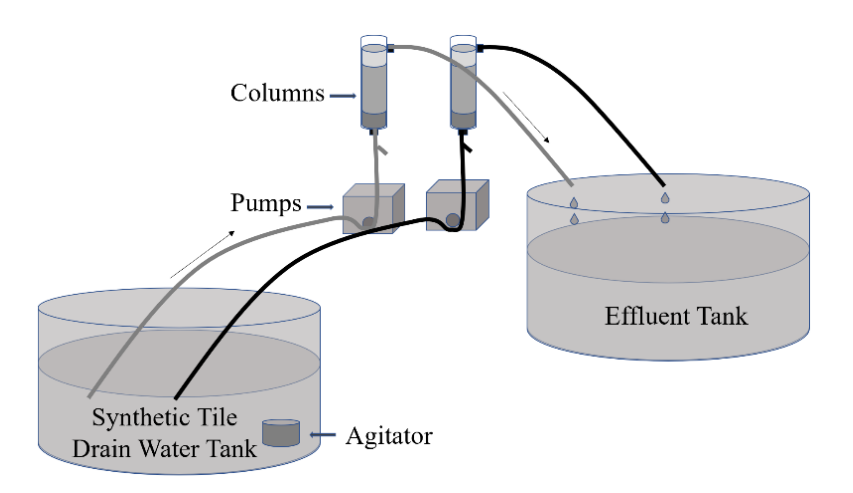


Figure 14: Diagram of adsorption media columns connected to the influent and effluent 110gallon tanks

MasterFlex tubing (item # HV-96412-17) was attached to the hose barb fitting on the bottom of the endcap and the T-shaped fitting (item # HV-30613-20). Additional plastic tubing was used to go around the MasterFlex tubing and this plastic tubing brought water from the influent 10-gallon tank up to the bottom of the columns. Plastic tubing was attached to the hose barb fitting at the top of the column to convey the effluent solution into the waste container. Tin foil was wrapped around all the tubing to prevent algal growth, and zip ties were used at hose barb + tube connections, and tube + tube connections to prevent leaks and air bubbles. All tubing was replaced monthly or at the start of a new column study phase to minimize artifact impact of biofilm growth in the tubes and to prevent biofilm growth in the media column. The P concentration in the influent tank and influent testing location were measured to ensure the biofilm had not removed large amounts of P in the tank before entering the column.

To prepare each column, 60 mL of rinsed and dried pea gravel was added to the bottom of the columns to prevent the media from clogging the hose barb supplying the influent feed from bottom to the top of the column. Each media was sieved to a particle size between 1.18 mm and

2.36 mm and rinsed with DI water before going into the column. Flow rates for each column were tested after the columns were attached to a pump and there were no leaks. DI water was pumped through the columns with media during flow rate testing to ensure that no ions would adsorb to the media before testing began. After the target flow rate for the target EBCT was found. The flow rates for each column were checked daily. After the column stops undergoing testing, the media is collected, dried in an oven, stored, and labeled for possible future analysis.

4.6. Analytical Methods

Testing for SRP is important because this form of P is bioavailable to organisms that can utilize free-floating SRP in aqueous environments. Table 8 lists the different types of P test kits used in this research to test the SSD and RSD.

Table 8: Phosphorus test kits for use with the DR6000 and with the ranges of phosphorus or phosphate the kits can measure

Method Description	HACH Method Number	Range of Test Kit	EPA Equivalent Method	Source
Total Phosphorus Ultra-Low- Range (ULR)	TNT 843	10 - 500 μg/L PO4-P		[105, 106]
Total Phosphorus Low-Range (LR)	TNT 843	0.05 - 1.5 mg/L PO4-P	EPA 365.1, 365.3	[107]
Total Phosphorus High-Range (HR)	TNT 844	0.5 - 5.0 mg/L PO4-P		[108]

The initial soluble reactive P (SRP) content of the DI or tap (potable municipal) water was tested for possible phosphorus before starting an experiment. The SP and TP test methods were not recommended because the digestion of anti-corrosion compounds in the tap water containing phosphate ions release additional P into the solution [7, 8] For quality assurance and control

purposes, testing included a blank, a standard, and replicate. Hach brand DI water was used for the blank, a known concentration of 0.250 mg PO4-P/L was used for the standard, and various replication methods were used to ensure data accuracy. For BAEs, each jar was sampled in duplicate. For column experiments, one influent or effluent sample was chosen at random and duplicated. There was not enough replication to run statistical analyses, but enough to ensure confidence in all data presented throughout this thesis. Data quality was retested or unreported if the percent relative range between replicates was greater than 20%, or if the percent recovery for standards was outside a range of 80-110%. Table 9 and Table 10 summarize the batch adsorption and column study data quality discussed in chapter 5.

Table 9: Average percent relative range replicates used in batch adsorption and column experiments

Phosphorus	Batch adsorption	Column Study	Column Study	Column Study
Test Type	experiments	Phases 1a-1d	Phases 2a-2e	Phase 3
Total	3%	N/A	2.3%	3.9%
Phosphorus				
Soluble	5%	N/A	N/A	N/A
Phosphorus				
Soluble	4%	N/A	2.0%	2.1%
Reactive				
Phosphorus				

Table 10: Average percent recovery for standards used in batch adsorption and column experiments

Phosphorus	Batch adsorption	Column Study	Column Study	Column Study
Test Type	experiments	Phases 1a-1d	Phases 2a-2e	Phase 3
Total	N/A	97%	96%	101%
Phosphorus				
Soluble	N/A	N/A	N/A	N/A
Phosphorus				
Soluble	N/A	N/A	96%	101%
Reactive				
Phosphorus				

If the samples could not be tested immediately after collection, each was preserved by adding 0.1 mL of concentrated sulfuric acid until the pH reached 2 or lower. The samples were stored in a 6°C (43 °F) fridge covered with plastic film for a maximum of 48 hours for reactive P. To prepare a preserved sample for analyses, the sample was allowed to warm to room temperature (15–25°C or 59–77°F), then the pH of the sample was neutralized using a 5 M sodium hydroxide solution [109]. The volume of both the sulfuric acid to preserve and sodium hydroxide to neutralize were recorded and the result for that sample was corrected for dilution.

Chapter 5: Results & Discussion

This chapter discusses the media selected for batch adsorption and column experiments, media performance results in batch adsorption and column experiments, and an economic analysis of the selected media options from the column experiments.

5.1. Phosphorus Adsorption Media

For this application, media was first selected based on performance in other applications to see if there was qualitative potential for this application. Then it was evaluated on the following factors.

- Cost
- Structural stability
- Likely commercial availability

Below are descriptions of the selected media for this research. Table 11 below contains the P adsorption capacity, source, and commercial availability of each selected media type:

Table 11: Summary table of media options used in this research

Media Type	Phosphorus Adsorption	Manufacturer or	Commercially
	Capacity	Literature	Available (Y/N)
	(mg P/kg Media)	Source	
PO4Sponge	50,000	MetaMateria;	Yes, in a
Generation 1		Columbus, Ohio	monolith form
			only
PO4Sponge	N/A	MetaMateria;	No
Generation 2		Columbus, Ohio	
FerrIXA33E	2,250	[98]	Yes, in a bead
			form
HIX(Zr)-Nano	N/A	Purolite	No
Ferrous Sulfate	0.56	[94]	No, produced in-
Modified Biochar			house
Calcium-	239 (using a high	[110]	No, produced in-
Magnesium	initial phosphorus		house
Modified Biochar	concentration)		
Blast Furnace	200 to 9,150	Levy Plant 6;	Yes
Slag		Dearborn, MI	
Steel Furnace	120 to 3,330	Levy Plant 6;	Yes
Slag		Dearborn, MI	

5.1.1. PO4Sponge Generation 1

The PO4Sponge media is a proprietary product manufactured by MetaMateria, Columbus, OH. The PO4Sponge is composed of iron oxide nanocrystals of oxyhydroxide with an aluminosilicate bonded porous structure containing 80% interconnected pores & a hydraulic conductivity between 3-7 cm/s, a base surface area of 15 m²/gram, a density of approximately 0.53 grams/cm³, and can be manufactured into a monolith, a packed bed, or in a custom shape [76, 91, 111, 112]. It is important to note that the granular form of the PO4Sponge media used in this research is only produced for small-scale or laboratory purposes[113]. The hydraulic conductivity of the media allows water to easily pass through the media at low pressures due to the internal porosity that allows the water to reach those adsorption sites [76, 111].

The PO4Sponge has an adsorption capacity ranging from 25 mg P/g media for low P concentrations (< 2 mg P/L) and 80 mg P/g media for high P concentrations (> 5 mg P/L) [97, 114]. Competing ions found in subsurface drainage are not believed to be a concern for PO4Sponge [76, 113]. P removal is achieved at concentrations from 0.1 mg/L seen in agricultural drainage to 150 mg/L seen in industrial wastewater at food processing plants [111]. The PO4Sponge can remove P down to levels below 0.09 mg/L for lakes, streams, and agricultural water runoff [97]. Safferman et al. (2015) tested the media using effluent from multiple wastewater treatment plants and found that it reduced SP levels from 1 mg P/L to less than 0.3 mg P/L [112].

The cost of PO4Sponge is \$19.80/kg [91]. According to MetaMateria, the PO4Sponge can be regenerated 15-20 times and the regeneration process lowers the average media cost by 80% when compared to the cost of a single, non-regenerated use of this media [111]. P is also easily recovered as a calcium phosphate precipitate after the regeneration process. More information on

the PO4Sponge regeneration is in Appendix A.5. Figure 15 is a photograph of the PO4Sponge in its crushed form (passes through mesh size 10 and is retained on mesh size 40) and in its monolithic form. The reddish-orange color is from the iron oxide used in the manufacturing of this media.



Figure 15: The PO4Sponge nano-engineered phosphorus adsorption media monolith (left) and crushed monolith granules (right) [76]

5.1.2. PO4Sponge Generation 2

The second generation of the PO4Sponge is a proprietary product manufactured by MetaMateria in Columbus, OH. The second generation of the PO4Sponge media was a supplemental part of the research that provided more insights on future adsorption media developments in addition to commercially available adsorption media.

Figure 16 shows this media in its crushed form, which has less of a reddish-brown color



compared to the first version of the PO4Sponge media.

Figure 16: The second version of the PO4Sponge phosphorus adsorption media

5.1.3. FerrIXA33E

FerrIXA33E, or hybrid anion exchanger (HAIX), is a nano-engineered proprietary adsorption media from Purolite (manufactured in Philadelphia, PA) that contains iron. The diameter of one resin bead ranges from 0.30 mm to 1.20 mm [115]. The recommended EBCT for P removal is unknown. The adsorption capacity for the FerrIXA33E media was 2.25 mg/g when exposed to influent concentration of 0.200 mg/L [98]. A pH of 6.0 to 8.0 was found to be the condition where this media was at optimal performance and this media had an adsorption capacity between 1.90 and 2.30 mg P/g HAIX for a pH between 6.5 and 7.5, respectively [98].

The base cost of one cubic foot of new FerrIXA33E media is \$450. Purolite does not currently regenerate P off the FerrIXA33E media. However, Blaney et al. (2007) were able to regenerate the HAIX adsorption media with no noticeable loss in P adsorption capacity [98].

Figure 17 is a photograph of the FerrIXA33E media.



Figure 17: The FerrIXA33E phosphorus adsorption media

5.1.4. HIX(Zr)-Nano

The HIX(Zr)-Nano, also referred to as HAIX-NanoZr, (A520E) is another proprietary product manufactured by Purolite (Philadelphia, PA). The HIX(Zr)-Nano media was used in this research to gain insight on future adsorption media developments in addition to other commercially available adsorption media This product is only commercialized outside of the United States [116]. This media option has a resin diameter range of 300-1200 µm and can undergo regeneration and reuse for multiple cycles [117]. Figure 18 shows this adsorption media.



Figure 18: The HIX(Zr)-Nano phosphorus adsorption media

5.1.5. Ferrous Sulfate Modified Biochar

The ferrous sulfate biochar was selected because Fenglin et al. (2015) used this biochar to remove P from agricultural runoff with an initial TP concentration between 1.86 mg P/L and 2.47 mg P/L [94]. The EBCT used for BAEs was 2 hours, and the biochar removed over 99% of the TP, down to concentrations less than 0.02 mg P/L. From the Langmuir equation (R^2 =0.977), the q' value was 0.56 mg P/g media [94]. The base material is corn stover, which is defined as the stalk and leaves from the corn plant after harvest. Low-cob corn stover was obtained from Hamilton County, IA. Fifty grams of corn stover were cut into small pieces about 3cm long and dried in an oven at $105\,^{\circ}C$ for 12 hours. After drying, 40g of the cut and dried corn stover was soaked in 1 L of a 1 mol/L ferrous sulfate solution for 2 hours at room temperature. The soaked

modified corn stover was dried again in the oven at $105^{\circ}C$ for 24 hours. The dried and soaked corn stover was then pyrolyzed at $400^{\circ}C$ for 2 hours. After pyrolysis, the biochar was cooled, rinsed with DI water, and dried in the oven at $105^{\circ}C$ for 24 hours. After drying, the biochar is crushed and sieved to a target diameter of 0.25mm. There is no cost information associated with this specific type of biochar. Figure 19 shows the ferrous sulfate biochar after it was made for BAEs.



Figure 19: Ferrous sulfate biochar after pyrolysis

5.1.6. Calcium-Magnesium Modified Biochar

The production of calcium-magnesium modified biochar was based on research by Fang et al. (2015) [110]. This media was selected because it had a large P adsorption capacity at high initial P concentrations, and this research will determine if it can remove P at low initial P concentrations commonly observed in subsurface drainage and agricultural runoff. Fang et al. (2015) utilized this biochar in a BAE with biogas fermentation liquid having an initial P concentration of 4,000 mg P/L [110]. The soaking time used for BAEs was 12 hours, and the maximum adsorption capacity of the biochar was 327 mg P/g media [110]. The base material is made from corn cob (literature did not specify location type of corn cob) cut into $1cm \times 0.5cm \times 0.5cm$ pieces. The pieces are dried in an oven at $110^{\circ}C$ for 24 hours. Then, the corn cob pieces

were soaked in a 5 mol/L MgCl₂ solution for 2 hours then dried at 110°C for 24 hours. The corn cob pieces were soaked a second time in a 5 mol/L CaCl₂ solution for 3 hours then dried at 110°C for 24 hours. The modified pieces are then pyrolyzed at a temperature of 600°C for 3 hours. After pyrolysis, the biochar was cooled, rinsed with DI water, and dried in the oven at 60°C for 24 hours, and sieved through a 0.1mm-0.2mm mesh [110]. There is no cost information associated with this specific type of biochar. Figure 20 shows the calcium-magnesium biochar after it was made for BAEs.



Figure 20: Calcium-magnesium biochar after pyrolysis and sieving

5.1.7. Blast Furnace Slag

Blast furnace slag (BFS) is a non-metallic co-product produced in metallurgical smelting process. This industrial by-product, or waste media, can be used as a SP absorption media [102, 118, 119]. This media was chosen based on s performance and the possibility to add value to the waste product. Iron ore, coke, and a flux are melted together in a blast furnace, and lime is used as a flux because it chemically combines to aluminates and silicates of the ore and coke ash, ultimately forming the slag [120]. The cost of BFS is \$0.03/kg [121]. For particle sizes of 0 to 6 mm, the hydraulic conductivity of BFS ranged from 7.48x10⁻² to 2.69x10⁻⁴ cm/s [122]. Figure 7 shows the BFS after wet-sieving and drying.



Figure 21: The blast furnace slag after being wet-sieved dried in an oven & a zoomed in view of the media

Studies have shown that various sources of BFS have different adsorption capacities ranging from 0.2 to 9.15 mg P/g media [101, 123]. One study by Hussain et al. (2014) used BFS to treat lake water with initial P concentrations between 0.35 and 0.49 mg PO4-P/L, which are similar to initial concentrations observed in subsurface drainage [124]. The study compared an average EBCT of 0.4 days to an average EBCT of 1.1 days. The adsorption capacity after 0.4 and 1.1-day average EBCT were 0.066 and 0.073 mg PO4-P/g media, respectively. The authors concluded that the changes in EBCT did not impact the P removal [124].

5.1.8. Steel Furnace Slag

Steel furnace slag (SFS) (aka basic oxygen furnace steel slag) is a byproduct of the steel industry. Hot iron smelted in a basic oxygen furnace, or scrap metal smelted in an electric arc furnace, are the main methods to manufacture SFS [125]. Lime is injected during the smelting process as a fluxing agent, where the lime chemically adheres with silicates, aluminum oxides, magnesium oxides, manganese oxides, and ferrites to form the slag [125]. The steel slag is then poured, cooled, and processed to remove free-metallics and sized for commercial use [125]. The removal mechanism for SFS is calcium minerals on the SFS surface reacting with a phosphate or bicarbonate ion to produce either calcium phosphate or calcium carbonate, respectively [126].

The optimal conditions for calcium phosphate precipitation by the SFS are when the pH is 8 or above, and there are high concentrations of soluble calcium ions [126, 127]. This media was chosen based on its performance and added value to the waste product. The cost of SFS is \$0.03/kg [121]. Steel slag fines with a particle diameter of 0.075 mm had a hydraulic conductivity of 6.12x10⁻³ cm/s [128]. The specific gravity of SFS ranges from 3.2 to 3.6 [129]. Blanco et al. (2016) utilized SFS in a batch adsorption study with an initial P concentration of 5 mg P/L and achieved an adsorption capacity of 0.12 to 1.20 mg P/g media [86]. Sheng-gao et al. (2008) conducted a batch adsorption study with SFS using an initial concentration of 1000 mg P/L and achieved an adsorption capacity of 33.3 mg P/g media [87]. Both Sheng-gao et al. (2008) and Blanco et al. (2016) noted that increasing initial P concentrations increased the adsorption capacity of the media [86, 87].

5.2. Batch Adsorption Experiments

In this research, BAEs were a precursor to the column experiments to eliminate media options unable to remove SP under subsurface drainage conditions. Eight media were tested using different amounts and different initial concentrations of TP, SP, or SRP. Three different P tests were conducted during the BAEs as the project progressed as new methods were studied and implemented. For example, the TP test was done for early BAEs, but SRP was found to be the best suited P test towards the end of the project. Supplemental exploratory testing of some media was also conducted using the dual 24-hour method with DI water (no ions) and SSD (with ions) to determine if competing ions in the SSD impacted media performance. The subsections below describe the batch adsorption study testing results.

5.2.1. PO4Sponge Generation 1

After 24 hours of batch testing the media in SSD with an initial concentration of 0.200 mg SRP/L, the PO4Sponge Generation 1 media achieved 37%, 67%, 84%, and 84% removal using 0.1, 0.3, 0.5, and 1 g of media, respectively. The 84% removal using 1 g of media represents the highest possible removal percentage because this media removed SRP to the lower analytical detection limit.

MetaMateria states that the optimal P removal by the PO4Sponge Generation 1 media is achieved at a pH of 7. However, in laboratory experiments the pH was 8 to 9. The PO4Sponge Generation 1 media is a candidate for further column experiments.

5.2.2. PO4Sponge Generation 2

After 24 hours of batch testing, the PO4Sponge Generation media in SSD with an initial concentration of 0.200 mg SRP/L achieved 51%, 85%, and 85% removal using 0.1, 0.3, and 0.5 of media, respectively. As previously noted, 85% removal was the highest possible because of analytical detection limits.

The Generation 2 media removed 51% of SRP using 0.1 gram of media, which is more than the 37% removal by the Generation 1 media with the same amount of media. Both media options removed below detection limits when the media amount was 0.5 g or higher.

Competing ions had an impact on the Generation 2 media. In a dual 24-hour BAE, 0.1 g of media and an initial concentration of 0.200 mg P/L, the DI water solution removed 70.4% of SRP while the SSD removed 55%.

Since the PO4Sponge Generation 2 media is not commercialized, it is not a candidate for further column experiments.

5.2.3. FerrIXA33E

After 24 hours of batch testing FerrIXA33E in SSD, with an initial concentration of 0.300 mg SRP/L, 3%, 36%, 82%, and 92% removal resulted for 0.01, 0.1, 0.5, and 1 g of media, respectively.

Compared to the PO4Sponge Generation 1 media, the media performed the same for 0.1 g and 0.5 g of media. Compared to the PO4Sponge Generation 2 media, the FerrIXA33E media had less removal using 0.1 g of media.

The FerrIXA33E media is a candidate for further column experiments.

5.2.4. HIX(Zr)-Nano

The HIX(Zr)-Nano adsorption media had impressive P removal capabilities. At an initial concentration of 0.200 mg SRP/L, the HIX(Zr)-Nano removed 87% of SRP using 0.1 grams of media in both the SSD and the DI water with added P. With 0.3 grams and 0.5 grams of media, the SRP was removed to below detection limits.

Compared to the FerrIXA33E and PO4Sponge media, the HIX(Zr)-Nano media had a substantial greater removal using 0.1 g of media, even when the initial P concentration for the FerrIXA33E was greater. Compared to the PO4Sponge Generation 2 media, the HIX(Zr)-Nano media had a greater removal using 0.1 g of media.

Since the HIX(Zr)-Nano media is not commercialized, it is not a candidate for further column experiments.

5.2.5. Ferrous Sulfate Modified Biochar

SSD at an initial P concentration of 0.500 mg SRP/L, 0.15 g of ferrous sulfate modified biochar removed 21%, 23%, 26% and 28% after 2, 4, 6, and 24 hours, respectively. Since there was a

very minimal increase in SRP removal between 2 and 24 hours, the ferrous sulfate biochar was most likely adsorbing the P quickly in the beginning, but lost capacity after.

In a separate batch adsorption study using SSD, a higher initial concentration of 1.00 mg SRP/L was used. After 24 hours, 0.1 and 0.25 g of media removed 6% and 24% of SRP, respectively. Increasing the initial concentration did not increase SRP removal with the ferrous sulfate biochar, as both experiments exhibited similar removal. The results of the 1.00 mg SRP/L BAE further supported that the ferrous sulfate biochar media was not able to hold a large capacity of SRP, even if the initial SRP concentration was doubled, because it had no capacity to hold additional SRP.

The quick adsorption of P onto the media is a desirable characteristic to have when removing P from peak flow conditions when the flow rate is very high. However, the ferrous sulfate biochar is also quickly saturated and could require more frequent replacement. Since the ferrous sulfate biochar not currently able to be regenerated, the frequent replacement of the media would require an increased cost and labor to produce. Upon visual inspection, there were more fine particles in the bulk solution after the BAE was completed, indicating that the biochar was degrading under these conditions.

The ferrous sulfate biochar is not recommended for this application nor a candidate for further column experiments.

5.2.6. Calcium-Magnesium Modified Biochar

After 24 hours of immersing the media in SSD with an initial concentration of 0.200 mg SRP/L, the calcium-magnesium biochar achieved 0%, 6%, 17%, and 36% removal using 0.1, 0.3, 0.5, and 0.75 gram(s) of media, respectively. Compared to all the previous media options using

similar media amounts, the calcium-magnesium biochar has less removal. Upon visual inspection, there were more fine particles in the bulk solution after the BAE was completed, indicating that the biochar was degrading under these conditions.

The calcium-magnesium biochar is not recommended for this application nor a candidate for further column experiments.

5.2.7. Blast Furnace Slag

After 24 hours of immersing the media in SSD, with an initial concentration of 0.200 mg SRP/L, the BFS media achieved 0%, 0%, 0%, 1%, and 3% removal using 0.1, 0.2, 0.3, 0.5, and 0.75 gram(s) of media, respectively. Of all the media options, the BFS had the lowest removal.

Consequently, the BFS is not recommended for this application nor a candidate for further column experiments.

5.2.8. Steel Furnace Slag

After 24 hours of immersing the media in SSD with an initial concentration of 0.200 mg SP/L (note that this is not SRP), the SFS media achieved 7%, 12%, and 28% removal using 0.3, 0.6, and 1 gram(s) of media, respectively. The SFS was effective but requires larger quantities of media to remove P to become competitive with engineered media. Compared to the engineered media, the SFS has a lower capital cost due to its classification as a waste product from a common process. However, an economic analysis of capital and implementation costs will provide a more accurate cost of any adsorption media treatment system.

The opportunity to turn the SFS waste product into a value-added product makes the SFS media a candidate for further column experiments.

5.2.9. Selection of Media for Column experiments

The final media options selected for further column experiments are the PO4Sponge Generation 1, the FerrIXA33E, and the SFS.

The PO4Sponge Generation 2 and HIX(Zr)-Nano were not selected because they are not yet commercialized, but both exhibited enough removal to be candidates for P removal technology in future research. The ferrous sulfate biochar had rapid removal, but poor capacity, making it undesirable to implement for this application. Lastly, the calcium-magnesium and BFS had the lowest removals of all eight media options and were not recommended for this application or future column experiments.

5.3. Column experiments

The purpose of the column experiments was to estimate P removal and media capacity under different conditions and to gather data on media options to use in an economic analysis. The PO4Sponge Generation 1, FerrIXA33E, and SFS were selected from BAEs for these experiments. Changing conditions included (1) high and low P concentrations, (2) high and average flow rates to stimulate short and long EBCTs, respectively, and (3) on and off flow to the columns to simulate how the media responds when no drainage flows through the tile drains. The results of each column study phase 1a to 1d, phase 2a to 2e, and phase 3 are in the subsections below. The last subsection describes which media options were chosen for further feasibility studies. A summary of all ten phases is in Table 12. Note that three different P tests were conducted during the column experiments as the project progressed and new methods were studied and implemented. For example, the TP test was done for column phases 1a to 1d, but TP and SRP tests were used towards the end of the project. A more detailed summary table for each column study phase is in Appendix C, Table 26. Note that the mention of PO4Sponge from here

on refers to PO4Sponge Generation 1, not PO4Sponge Generation 2. Also note that the use of the term "saturation" in this section means that the media has absorbed the maximum amount of P under the given conditions.

Table 12: Summary of all column study phases and their characteristics

Phase	Media Type(s) Used	Fresh or Used Media	EBCT (min)	HRT (min)	Target Concentration (mg/L)	P Type	Subsurface drainage Type	Duration (days)
1a	PO4Sponge FerrIXA33E	Fresh	30	24 n/a	0.200 (for SSD only)	TP	SSD and RDTW	124
1b	PO4Sponge FerrIXA33E	Used	60	48 n/a	0.200 to 0.500	TP	SSD	34
1c	PO4Sponge FerrIXA33E	Used	60	48 n/a	Field Conditions	TP	RSD only	7
1d	PO4Sponge FerrIXA33E	Used	60	48 n/a	1.00	TP	SSD	6
2a	PO4Sponge SFS	Fresh	5	4	0.500	TP and	SSD	9
	PO4Sponge		1.0	8	0.500	SRP TP	aap	
2b	SFS	Used	10	6	0.500	and SRP	SSD	5
2c	PO4Sponge SFS	Used	20	16 11	0.500	TP and SRP	SSD	8
2d	PO4Sponge SFS	Used	20	16 11	2.00	TP and	SSD	19
2e	PO4Sponge	Used	60	48	2.00	SRP TP and	SSD	4
26	SFS	USCU	00	34	2.00	SRP TP	SSD	+
3	PO4Sponge SFS	Fresh	5	3	0.500	and SRP	SSD	10

5.3.1. Phase 1a: Fresh PO4Sponge Generation 1 and FerriXA33E media with RSD and SSD at an EBCT of 30-minutes and target initial TP concentration of 0.200 mg TP/L

Phase 1a allowed methods and protocols to be fully developed. As a result, under-range data was a common issue for both columns removing TP from SSD and RSD. Further, the initial TP concentration of RSD was often diluted by storm flow and measured under the detection limit.

All results for Phase 1a are summarized below.

Each column received either RSD water or SSD as the influent feed at an EBCT of 30 minutes. The SSD was formulated with a target concentration of TP of approximately 0.200 mg TP/L. However, the RSD did not have a controllable concentration because it depended on real-time and site-specific conditions impacting the tile drain at the time of collection.

Approximately 50% TP removal with an influent TP concentration as low as 0.105 mg TP/L resulted for the following media.

- Granular PO4Sponge in RSD
- Granular and monolithic PO4Sponge n SSD
- FerrIXA33E in SSD

The similar TP removal trends between the granular and monolithic forms of PO4Sponge media is important as lab testing relies heavily on the granular form of the media. Additionally, the similar removal between the granular and monolithic PO4Sponge media columns demonstrated that the upwards flow through the granular PO4Sponge column and downwards flow through the granular PO4Sponge column did not impact media capacity and P removal. However, a monolith of PO4Sponge is more economically produced and easier to manage. All results for Phase 1a are in Appendix C.

5.3.2. Phase 1b: Used PO4Sponge and FerriXA33E media with SSD at an EBCT of 60minutes

The purpose of phase 1b was to test if doubling the EBCT increased the amount of TP adsorption. For the granular PO4Sponge, initially when the EBCT was doubled to 60-minutes, the influent and effluent TP concentrations went from 0.525 mg TP/L to 0.251 mg TP/L, respectively, and towards the end of the phase, the influent and effluent TP concentrations went from 0.450 mg TP/L to 0.432 mg TP/L, respectively. When the initial concentrations were higher than 0.400 mg TP/L, effluent concentrations decreased because the larger initial concentration gave the media additional capacity under those conditions to continue adsorbing the TP. However, the media was showing possible signs of saturation when influent concentrations were around 0.400 mg TP/L because the resulting effluent concentrations increased. This indicated possible de-adsorption of TP off the media back into the solution.

The PO4Sponge and FerrIXA33E media reached saturation between the end of phase 1a and the end of phase 1b. The doubled EBCT temporarily increased media capacity and TP removal until the media became saturated again. All results for Phase 1b are in Appendix C.

5.3.3. Phase 1c: Used PO4Sponge Generation 1 and FerrIXA33E media with RSD at an EBCT of 60-minutes

After Phase 1b, the pumps were turned off for three weeks then back on to stimulate the effects of pulse-loading in the tile drain. Pulse-loading in tile drains simulate an on and off water flow pattern within the tile drain, which is important to consider for the summer months. This experiment was conducted to determine if media could dry out and cake together. If caking occurs, the water can bypass the bulk volume of the media by rerouting along the outside of the media and will not receive the proper treatment.

RSD was used in place of SSD to observe the media performance. Since adsorption media relies on equilibrium kinetics, there was a higher concentration of TP in the effluent than the influent during phase 1c because the influent feed in phase 1c had a lower concentration of P than the feed in phase 1b, which caused de-adsorption of TP back into the water off the media Since no additional TP was removed, the PO4Sponge and FerrIXA33E media reached capacity and were saturated under the RSD conditions after phase 1c. Further, no media caking was observed. All results for Phase 1c are in Appendix C.

5.3.4. Phase 1d: Used PO4Sponge Generation 1 and FerriXA33E media with SSD at an EBCT of 60-minutes and initial SRP concentration of 1.00 mg SRP/L

A high influent TP concentration of 1.00 mg TP/L was fed into the columns to see if the media would continue to remove TP at a higher concentration even if the media were saturated at lower concentrations.

The PO4Sponge and FerrIXA33E media achieved a 50% TP removal for the first two days but this removal ceased by day 5 as the media became saturated under the high influent concentration.

At the end of phase 1d, the media was saturated and loaded under the high influent conditions seen in subsurface drainage and no further experiments to continue loading the media were necessary. The media was removed from the columns, labeled, and stored in case further analysis was needed. All results for Phase 1d are in Appendix C.

Overall, phase 1a to 1d demonstrated that low initial TP concentrations will saturate the media. However, it was also observed that increasing the initial TP concentration does not greatly increase the media capacity and longevity because the media would continue to saturate quickly in response to increasing concentrations.

5.3.5. Phase 2a: Fresh PO4Sponge and SFS with SSD at an EBCT of 5-minutes and initial SRP concentration of 0.500 mg SRP/L

After phase 1d, the columns were emptied and cleaned and two columns with new media, SFS and PO4Sponge, were initiated. The goal of phase 2a was to determine if the media would respond to greater flow with an above average SRP concentration. These conditions would be expected during storm events or snowmelt, where large volumes of water enter the tile drain within 24 to 48 hours after draining through the soil [19]. The phase 2a columns operated at a target initial SRP concentration of 0.500 mg SRP/L, an EBCT of 5-minutes, and used SSD to simulate these conditions. The HRT for the PO4Sponge and SFS were 4 and 3 minutes, respectively.

SRP removal was observed during the first three days. However, subsequent testing three and five consecutive days later showed no removal because the media reached capacity under these conditions and unable to remove additional SRP.

In addition, the sampling periods were too far apart to capture the changes within the first 0 to 24 hours for the PO4Sponge and SFS. Phase 3 of the column experiments replicates the phase 2a study to document the removal between 0 and 24 hours. Capturing the changes between 0 and 24 hours is crucial to determine when the PO4Sponge and SFS began removing SRP and when the removal of SRP leveled off.

All results for Phase 2a are in Appendix C, and results for phase 3 are in a section later.

5.3.6. Phase 2b: Used PO4Sponge Generation 1 and SFS with SSD at an EBCT of 10minutes and initial concentration of 0.500 mg SRP/L

To determine if the SFS and PO4Sponge adsorption media required a longer EBCT to remove SRP, the same media was kept in the columns and the EBCT was doubled to 10 minutes by halving the flow rate to each column. The concentration of SRP in the influent remained at 0.500 mg SRP/L. The HRT for the PO4Sponge and SFS were 8 and 6 minutes, respectively.

Testing on the first day of this phase and three days later showed no SRP removal for both the PO4Sponge and, indicating that the media was still saturated and needed a longer EBCT still to remove SRP from the influent stream. All results for Phase 2b are in Appendix C.

5.3.7. Phase 2c: Used PO4Sponge Generation 1 and SFS with SSD at an EBCT of 20minutes and initial concentration of 0.500 mg SRP/L

The EBCT for the SFS and PO4Sponge was doubled to 20-minutes to determine if the media could remove more SRP from the SSD with the increased contact time. The concentration of SRP in the influent remained at 0.500 mg SRP/L. The HRT for the PO4Sponge and SFS were 16 and 11 minutes, respectively.

No SRP removal was seen throughout the entire duration of Phase 2c, indicating that the media was still at equilibrium and an increase in EBCT or initial concentration was needed to determine if the media could still remove SRP. All results for Phase 2c are in Appendix C.

5.3.8. Phase 2d: Used PO4Sponge Generation 1 and SFS with SSD at an EBCT of 20minutes and initial concentration of 2.00 mg SRP/L

After no SRP removal was observed by doubling the EBCT to 20 minutes, the initial SRP concentration was increased from 0.500 mg SRP/L to 2.00 mg SRP/L, which is the upper limit

for SRP concentrations observed in subsurface drainage under field conditions shown in Table 3. The EBCT remained at 20-minutes. The HRT for the PO4Sponge and SFS were 16 and 11 minutes, respectively.

The PO4Sponge media exhibited over 50% SRP removal during the first day of this phase; however, SRP removal significantly declined over the next three days, then the SRP removal was negligible over the following two days, indicating that the PO4Sponge media reached equilibrium under these conditions.

The SFS exhibited little to no SRP removal throughout the duration of phase 2d, indicating that it had also reached equilibrium under these conditions. All results for Phase 2d are in Appendix C.

5.3.9. Phase 2e: Used PO4Sponge Generation 1 and SFS with SSD at an EBCT of 60minutes and initial concentration of 2.00 mg SRP/L

The goal of phase 2e was to observe if the media removed SRP at an EBCT of 60-minutes and at 2.00 mg SRP/L. The longer EBCT is not practical for field applications due to the corresponding large size of a contractor, but this experiment was of interest to understand if the PO4Sponge and SFS could continue removing SRP. This phase followed what was conducted in earlier phases, which utilized longer EBCTs and higher initial SRP concentrations. The HRT for the PO4Sponge and SFS were 48 and 34 minutes, respectively.

The SFS and PO4Sponge removed 5% and 17% SRP, respectively, during the first sampling period, then both removed 11% SRP during the second testing period. These trends strongly indicated that both media were saturated and that a higher EBCT for these relatively low influent SRP concentrations did not have a significant impact. All results for Phase 2e are in Appendix C.

The SFS media was difficult to remove from the column after this phase because it had hardened inside due to the formation of calcium carbonate (see

Figure 22). Calcium carbonates form on the slag instead of calcium phosphate when bicarbonate and dissolved forms of CO₂ are present in the subsurface drainage due to water infiltrating through calcareous soils and microbial respiration [126, 127]. This decreases the capacity of the SFS due to (1) the bicarbonate and phosphate ions competing to adsorb to the calcium minerals on the SFS and (2) the formation of calcium carbonate decreases the pH and soluble calcium concentration which negatively impacts the SFS's ability to precipitate phosphate ions as calcium phosphate [124, 125]. Additionally, it was noted that SFS has a decrease in P removal via calcium phosphate precipitation when the pH of the solution is below 8.5 [126, 127]. Surface runoff was not found to be an issue for the SFS because it did not contain bicarbonates that cause calcium carbonates [126].



Figure 22: Hardened steel furnace slag media after the end of column study phase 2e

5.3.10. Phase 3 – Replication of Phase 2a: Fresh PO4Sponge Generation 1 and SFS with SSD at an EBCT of 5-minutes and initial concentration of 0.500 mg SRP/L

Phase 3 tested the hypotheses concluded at the end of phase 2a. The same media volume and SSD formulation was used throughout phase 3, identical to phase 2a. All results for Phase 3 are in Appendix C.

Both the PO4Sponge and SFS were able to remove SRP to below detection limits up to 5 hours after the columns were turned on. After 24 hours, the SFS was removing approximately 50% SRP, while the PO4Sponge was still removing SRP to below detection limits. After 7 days, the SFS was saturated. The PO4Sponge, however, was still exhibiting up to 20% SRP removal after 10 days of operation.

By capturing the SRP removal data multiple times per day over multiple days, it was determined that the PO4Sponge is better suited for long-term SRP removal for large storm flows due to its higher adsorption capacity. The SFS can remove SRP for large storm flows, but for a shorter duration since it has a smaller adsorption capacity compared to the PO4Sponge. Figure 23 compares the loading of SRP onto both the PO4Sponge and SFS over the duration of Phase 3. From Figure 23, both the PO4Sponge and SFS had similar capacities for the first 24 hours. However, the PO4Sponge had an increased capacity after 24 hours compared to the SFS's capacity, which leveled off due to media saturation.

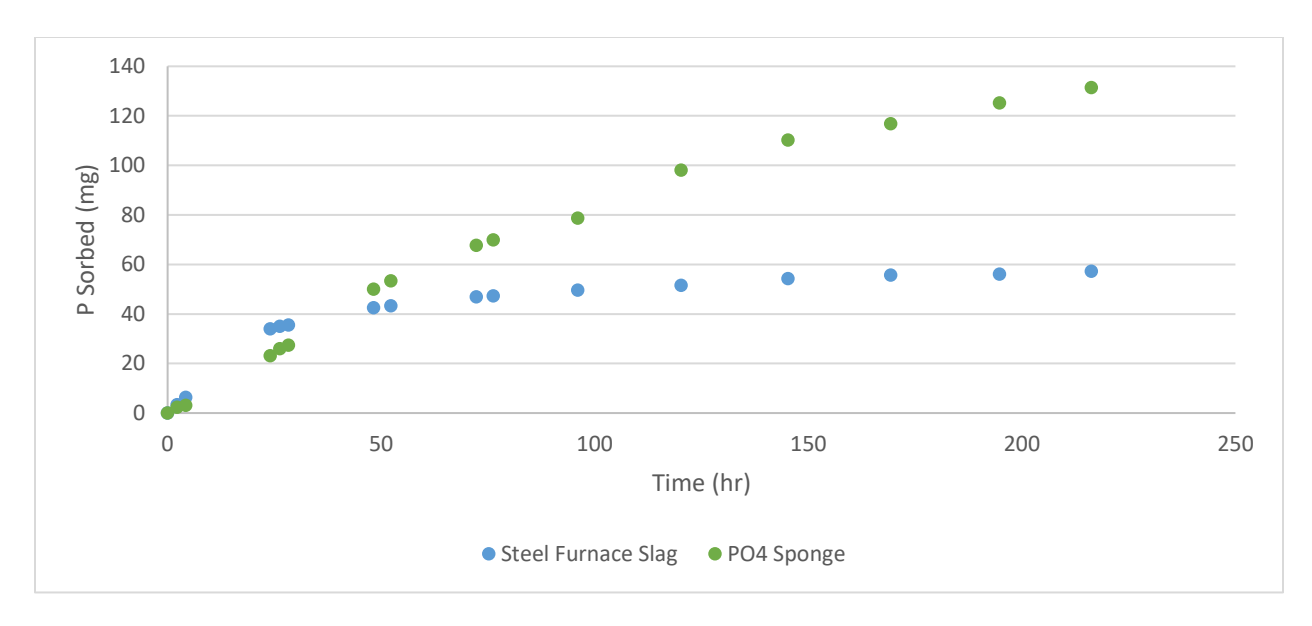


Figure 23: Relationship between the SRP loaded onto the PO4Sponge vs. SFS

5.3.11. Selection of Media for Feasibility Studies

After starting column phase 1a, the manufacturer of the FerrIXA33E reached out and did not recommend the FerrIXA33E media for this application because its hydraulic conductivity, the ease for water to travel through the media, was low. Based on this information, the FerrIXA33E media was not a candidate for further feasibility studies.

Based on the results in phase 3, both the PO4Sponge and SFS were able to remove SRP in peak flow conditions exhibiting high SRP concentrations. However, regeneration of SFS is not demonstrated so it cannot be reused, as compared to PO4Sponge. Both the PO4Sponge and SFS were selected as candidates for further economic analysis.

5.4. Economic Analysis

5.4.1. Media Performance in Batch Adsorption and/or Column experiments

Based on the BAEs, all commercialized media except for the BFS are suitable choices for treating subsurface drainage based on P removal performance. However, both the magnesium calcium and ferrous sulfate modified biochar are not competitive compared to the PO4Sponge

and SFS. This is evident as 0.1 grams, the PO4Sponge removed 41.2% of SRP at an initial concentration of 0.200 mg P/L but 0.500 mg P/L of ferrous sulfate modified biochar only removed 32.1% of SRP.

The SFS and the magnesium calcium modified biochar had similar performance for similar media amounts and the same initial SRP concentration. Specifically, 1.0 gram of SFS removed 35.5% of SRP, and 0.75 grams of magnesium calcium modified biochar removed 36.3% of SRP for an initial SRP concentration of 0.200 mg P/L.

While the FerrIXA33E media exhibited relatively high P sorption, the manufacturer recommended that this media not be used for this application because of its low hydraulic conductivity. This was particularly true as the real tile drain occasionally had sediment, which could clog this media.

Both the SFS and the PO4Sponge P adsorption media seemed to be well suited for subsurface drainage and removed P during stimulated storm flow conditions with a high SRP concentrations of 0.500 mg P/L. The SFS was exhausted after 7 days and the PO4Sponge was still removing up to 20% of SRP after 10 days.

5.4.2. Capital and Operational Costs

Biochar has been studied mainly as a soil amendment and recently as a water treatment technology. The cost to produce biochar on-site is high due to the costs of the equipment required for pretreatment and pyrolysis. One example of a lab-scale mobile farm unit made specifically for biochar production costs \$50,000, without the cost of materials to produce biochar [130].

Cost estimates associated with the PO4Sponge and SFS are shown in Table 13. Note that the value of regenerated calcium phosphate is priced based on reagent grade calcium phosphate, which is more expensive than technical grade calcium phosphate. Labor costs are associated with the media installation and removal when the PO4Sponge is regenerated, or the SFS is removed and disposed. The contactor capital and installation costs are only charged at the time of contactor installation. Appendix D.2. contains all calculations used in Table 13.

Table 13: Cost estimates for the PO4Sponge Generation 1 media and SFS

Item	PO4Sponge Generation 1	SFS
Media Capital Cost	\$19/kg [91]	\$0.06/kg (Quote from Edward Levy Company)
Contactor Capital Cost	\$6,685	\$10,869
Labor Cost	\$480	\$480
Contactor Installation Cost	\$640	\$640
Regeneration	\$2/kg/regeneration + shipping [91]	N.A.
Vacuum Truck Rental	\$725/truck/day	\$725/truck/day
Disposal Cost	\$28/yd ³ +\$12/truck	\$28/yd ³ +\$12/truck
Value of Regenerated Calcium Phosphate	\$0.64/g (Fisher Scientific; catalog no. C133-500)	N.A.

5.4.3. Media Implementation in Tile Drains

A case study was conducted to demonstrate the protocol and determine the rough size and cost of deploying media within subsurface tile drains. Site-specific modeling was conducted using confidential data from a, heavily monitored tiled farm field, "Site BN". Table 14 provides a summary of the flow and SRP concentrations for "Site BN".

Table 14: "Site BN" tile drain data for drainage flow rate and SRP ranges

Month	Flow rate range (m³/day)	SRP range (mg P/L)	# of times the SRP concentration was above 0.050 mg P/L	Media recommended during this time?
October	0-13.51	0-0.05	2	No
November	11.73-936.63	0.003-0.050	2	No

Table 14 (cont'd)

December	4.29-848.73	0.003-0.061	1	No
January	1.42-551.60	0.003-0.132	2	Yes
February	6.64-446.06	0.014-0.481	4	Yes
March	1.57-865.27	0.004-0.093	4	Yes
April	16.46-1134.34	0.003-0.332	5	Yes
May	19.23-1009.4	0.0001-0.305	6	Yes
June	2.10-1253.40	0-0.070	2	Yes
July	0-39.1	0.004-0.168	2	No

With variable dry-rate fertilizer application and snow melt in the spring, the most crucial time for the P adsorption media to be deployed is January thru June, a total of 6 months. From the preliminary "Site BN" data, the daily flow rate was multiplied by the daily SRP concentration to obtain the daily mass of SRP leaving the subsurface tile drain via subsurface drainage. The total daily mass of SRP from January to June was summed to obtain total amount of SRP requiring treatment by the media. The resulting total SRP discharged from 14.9 acres of subsurface tile drains was 1.66 kg of SRP during this period. Additionally, the average pH between January and June was 7.59 (max = 8.07 & min = 7.20). The pH of the tile drainage is important for the SFS because a pH above 8 can cause spontaneous calcium phosphate precipitation, but calcium carbonate formation below a pH of 8 [126].

Rough design and cost estimates were conducted for each media choice based on the cost information in Table 13. Data from column study Phase 3 was utilized to estimate how much media was needed to remove the 1.66 kg of SRP in the tile drain between January and June. The detailed calculations are in Appendix D.2. The calculated media volume to remove 1.66 kg of SRP was 4.80 m³ and 13.91 m³ for the PO4Sponge and SFS, respectively. The saturated P adsorption capacity of the PO4Sponge and SFS from column experiment phase 3 was halved to achieve these media volumes. Halving the capacity doubles the volume of media, reducing the

chance of media saturation in the subsurface tile drain. If the media is saturated, it risks desorption of P back into the subsurface drainage. Using the "Site BN" daily flow rate data between January and June, the maximum and minimum EBCT and HRT were calculated for a treatment system using this volume of PO4Sponge or SFS. The maximum and minimum daily calculated EBCT and HRT for the PO4Sponge and SFS is shown in Table 15 and Table 16, respectively. Note that the minimum EBCT or HRT is the most critical design consideration because the media must remove SRP from peak flow rate conditions.

Table 15: The maximum and minimum calculated empty bed contact times for the PO4Sponge and steel furnace slag based on daily flow rates from "Site BN" data

Media →	PO4Sponge		Steel Furnace Slag	
Month	Maximum EBCT (min)	Minimum EBCT (min)	Maximum EBCT (min)	Minimum EBCT (min)
January	4856	13	14072	36
February	1041	15	3016	45
March	4410	8	12779	23
April	420	6	1217	18
May	359	7	1042	20
June	3223	6	9339	16

The minimum EBCT for the PO4Sponge was 6 minutes, and this EBCT occurred in April and June. The minimum EBCT for the SFS was 16 minutes, and this EBCT occurred in June.

Table 16: The maximum and minimum calculated hydraulic retention times for the PO4Sponge and steel furnace slag based on daily flow rates from "Site BN" data

Media →	PO4Sponge		Steel Furnace Slag	
Month	Maximum HRT	Minimum HRT	Maximum HRT	Minimum HRT
	(min)	(min)	(min)	(min)
January	3885	10	8021	21
February	832	12	1719	26
March	3526	6	7284	13
April	336	5	694	10
May	288	5	594	11
June	2578	4	5323	9

The minimum HRT for the PO4Sponge was 4 minutes, and this HRT occurred in June. The minimum HRT for the SFS was 9 minutes, and this HRT also occurred in June.

Further, the PO4Sponge media is regenerated once a year and the SFS is replaced once a year because after the P is loaded onto the media between January and June, there is not enough capacity left to use the media into next year. Three scenarios were developed: (1) Scenario A – the cost of the PO4Sponge plus the cost to regenerate by the manufacturer, (2) Scenario B – the cost of the PO4Sponge plus the cost to regenerate onsite, (3) Scenario C – the cost of the SFS plus the cost of disposal. Figure 24 shows the flow diagram for each scenario.

Table 17, Table 18, and Table 19 summarize the rough cost estimate over 15 years for scenario A, B and C, with values normalized to a 1-year period. For scenarios A and B, year 0 is the point in time where the PO4Sponge and its contactor are installed, years 1 to 14 are the times when the PO4Sponge is removed and shipped round-trip for regeneration, and year 15 is the time when the PO4Sponge has reached its 15-year lifespan and requires removal and disposal from the system. Similarly, for scenario C, year 0 is the point in time where the SFS and its contactor are installed, and years 1 to 15 are the times when the SFS requires yearly removal, disposal, and reinstallation with fresh media. The time value of money was not incorporated into these tables, but the large upfront investments in the contactor and/or media will increase the cost to implement this technology if the time value of money was included. Detailed calculations are in Appendix D.2.

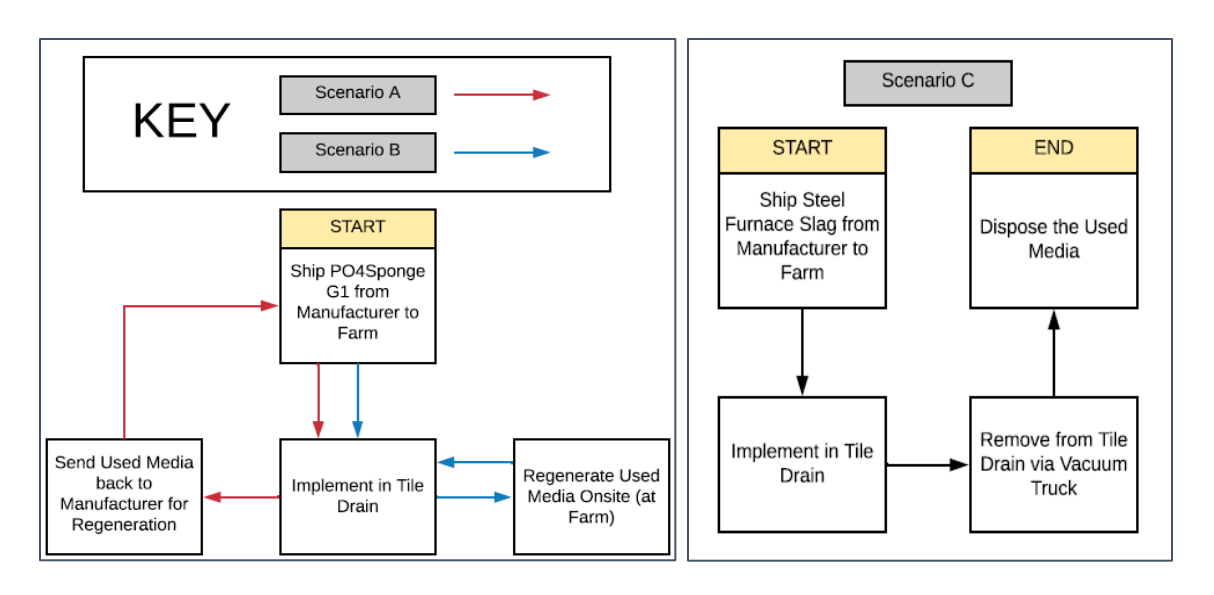


Figure 24: The media flow diagram for scenarios A, B, and C

Table 17: Rough cost estimates for scenario A over a 15-year period

	Year 0	Year 1 to 14	Year 15		
Media Capital Cost	\$53,623	N/A	N/A		
Contactor Capital Cost	\$6,685	N/A	N/A		
Contactor Installation	\$640	N/A	N/A		
Cost					
Labor to Install/Re-Install	\$480	\$480	N/A		
Media in Contactor					
Shipping Cost	\$201	\$370	N/A		
Regeneration Cost	N/A	\$5,645	N/A		
Labor to Remove Media	N/A	\$480	\$480		
from Contactor					
Removal Cost via	N/A	N/A	N/A		
Vacuum Truck					
Disposal Cost	N/A	N/A	\$188		
Annual Cost (Separate)	\$61,215/year	\$6,975/year	\$668/year		
Total Cost (Separate)	\$61,215	\$97,643	\$668		
Total Cost (Together)	\$159,526 for 15 years				
Annual Cost	\$10,635/year				
Annual Cost Per Acre	\$714/acre/year				
(14.9 acres)					

 Assume that year 14 is the last time the media is shipped back to the farm after regeneration and that there is no shipping or regeneration after year 15, just the cost of labor to remove the media and disposal costs Assume that the farmer can transport the PO4Sponge to the disposal site without the use of a vacuum truck

Table 18: Rough cost estimates for scenario B over a 15-year period

	Year 0	Year 1 to 14	Year 15		
Media Capital Cost	\$53,623	N/A	N/A		
Contactor Capital Cost	\$6,685	N/A	N/A		
Contactor Installation	\$640	N/A	N/A		
Cost					
Labor to Install/Re-Install	\$480	\$480	N/A		
Media in Contactor					
Shipping Cost	\$201	N/A	N/A		
Regeneration Cost	N/A	\$1,088	N/A		
Labor to Remove Media	N/A	\$480	\$480		
from Contactor					
Removal Cost via	N/A	N/A	N/A		
Vacuum Truck					
Disposal Cost	N/A	N/A	\$188		
Annual Cost (Separate)	\$61,215/year	\$2,047/year	\$668/year		
Total Cost (Separate)	\$61,215	\$28,661	\$668		
Total Cost (Together)	\$90,554 for 15 years				
Annual Cost	\$6,036/year				
Annual Cost Per Acre	\$405/acre/year				
(14.9 acres)					

- Assume that year 14 is the last time the media is regenerated, and there is no regeneration after year 15, just the cost of labor to remove the media and disposal costs
- Assume that the farmer can transport the PO4Sponge to the disposal site without the use of a vacuum truck

Table 19: Rough cost estimates for scenario C over a 15-year period

	Year 0	Year 1 to 14	Year 15
Media Shipping & Capital	\$1,130	\$1,130	N/A
Cost			
Contactor Capital Cost	\$10,869	N/A	N/A
Contactor Installation	\$640	N/A	N/A
Cost			
Labor to Install/Re-Install	\$480	\$480	N/A
Media in Contactor			
Regeneration Cost	N/A	N/A	N/A

Table 19 (cont'd)

Labor to Remove Media	N/A	\$480	\$480	
from Contactor				
Removal Cost via	N/A	\$1,909	\$1,909	
Vacuum Truck				
Disposal Cost	N/A	\$556	\$556	
Annual Cost (Separate)	\$13,119/year	\$4,529/year	\$2,922 /year	
Total Cost (Separate)	\$13,119	\$63,406	\$2,922	
Total Cost (Together)	\$79,078 for 15 years			
Annual Cost	\$5,272/year			
Annual Cost Per Acre	\$354/acre/year			
(14.9 acres)				

 Assume that no new SFS media is purchased at the start of year 15, there are only removal and disposal costs

From Table 17, Table 18, and Table 19, the SFS was the most cost-effective option. Table 20 shows the percent difference in the annual cost per acre between scenarios A, B, and C. The percent difference in annual cost per acre between scenario B and C was 14%, making scenario B the next most cost-effective option. Scenario A is 67% more expensive as scenario C, and 55% more expensive as scenario B. If the PO4Sponge is regenerated on site it about half as expensive as the PO4Sponge regenerated by the manufacturer due to less shipping costs. All cost calculations and assumptions for those calculations are in Appendix D.2.

Table 20: Calculated percent difference in the annual cost per acre for scenarios A, B, and C

Scenario	A	В	C
Annual Cost Per Acre	\$714	\$405	\$354
Percent Difference Compared to Scenario A	N/A	55%	67%
Percent Difference Compared to Scenario B	55%	N/A	14%
Percent Difference Compared to Scenario C	67%	14%	N/A

In addition to the above analysis, the annual cost per acre for scenarios A, B, and C were compared to the annual revenue per acre of rotational field corn. For a high productivity soil producing 211 bushels/acre at a harvest price of \$3.80/bushel, the expected revenue per acre for

rotational corn is \$359 [131]. For average and low productivity soils producing 176 and 141 bushels/acre, respectively, the expected revenue per acre for rotational corn is \$246 and \$155 per acre, respectively [131]. Based on these expected revenues per acre, none of scenarios in this case study have an associated cost that allows the farmer to implement this technology with a sizeable revenue afterwards. The next section further analyzes if the annual media cost per acre changes with changing treatment requirements.

5.4.4. Further Analysis on Media Feasibility

In addition to the case study performed on "Site BN" to treat 1.66 kg of SRP lost in the tile drains, an Excel spreadsheet called "Media_Feasibility_Study_Extension_V2.xlsx" utilized the calculations in Appendix D.2. to calculate the change in total annual cost per acre depending in response to the change in mass of SRP requiring treatment. The mass of SRP requiring treatment ranged from 0.5 kg to 5 kg of SRP, and the results are shown in Table 21 and Figure 25.

Table 21: Results from the calculations comparing total annual cost to the mass of SRP requiring treatment

	Total Annual Cost (\$)		
Mass of SRP Requiring Treatment (kg)	Scenario A	Scenario B	Scenario C
0.50	\$298	\$189	\$224
1.00	\$477	\$282	\$257
1.50	\$656	\$375	\$343
1.66	\$714	\$405	\$354
2.00	\$835	\$468	\$376
2.50	\$1,014	\$561	\$409
3.00	\$1,193	\$654	\$495
3.50	\$1,372	\$747	\$528
4.00	\$1,551	\$840	\$614
4.50	\$1,730	\$933	\$647
5.00	\$1,909	\$1,026	\$681

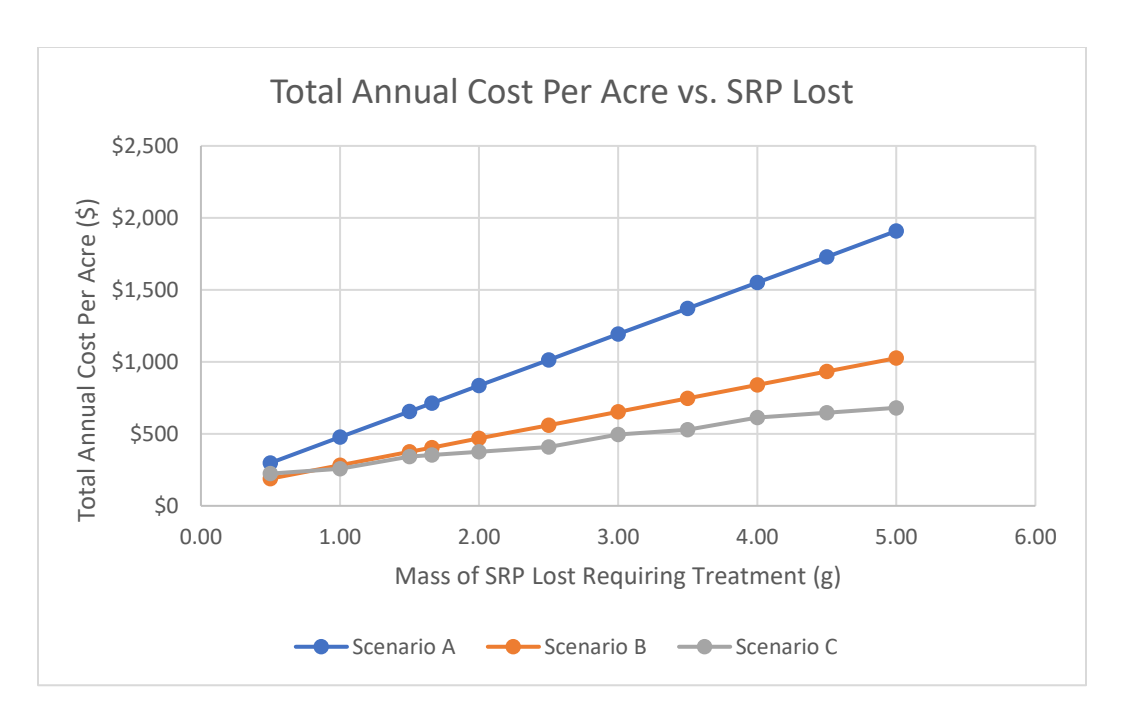


Figure 25: Graphical representation of Table 21

For all three scenarios, the total annual cost of the media increased when the amount of SRP requiring treatment was also increased. The slope of the line represents the change in total annual cost as the amount of SRP requiring treatment increases. Scenario A, the PO4Sponge with regeneration by the manufacturer, had the steepest slope (trendline: y=357.97x+119.15), scenario B, the PO4Sponge with on-site regeneration, had a less-steep slope (trendline: y=185.99x+96.051), and scenario C, the SFS with removal and no regeneration, had the least steep slope (trendline: y=105.39x+168.63).

From these results, both visually and numerically, scenario A is the most expensive option due to the highest increase in cost per increase in mass SRP treated. This is due to the cost of three shipping events where the PO4Sponge media went back and forth between the farm (assumed as "Site BN") and the manufacturer, MetaMateria. Scenario B was less expensive than scenario A since the regeneration was assumed to be less expensive to conduct on-site and there were fewer associated shipping costs since the regeneration took place on-site.

When the treatment requirements were 0.50 kg, scenario B was \$35/acre cheaper than scenario C. However, once the amount of SRP requiring treatment was 1.00 kg or more, scenario B was more expensive than scenario C. In conclusion, scenario C, the SFS with removal and no regeneration proved to be the most cost-effective option for farmers considering this new adsorption media technology to remove 1 kg or more SRP from subsurface drainage.

In addition to the cost of media implementation, the following factors will impact the practical application of this treatment system:

- The volume of media impacts the contactor size and cost. The size matters because it may take up a large area of profitable cropland depending on placement.
- The installation of the contactor needs to occur outside the growing season to minimize loss of crop/profit. However, the soil cannot be too wet to allow equipment to drive across the field and dig to install the contactor.
- The location of the contactor needs to be accessible and minimize disturbance to the cropland when media is installed/removed for replacement, maintenance, or regeneration

Chapter 6: Conclusions and Future Research

The goal of this research was to determine the media option best suited for removing and managing P in agricultural subsurface drainage. The SFS was the most cost-effective option based on a case-study and additional analysis. The most expensive option was the use of PO4Sponge media to remove P, then regenerating it at the manufacturer. This was due to the cost of shipping required to transport the media to and from the site for regeneration. The second most expensive option was the use of PO4Sponge media to remove P, then regenerating the media on-site because there were fewer associated shipping costs.

Although the SFS was the most cost-effective option to treat subsurface drainage, a recent field study by Penn et al. (2020) concluded that the calcium carbonate production caused the slag to underperform in the field study in comparison to the laboratory studies [127]. This was hypothesized because the bicarbonate consumed the calcium on the slag by precipitating as calcium carbonate, causing (1) clogging of the pore space on the slag, (2) decreasing flow and pH, and (3) the prevention of calcium phosphate precipitation [127].

Penn et al. (2020) recommended the SFS to treat SP in subsurface drainage if the slag is replaced every 4 to 6 months [127]. This recommendation is aligned with the yearly media replacement assumption outlined in the economic analysis. However, the SFS media should be removed sooner rather than later to prevent the calcium carbonates from binding the slag together, making removal more difficult the longer it is left in the system. In the future, the SFS could be coated with metal oxides to reduce the impact of calcium carbonates on the media surface by making the SFS's main adsorption mechanism chemisorption instead of calcium phosphate precipitation. This could increase media longevity and removal for subsurface drainage and other applications.

The other six media options, the PO4Sponge Generation 2, FerrIXA33E, HIX(Zr)-Nano, ferrous sulfate biochar, calcium magnesium biochar, and BFS, were ruled out for the following reason:

- The PO4Sponge Generation 2 and HIX(Zr)-Nano are not yet commercialized, but both exhibited better removal than the current, commercially available options.
- The FerrIXA33E was not recommended for this application by the manufacturer due to low hydraulic conductivity.
- The ferrous sulfate biochar was effective at low EBCTs but had poor capacity.
- The calcium-magnesium and BFS had no removal.

Additionally, even if the ferrous sulfate and calcium-magnesium biochar options had better performances in the BAEs, the current availability and reliability of the media is unknown, making these media options undesirable at this time. As research continues, the pretreatment of biochar to maximize P sorption may become competitive with the other options. The production of a commercial biochar designed for P recovery was identified, "Black Owl Biochar". However, this company could not be reached and could be out of business.

Biochar as a soil amendment should be researched to see if the ferrous sulfate and calcium magnesium biochar can mitigate P in the soil before it reaches subsurface drainage. When applied as a soil amendment, biochar has the potential to aid in multiple processes that contribute to plant growth. Biochar improves the amended soil's water holding capacity, which assists in the retention of nutrients ultimately improving fertilizer efficiency [132]. Additionally, biochar has the ability to sequester carbon from the atmosphere and store it in the soil [133]. This ability increases the organic carbon in the soil, which encourages microbial activity, while also mitigating both anthropogenic atmospheric impact and climate change by sustainably fixing

carbon dioxide from the atmosphere [133]. Lastly, biochar has a longer lifetime than any other form of supplemental soil organic matter such as humic substances, which allows for continuous benefits through the extended lifetime of the biochar [134]. These benefits provide the opportunity to contribute to long-term increased crop yields and agricultural sustainability. The ability for the media to leach heavy metals into the subsurface drainage was not tested in this research but is highly encouraged for the engineered media.

If this research is desired to determine the cost of media for a different site, an independent analysis of each site-specific condition is recommended to determine costs for that set of farm-specific conditions. Additionally, more research could be conducted to examine multiple farm-specific conditions and develop a model to include (1) multiple regeneration locations across the US to mitigate shipping costs, (2) variable media costs to determine the target media price to make engineered media more cost effective than the SFS, and (3) the impact of soil texture, climate, and legacy soil P on subsurface drainage SRP concentrations.

The regeneration of various P adsorption media and its recovery as calcium phosphate, a value-added product, was not studied in BAEs or column experiments, but future work on promising adsorption media should include regeneration studies to determine if engineered, natural, and waste materials can undergo regeneration. Although the other six media were not selected for the final feasibility step of this research, this does not disqualify those media types from future research in different applications. In fact, it is encouraged to further research and develop these promising media options. Different combinations of engineered, natural, and waste adsorption media in one treatment system could also be analyzed to determine cost-effective designs.

More research is warranted on the design and implementation of P adsorption media in subsurface tile drains. An important factor to consider is that the conditions in a controlled

laboratory setting are not as predictable in terms of media capacity and the adsorption kinetics. Biological factors such as microorganisms in the subsurface drainage, weather and climate patterns, and history of land use will impact the performance of the treatment system. To implement, a field demonstration is needed to monitor flow and SRP concentrations to obtain the amount of SP leaving the drained area. Then, the volume of P adsorption media can be determined. At the subsurface tile drain outlet or other location within the tile drain, a contactor needs to be present to hold the media in place and allow water to pass through, which is important during times of peak flow. When selecting a holding vessel for the adsorption media, it is also important to consider the placement of the system so the media can be switched out to perform maintenance, regeneration, or replacement.

Additionally, research should be done on utilizing saturated engineered, natural, and waste adsorption media as a source of SRP for hydroponic systems that depend on nutrients in the bulk solution for plant root uptake [135]. Equilibrium desorption of SRP back into the bulk solution could be controlled with different media amounts. For waste media, such as the SFS that is disposed after use, this could be another method to extend the life and use of the media. Research on hydroponically treating subsurface drainage is also an option [136, 137]. Saturated adsorption media could also be mixed into the soil to observe if biological or chemical processes can desorb and utilize the adsorbed SRP to enhance soil fertility [138].

APPENDICES

APPENDIX A – Supplemental Material

A.1. Merit Labs ion analyses PDFs

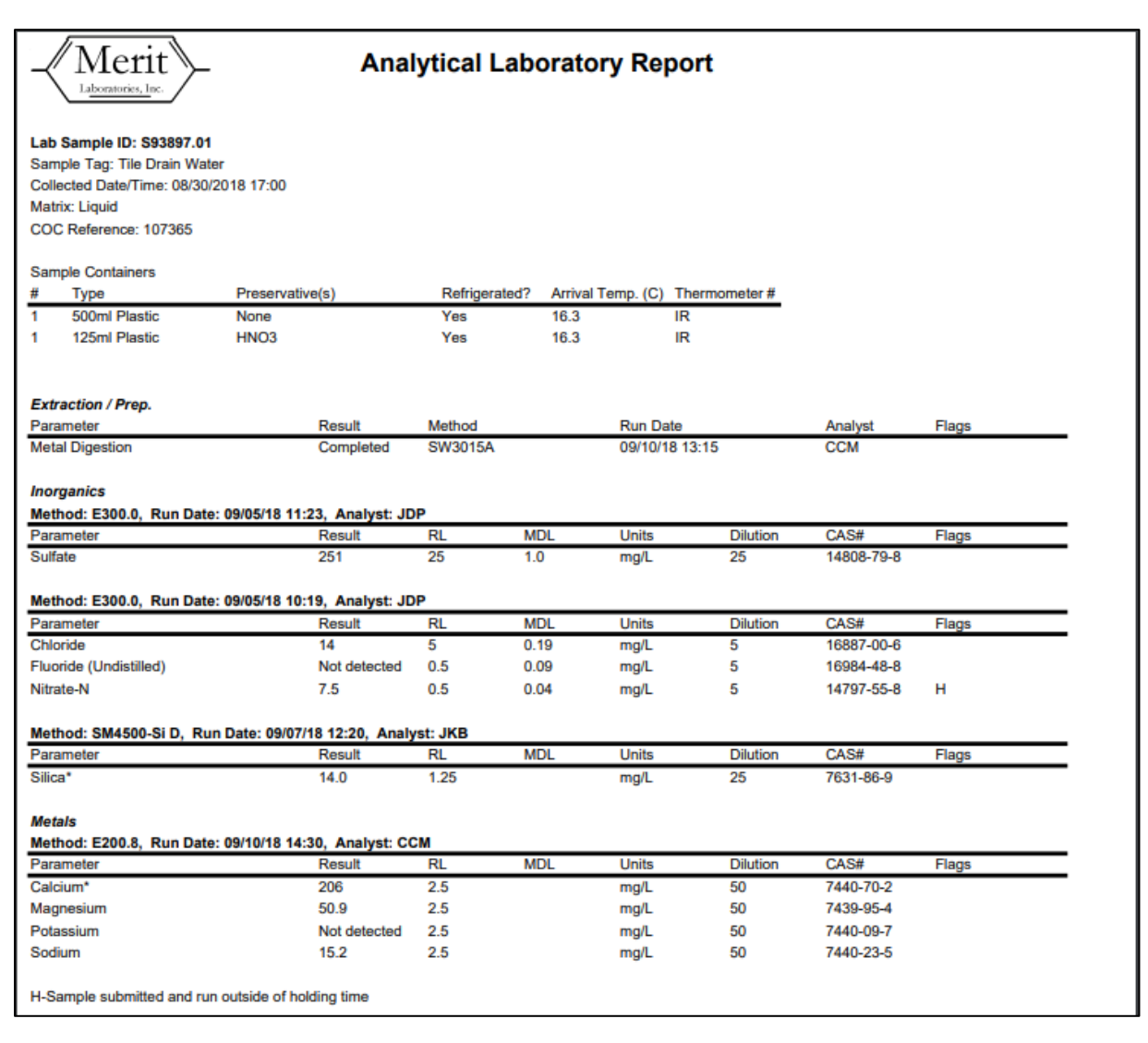


Figure 26: First set of results from the commercial laboratory ion analyses of RSD collected from "Site BN"

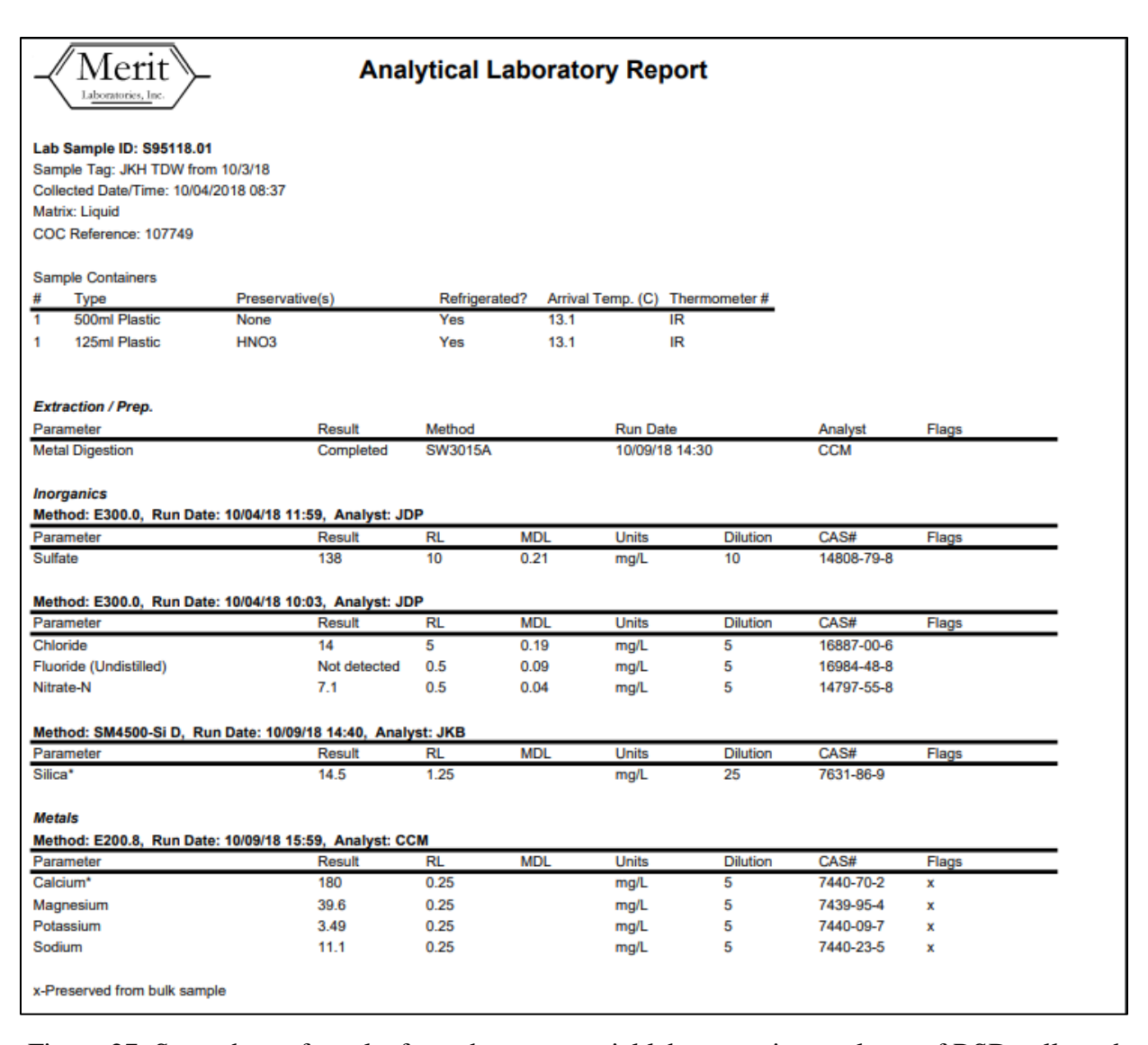


Figure 27: Second set of results from the commercial laboratory ion analyses of RSD collected from "Site BN"

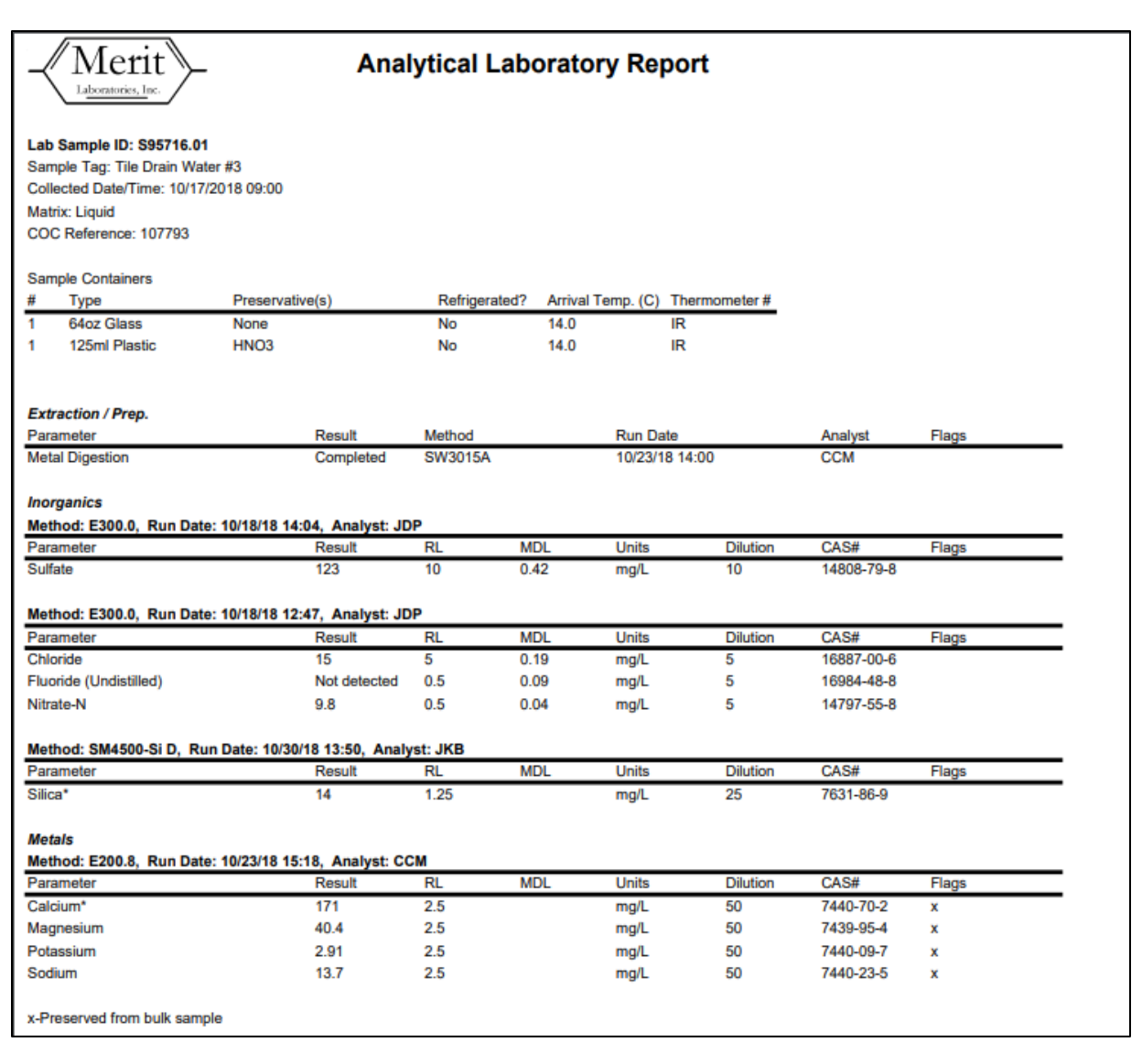


Figure 28: Third set of results from the commercial laboratory ion analyses of RSD collected from "Site BN"

A.2. Standard Operating Procedures

A.2.1. Biochar production procedure

A.2.1.1. Ferrous Sulfate Biochar

Solution Preparation

Table 22: Ferrous sulfate biochar solution preparation

Substances	Final Conc. (mol/L)	Vol. DI Water (L)	Amt. Needed (g)
FeSO4 • 7H2O	1	1	278.01

- 1. Put 1 L of DI water in graduate cylinder 1000 ml
- 2. Pure 500 ml of DI water in to 2000 ml beaker
- 3. Add 278.01 g of FeSO4 7H2O into the beaker
- 4. Mix them on the stir plate
- 5. Heat the beaker up to 64 Celsius
- 6. Measure the pH

Note: After step 1, work under fume hood

Storage: Keep container tightly closed in a dry and well-ventilated place. Recommended storage temperature 2 - 8 °C Storage class (TRGS 510): 13: Non-Combustible Solids

FERROUS SULFATE is a greenish or yellow-brown crystalline solid. Density 15.0 lb/gal. Melts at 64°C and loses the seven waters of hydration at 90°C. The primary hazard is the threat to the environment. Immediate steps should be taken to limit its spread to the environment. Used for <u>water</u> or sewage treatment, as a fertilizer ingredient.

pH 3.0 - 4.0 at 50 g/l at 25 °C (77 °F) e) Melting point/freezing point Melting point/range: 64 °C (147 °F)

Corn Stover Preparation

- 1. Collect 50g corn stover and cut into 3 cm long pieces
- 2. Dry the corn stover in an oven for 12 hours at 105 degrees C
- 3. Immerse 40 g corn stover in 1 L of ferrous sulfate solution (1 mol/L) for 2 hours at room temperature

Pyrolysis

- 1. Prepare materials for pyrolysis
 - 1. Measure 1g of corn stover into 3 small crucibles
 - 2. Place crucibles inside reactor and seal top with screws and bolts
 - 3. Place reactor inside furnace and connect top ports to gas outlet, gas inlet, and the thermometer. Secure tightly with wrench to avoid leakage
- 2. Purge reactor chamber with nitrogen gas for 1 hour at 1 mL/min, monitoring to make sure gas flow remains constant
- 3. Set initial furnace temperature to 450 deg. C and begin heating, adjusting until the reactor stabilizes at 400 deg. C
- 4. Leave in the furnace for 2 hours, recording every ten minutes the set oven temperature, actual reactor temperature, and gas flow rate
- 5. Reduce oven temperature to 25 deg. C to begin cooling, leaving the door slightly open. Once the reactor temperature reaches 200 deg. C, fully open the oven door, and use a fan to accelerate cooling. Using gloves, remove the gas outlet to clean using acetone
- 6. Remove the reactor from the oven at 40 deg. C, wearing gloves and lab coat
- 7. Rinse with DI water to remove impurities
 - 1. Get 120 mL distilled water
 - 2. Rinse top and middle/bottom biochar twice separately, using 30 mL DI water each rinse and filtering using the glass funnel and filter paper
 - 3. Once water is fully drained into the bottle, remove the filter, scrape out the biochar and place in a new container
- 8. In an oven, dry at 80 C for 2 hours, or until a fine, dry powder is achieved. (It might not take long because it will be hydrophobic) on a thin layer on a flat tray; caution, will blow away.
- 9. Seal in a container before use

A.2.1.2. Calcium-Magnesium Biochar

Solution Preparation

1. Prepare solution 5M MgCl2 • 6H2O

Table 23: Calcium-magnesium biochar MgCl₂ solution preparation

Substances	Final Conc. (mol/L)	Vol. DI Water (L)	Amt. Needed (g)
MgCl2 • 6H2O	5	1	1016.55
		0.5	508.275
		0.4	406.62

- 1.1. Put 1 L of DI water in graduated cylinder 1000 ml
- 1.2. Pour 500 ml of DI water into 2000 ml beaker
- 1.3. Add 1016.55 g of MgCl2 6H2O into the beaker
- 1.4. Mix on stir plate and add additional 500 mL of water

Note: Perform steps after 1.1 under fume hood

2. Repeat 1. to prepare 5M CaCl₂ solution

Table 24: Calcium-magnesium biochar CaCl₂ solution preparation

Substances	Final Conc. (mol/L)	Vol. DI Water (L)	Amt. Needed (g)
CaCl2	5	1	554.89
		0.5	277.445

Corn Cob Preparation

- 1. Cut kernels out of cob and cut cob into 1 cm long, 0.5 cm wide pieces
- 2. Dry corn cob in oven at 110 deg C for 24 hours
- 3. Immerse corn cob in 5 mol/L MgCl₂ solution at a solid-liquid ratio of 1g to 6 mL for 2 hours at room temperature, stirring the acid beforehand
 - a. Filter out any remaining liquid afterwards using filter paper and a glass funnel
- 4. Dry corn cob at 110 C for 24 hours

- 5. Immerse corn waste (cob) in 5 mol/L of a CaCl₂ solution at a solid-liquid ratio of 1g to 4 mL for 2 hours at room temperature
 - a. Filter out any remaining liquid afterwards using filter paper and a glass funnel
- 6. Dry corn cob in oven at 110 C for 24 hours

Pyrolysis

- 1. Prepare materials for pyrolysis
 - 1. Measure 1g of corn stover into 3 small crucibles
 - 2. Place crucibles inside reactor and seal top with screws and bolts
 - 3. Place reactor inside furnace and connect top ports to gas outlet, gas inlet, and the thermometer
- 2. Purge reactor chamber with nitrogen gas for 1 hour at 1 mL/min, monitoring to make sure gas flow remains constant
- 3. Set initial furnace temperature to 650 C and begin heating, adjusting until the reactor stabilizes at 600 C
- 4. Leave in the furnace for 3 hours, recording every ten minutes the set oven temperature, actual reactor temperature, and gas flow rate
- 5. Reduce oven temperature to 25 deg. C to begin cooling, leaving the door slightly open. Once the reactor temperature reaches 200 deg. C, fully open the oven door, and use a fan to accelerate cooling. Using gloves, remove the gas outlet to clean using acetone
- 6. Remove the reactor from the oven at 40 deg. C, wearing gloves and lab coat
- 7. Rinse with DI water to remove impurities
 - 1. Get 120 mL distilled water
 - 2. Rinse top and middle/bottom biochar twice separately, using 30 mL DI water each rinse and filtering using the glass funnel and filter paper
 - 3. Once water is fully drained into the bottle, remove the filter, scrape out the biochar and place in a new container
- 8. In an oven, dry at 80 C for 2 hours, or until a fine, dry powder is achieved. (It might not take long because it will be hydrophobic) on a thin layer on a flat tray; caution, will blow away.
- 9. Seal in a container before use

A.3. SOP for Batch Adsorption Experiments

A.3.1. Preparing the Synthetic Subsurface drainage Water

Each container used for a BAE received 1 L of SSD or RSD. To prepare the SSD, each chemical compound was mixed with 2 L of DI water, then was slowly poured back into a 5-gallon bucket. After all the compounds were mixed and added to the 5-gallon bucket, the 5-gallon bucket was placed on top of the mixing plate and stirred for 5-minutes. Next, the initial SRP concentration was tested to ensure that it was within $\pm 10\%$ of the target initial SRP concentration.

A.3.2. Preparing and Running the Batch Adsorption Experiments

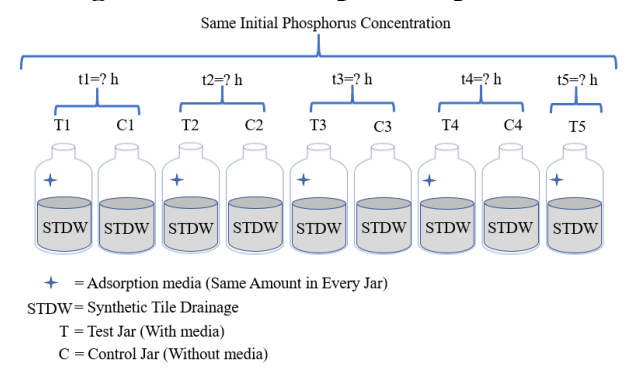


Figure 29: Diagram of a standard batch adsorption study (non-24-hour batch adsorption study)

T1	T2	Т3
C4	T5	T4
C1	C2	СЗ

Figure 30: The placement configuration for jars in a standard batch adsorption study (non-24-hour batch adsorption study)

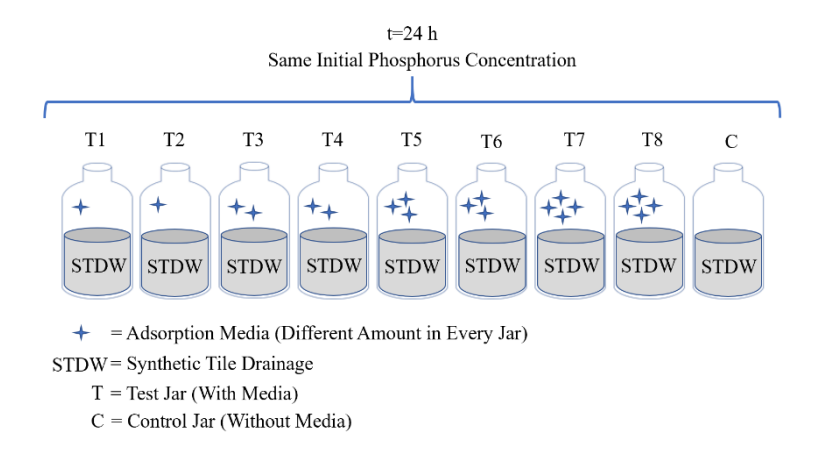


Figure 31: Diagram of the standard 24-hour batch adsorption study

T1	T2	Т3
Т8	С	T4
Т7	Т6	T5

Figure 32: The placement configuration for jars in a standard 24-hour batch adsorption study

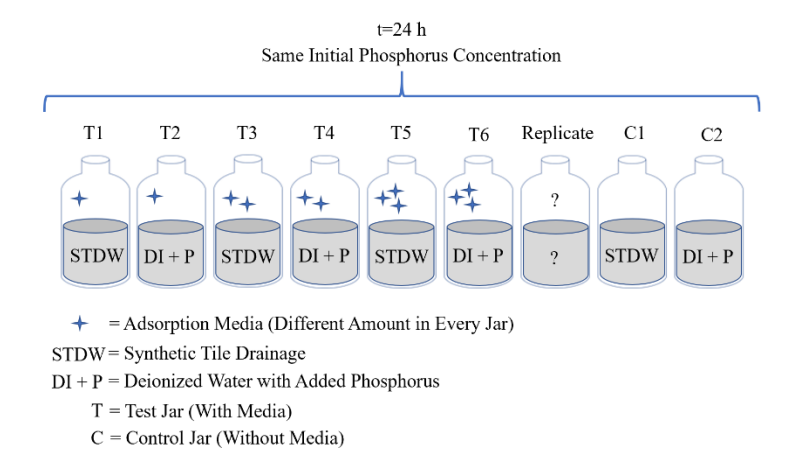


Figure 33: Diagram of a dual 24-hour batch adsorption study

T1	C1	T4
T2	R	T5
Т3	C2	Т6

Figure 34: The placement configuration for jars in a dual 24-hour batch adsorption study

Table 25: When and which jars should be taken out together based on the batch adsorption experiment type and the corresponding placement configurations

Batch Adsorption Experiment Type	Which and When Jars are taken out
Standard	T1 + C1 at t1
	T2 + C2 at $t2$
	T3 + C3 at $t3$
	T4 + C4 at t4
	T5 at t5 (or at t4 so T5 acts as a replicate as T4)
Standard 24-hour	All taken out at 24 hours
Dual 24-hour	All taken out at 24 hours

A.4. SOP for Column Experiments

The following method was conducted to empty and fill the 110-gallon tank used to hold the influent SSD for the column experiments.

If there is SSD remaining inside the 110-gallon tank, that remaining water was collected into clean 5-gallon buckets. The 5-gallon buckets were used to hold the SSD so the columns could continue pulling influent SSD while the 110-gallon tank was being refilled. The influent tubes were transferred from the 110-gallon tank to the 5-gallon bucket, and the 5-gallon bucket was refilled using leftover SSD from other 5-gallon buckets when needed. This was advantageous because the last bits of SSD could increase the water height in the 5-gallon bucket since the bottom surface area of the 5-gallon buckets was much smaller than the bottom surface area of the 110-gallon tank.

After scrubbing and rinsing the empty 110-gallon tank with tap and DI water, respectively, tap water was left to run for 10-minutes to purge any particulate matter out of the pipes, which ensures a uniform water composition. After purging, two samples of tap water, taken one minute apart, should be tested to see if there is SRP in the water. The results of the tap water test should be entered into the excel sheet to calculate the amount of each chemical compound required in

the SSD formulation. After testing the initial SRP concentration, the tap water was connected to a flowmeter by attaching one end of a tube to the outlet of the sink and letting the other end rest inside a 5-gallon bucket. Four 5-gallon buckets were kept on hand and filled first with tap water before filling the 110-gallon tank so that water could be used for mixing the chemical compounds in the SSD formulation.

Each chemical compound was mixed with 3 L of tap water using a 4 L beaker and a mixing plate set to 1100 RPM for four minutes, then was slowly poured back into the 110-gallon tank. Mixing individual chemical compounds allowed them to solubilize so they could be confidently added to the larger mixture without worry that the chemicals were not completely solubilized and settled at the bottom of the 110-gallon tank. The chemical compounds that were the most difficult to mix were magnesium sulfate and calcium sulfate because they turned the water an opaque milky white color if too much of the chemical was added into the mixing water, this is shown in Figure 35.



Figure 35: Mixing the magnesium sulfate and calcium sulfate chemical compounds turned the water a milky white color

After the four 5-gallon buckets were filled with tap water, the tube attached to the flowmeter that was not connected to the sink was placed inside a PVC pipe resting against the inner wall of the

110-gallon tank and secured to that PVC pipe using zip ties. The purpose of the PVC pipe was to ensure all the water made it into the tank.

The flowmeter was set to units of gallons per minute (GPM) and this value was, on average, about 2 GPM, which required the tap water to be turned on for 55-minutes. A timer was usually set for 45-minutes to signal someone to watch the reading on the flowmeter until a total of 100 gallons went from the sink thought the flowmeter and into the 110-tank or buckets. The amount of water in the separated buckets and the tank equated to 100 gallons.

A plastic sheet covered the top of the 110-gallon tank once it was filled to keep contaminants out of the water. Two SunSun JVP-201 1585 GPH Wavemaker Powerhead Dual Aquarium Circulation Pumps were used to mix the water in the tank while the tank was filled

After the SSD was formulated, two samples were taken and the SRP concentration was measured to ensure that it was within $\pm 10\%$ of the target concentration. After the initial concentration testing, the inlet tubes for the columns were transferred back into the 110-gallon tank and the 5-gallon buckets were washed with soap and DI water. If there were 5-gallon buckets containing the leftover SSD, they were labeled with the date and initial concentration of that SSD. The leftover SSD was kept on hand in case there was a need for additional SSD while filling the tank. For example, if the water level in the 110-gallon tank was running low, the remaining water was collected into 5-gallon buckets in case there was not enough time to make additional SSD. However, the addition of water from different batches could result in inconsistent/non-target levels of SP, and this method should only be used as a last resort.

A.5. Regeneration Information for the PO4Sponge

All information is from reference [139]

Regeneration is a chemical method to remove adsorbed SP ions off the media. A mild sodium hydroxide solution (1M NaOH) removes SP off the PO4Sponge. Calcium chloride (CaCl₂) is then added to the NaOH and SP solution, this precipitates SP out as calcium phosphate. This process is repeated six to seven times to achieve over 99% SP removal from the PO4Sponge. MetaMateria describes the resulting calcium phosphate powder as a high purity product suitable for food manufacturing or other non-fertilizer products. After regeneration, the PO4Sponge can be reused for the same or other applications.

The PO4Sponge absorbs competing ions in addition to P. These competing ions may not precipitate off the media during regeneration, resulting in a decreased media capacity.

MetaMateria states that the PO4Sponge can be regenerated 15 to 20 times for most applications.

Regeneration can either be done on-site or by MetaMateria.

APPENDIX B – Batch adsorption experiments

B.1. Additional Note on Methods used in Batch adsorption experiments

In earlier methods, 2 L of synthetic subsurface drainage was used, but there was concern over the amount of headspace in the tops of the jars (about 1 inch). If the subsurface drainage was unable to mix via horizontal shaking to easily distribute the ions in the subsurface drainage around the entire container, there was a concern for stratification of P in the jar. Stratification in this context refers to the P removal mainly in the bottom portion near where the media sunk down and not in other areas towards the top of the jar.

Switching to 1 L of subsurface drainage also reduced the amount of subsurface drainage needed for each experiment overall, conserving the real subsurface drainage or reducing the chemicals and time required to make the synthetic subsurface drainage. There was no major observed change between the two methods, but the 1 L of subsurface drainage per jar is the recommended amount to use for these batch adsorption experiments.

B.2. Batch Adsorption Study Media Comparison Tables

B.2.1. Engineered Media: PO4Sponge Generation 1, PO4Sponge Generation 2, FerrIXA33E, and HIX(Zr)-Nano

					Total Phosphor	us							
M = 4 = 4 == = = = (=)	PO4Sponge G1				PO4Sponge G2			FerrIXA33		HIX(Zr)	-Nano		
Media Amount (g)	Time (hr)	Initial Conc. (mg/L)	Removal (%)	Time (hr)	Initial Conc. (mg/L)	Removal (%)	Time (hr)	Initial Conc. (m	g/L) Removal	%) Time (hr	Initial Conc.	(mg/L)	Removal (%)
0.01													
0.015													
0.0182													
0.06													
0.1													
0.133													
0.15													
0.2													
0.25													
0.3													
0.3571													
0.45													
0.5													
0.6													
0.75													
1													

Figure 36: There was no recorded data for total phosphorus during the batch adsorption experiments for PO4Sponge generation 1, PO4Sponge generation 2, FerrIXA33E, and HIX(Zr)-Nano

					Soluble Phospho	rus						
Media Amount (g)	PO4Sponge G1			PO4Sponge G2			FerrIXA33E				HIX(Zr)-Nano	
	Time (hr)	Initial Conc. (mg/L)	Removal (%)	Time (hr)	Initial Conc. (mg/L)	Removal (%)		Initial Conc. (mg/L)		Time (hr)	Initial Conc. (mg/L)	Removal (%)
0.01							24	0.296	5%			
0.015												
0.0182												
0.06												
0.1	24	0.193	36%	24	0.215	53%	24	0.296	37%	24	0.199	74%
	24	0.199	40%							24	0.22	51%
0.133												
0.15												
0.13												
0.2												
0.25												
	24	0.193	69%	24	0.215	87%				24	0.199	86%
	24	0.199	68%							24	0.22	76%
0.3												
0.5												
0.3571												
0.45												
0.5	24	0.193	85%	24	0.215	87%	24	0.296	81%	24	0.199	86%
0.5	24	0.199	86%							24	0.22	84%
0.6												
0.75	24	0.193	85%							24	0.199	87%
1							24	0.296	92%			

Figure 37: Soluble phosphorus data recorded during the batch adsorption experiments for PO4Sponge generation 1, PO4Sponge generation 2, FerrIXA33E, and HIX(Zr)-Nano

					Soluble Reactive Pho	sphorus							
M - di - A (-)		PO4Sponge G1			PO4Sponge G2			FerrIXA33E			HIX(Zr)-Nano		
Media Amount (g)	Time (hr)	Initial Conc. (mg/L	Removal (%)	Time (hr)	Initial Conc. (mg/L)	Removal (%)	Time (hr)	Initial Conc. (mg/L)	Removal (%)	Time (hr)	Initial Conc. (mg/L) Removal (%)	
0.01							24	0.296	3%				
0.015													
0.0182													
0.06													
0.1	24	0.191	37%	24	0.22	51%	24	0.296	36%	24	0.195	87%	
0.1	24	0.196	38%							24	0.215	53%	
0.133													
0.15													
0.13													
0.2													
0.25													
0.3	24	0.191	68%	24	0.22	85%				24	0.195	87%	
0.3	24	0.196	67%							24	0.215	80%	
0.3571													
0.45													
0.5	24	0.191	84%	24	0.22	85%	24	0.296	82%	24	0.195	87%	
0.5	24	0.196	84%							24	0.215	88%	
0.6													
0.75	24	0.191	84%							24	0.195	88%	
1							24	0.296	92%				

Figure 38: Soluble reactive phosphorus data recorded during the batch adsorption experiments for PO4Sponge generation 1, PO4Sponge generation 2, FerrIXA33E, and HIX(Zr)-Nano

B.2.2. Non-Engineered Media: Ferrous Sulfate Biochar, Calcium-Magnesium Biochar, Blast Furnace Slag, and Steel Furnace Slag

					Total Phosphor	us								
H-di- A	FeSO4 Biochar				Ca-Mg Biochar			BFS				SFS	5	
Media Amount (g)	Time (hr)	Initial Conc. (mg/L)	Removal (%)	Time (hr)	Initial Conc. (mg/L)	Removal (%)	Time (hr)	Initial Conc. (mg/L)	Removal (%)	Time (hr)	Initial Conc.	(mg/L)	Removal (%)
0.01														
	1	0.281	1%	1	0.263	-3%								
0.015	2	0.281	6%	2	0.263	-3%								
0.015	3	0.281	8%	3	0.263	2%								
	24	0.281	9%											
				6.33	0.274	4%								
0.0182				10.33	0.274	-5%								
				14	0.274	3%								
0.06														
0.1														
	1.17	0.230	-5%											
0.133	2.17	0.230	-6%											
	22	0.230	4%											
	23	0.230	3%											
0.15														
0.2														
0.25														
0.3														
0.3571														
0.45														
0.5														
0.6														
0.75														
1														

Figure 39: Total phosphorus data recorded during the batch adsorption experiments for the ferrous sulfate biochar, calcium-magnesium biochar, blast furnace slag, and steel furnace slag

	 -				Soluble Phospho	rus		ş				
Media Amount (g)		FeSO4 Biochar			Ca-Mg Biochar		BFS				SFS	
media Amount (g)	Time (hr)	Initial Conc. (mg/L)	Removal (%)	Time (hr)	Initial Conc. (mg/L)	Removal (%)	Time (hr)	Initial Conc. (mg/L)	Removal (%)	Time (hr)	Initial Conc. (mg/L) Removal (%
0.01												
0.015												
0.0182												
0.06	24	0.519	18%									
0.1	24	0.993	7%	24	0.21	0%	24	0.227	0%			
0.1	24	0.519	40%				24	0.228	1%			
0.133			_									
	2	0.493	24%									
0.15	4	0.493	23%									
0.13	6	0.493	24%									
	24	0.493	28%									
0.2							24	0.227	1%			
0.25	24	0.993	24%									
				24	0.21	8%	24	0.228	2%	24	0.261	7%
										1	0.552	0%
0.3										3	0.552	1%
0.5										19	0.552	-4%
										22	0.552	4%
										25	0.552	7%
0.3571							24	0.227	2%			
0.45										24	0.261	7%
0.5				24	0.21	18%	24	0.227	3%			
0.5							24	0.228	1%			
										1	0.242	-1%
										3	0.242	5%
0.6										20	0.242	18%
										25	0.242	
										24	0.261	12%
0.75	24	0.993	64%	24	0.21	37%	24	0.228	4%			
0.73												
1										24	0.261	28%

Figure 40: Soluble phosphorus data recorded during the batch adsorption experiments for the ferrous sulfate biochar, calcium-magnesium biochar, blast furnace slag, and steel furnace slag

					Soluble Reactive Pho	sphorus						
11 - di - 1 (-)		FeSO4 Biochar			Ca-Mg Biochar			BFS			SFS	
Media Amount (g)	Time (hr)	Initial Conc. (mg/L)	Removal (%)	Time (hr)	Initial Conc. (mg/L)	Removal (%)	Time (hr)	Initial Conc. (mg/L)	Removal (%)	Time (hr)	Initial Conc. (m	g/L) Removal (%)
0.01												
0.015												
0.0182												
0.06	24	0.523	19%									
0.1	24	1.01	6%	24	0.208	-1%	24	0.220	-2%			
0.1	24	0.523	40%				24	0.223	0%			
0.133												
	2	0.494	21%									
0.15	4	0.494	23%									
0.13	6	0.494	26%									
	24	0.494	28%									
0.2							24	0.220	-1%			
0.25	24	1.01	24%									
0.3				24	0.208	6%	24	0.223	-2%			
0.3571							24	0.220	2%			
0.45												
0.5				24	0.208	17%	24	0.220	3%			
0.5							24	0.223	-1%			
0.6												
0.75	24	1.01	68%	24	0.208	36%	24	0.223	3%			
1												

Figure 41: Soluble reactive phosphorus data recorded during the batch adsorption experiments for the ferrous sulfate biochar, calcium-magnesium biochar, blast furnace slag, and steel furnace slag

APPENDIX C – Column experiments

C.1. Additional Note on Methods used in Column experiments

There was a method that utilized two 5-gallon buckets, two for each column to hold and capture the influent and effluent feeds, respectively, during days 0 to 46 of column study phase 1a. There was no concern over the data quality changing when the 110-gallon tank method was implemented. The change from the 5-gallon buckets to the 110-gallon tank on day 47 was advantageous in because it decreased the amount of manual labor required to fill and empty the buckets. The 5-gallon buckets had to be attended to every day, where the 110-gallon tank could be left alone, except for refilling the tank, for over a day. Each 5-gallon bucket required an individual supply of SSD to fill the influent bucket and required the emptying of the effluent bucket into the sink to prevent overflows. The switch to the 110-gallon tank method also ensured that each column was receiving the same influent feed made at the same time, so less testing was needed to test the influent feed of a single tank versus five 5-gallon buckets.

Figure 42 shows the original 5-gallon bucket method, and Figure 43 shows the improved 110-gallon tank method.



Figure 42: The original 5-gallon bucket method used for column experiments



Figure 43: The improved 110-gallon tank method used for column experiments

C.2. Column Study Influent and Effluent Graphs

Table 26: Summary of column phases and influent conditions for each column

Phase and Duration	Column	Feed Type	Average l	Influent ation (mg/L)	EBCT (min.)
	PO4Sponge Monolith	SSD	TP SRP	0.242	30
	Mononun			N/A	
	DO 45	RSD (day 0-70)	TP	0.224	20
	PO4Sponge Granular (a)	-	SRP	N/A	30
l 1a	Granulai (a)	SSD (day 71-124)	TP SRP	0.253 N/A	
(124 days)	Control (no	-	TP	0.237	30
(12+ days)	Control (no media)	SSD	SRP	0.237 N/A	30
			TP	0.276	30
	PO4Sponge Granular (b)	SSD	SRP	0.276 N/A	30
	Granulai (b)		TP	0.252	
	FerrIXA33E	SSD	SRP	N/A	30
	DO4Crana		TP		
	PO4Sponge Monolith	SSD	SRP	0.648	30
	PO4Sponge		TP	0.620	
	Granular (a)	SSD	SRP	0.495	60
1b	Control (no	aab	TP	0.550	60
(34 days)	media)	SSD	SRP	0.570	60
-	PO4Sponge	SSD	TP	0.626	60
	Granular (b)	22D	SRP	0.540	60
	FerrIXA33E	SSD	TP	0.614	60
	FeIIIAASSE	33D	SRP	0.582	00
	PO4Sponge	RSD	TP	0.156	60
	Monolith	KSD	SRP	0.118	60
	PO4Sponge	RSD	TP	0.259	60
	Granular (a)	KSD	SRP	0.193	00
1c	Control (no	RSD	TP	0.243	60
(7 days)	media)	KSD	SRP	0.176	00
	PO4Sponge	RSD	TP	0.266	60
	Granular (b)	KDD	SRP	0.210	00
	FerrIXA33E	RSD	TP	0.211	60
	TOTTAMOSE	IND	SRP	0.178	30

Table 26 (cont'd)

	PO4Sponge Monolith	SSD	TP SRP	1.24 0.924	60
	PO4Sponge Granular (a)	SSD	TP SRP	1.03 0.792	- 60
1d (6 days)	Control (no media)	ontrol (no		1.19 0.814	- 60
	PO4Sponge Granular (b)	SSD	TP SRP	1.12 0.880	- 60
	FerrIXA33E	SSD	TP SRP	1.07 0.83	- 60
2a	PO4Sponge Granular	SSD	TP SRP	0.997 0.508	5
(9 days)	Steel Furnace Slag	SSD	TP SRP	0.979 0.390	- 5
2b	PO4Sponge Granular	SSD	TP SRP	0.881 0.548	10
(5 days)	Steel Furnace Slag	SSD	TP SRP	0.873 0.551	- 10
2c	PO4Sponge Granular	SSD	TP SRP	0.615 0.444	- 20
(8 days)	Steel Furnace Slag	SSD	TP SRP	1.16 0.446	- 20
2d	PO4Sponge Granular	SSD	TP SRP	1.72 1.23	20
(19 days)	Steel Furnace Slag	SSD	TP SRP	1.89 1.20	- 20
2e	PO4Sponge Granular	SSD	TP SRP	N/A 1.45	- 60
(4 days)	Steel Furnace Slag	SSD	TP SRP	N/A 1.37	60
3	PO4Sponge Granular	SSD	TP SRP	0.786 0.473	5
(10 days)	Steel Furnace Slag	SSD	TP	0.887	5

C.2.1. Column experiments – Phase 1a (Total Phosphorus – No Soluble Reactive Phosphorus)

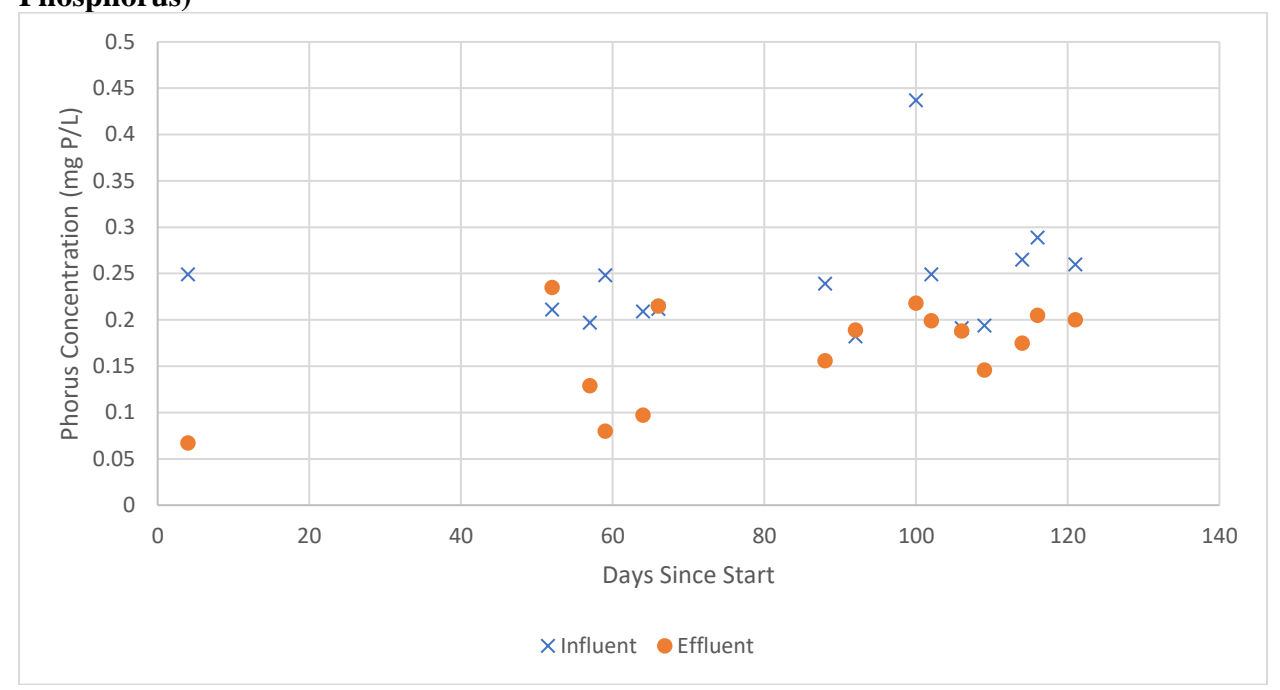


Figure 44: Phase 1a column with the PO4Sponge monolith media receiving SSD

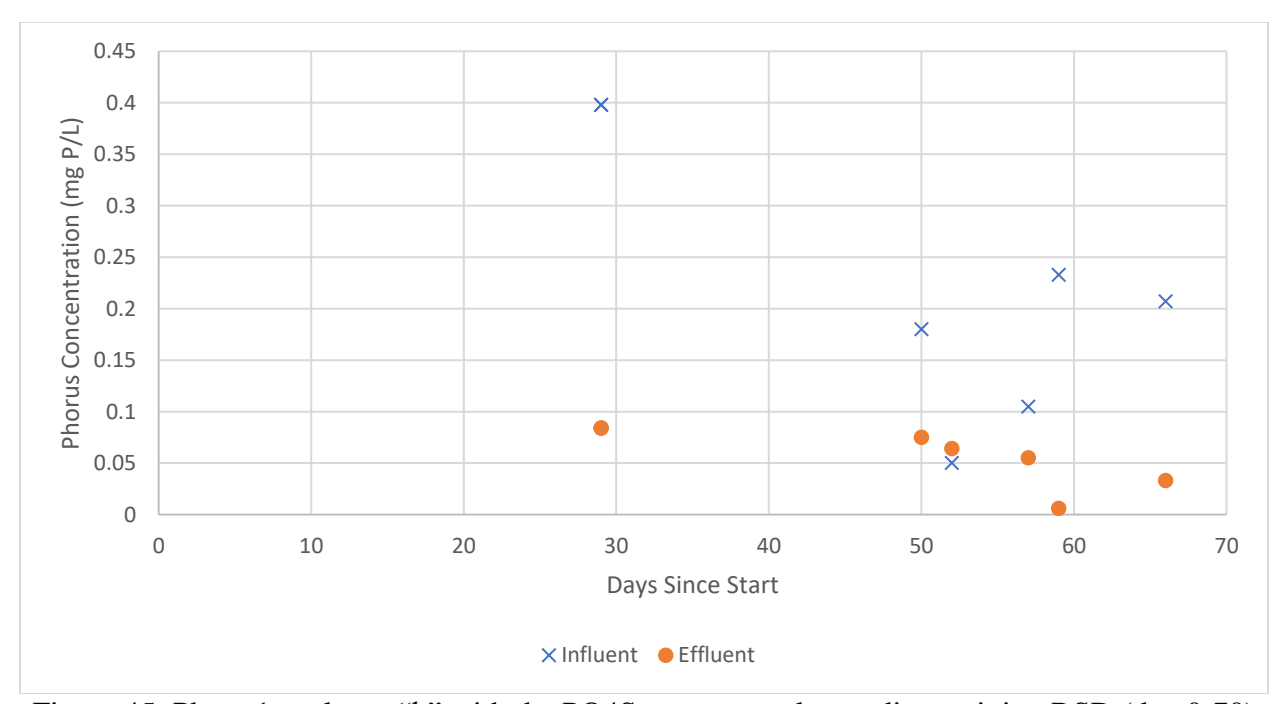


Figure 45: Phase 1a column "b" with the PO4Sponge granular media receiving RSD (day 0-70)

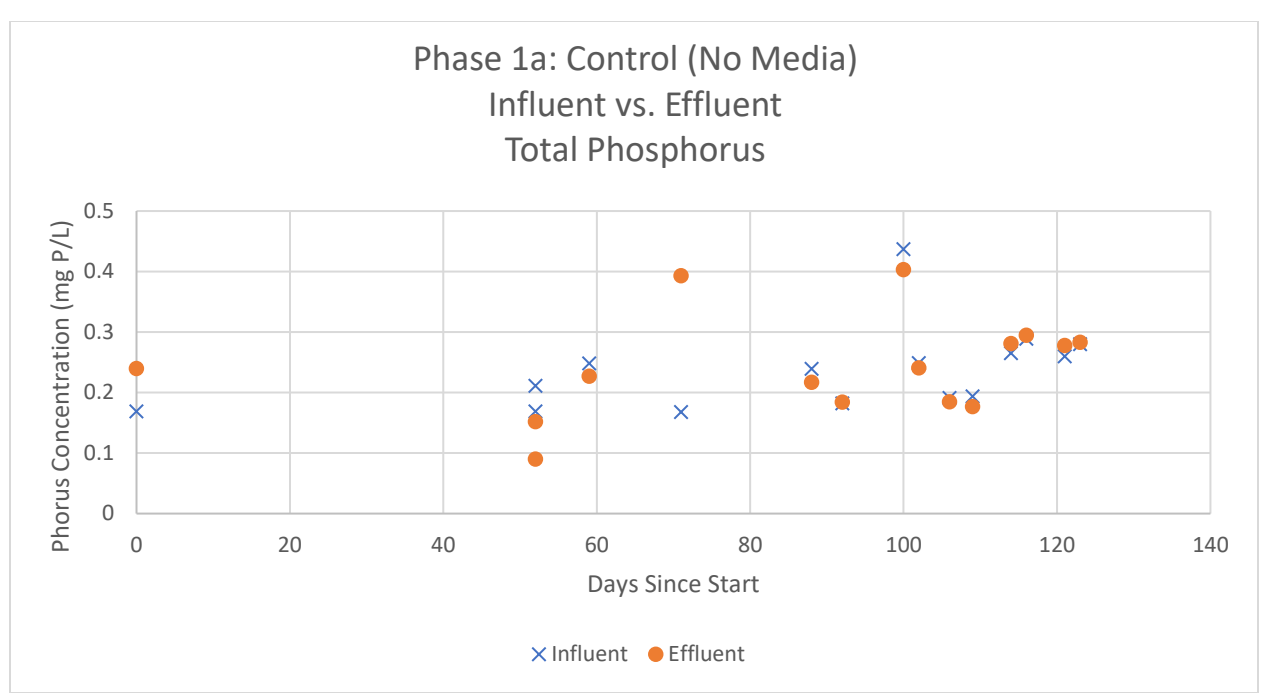


Figure 46: Phase 1a control column with no media receiving SSD

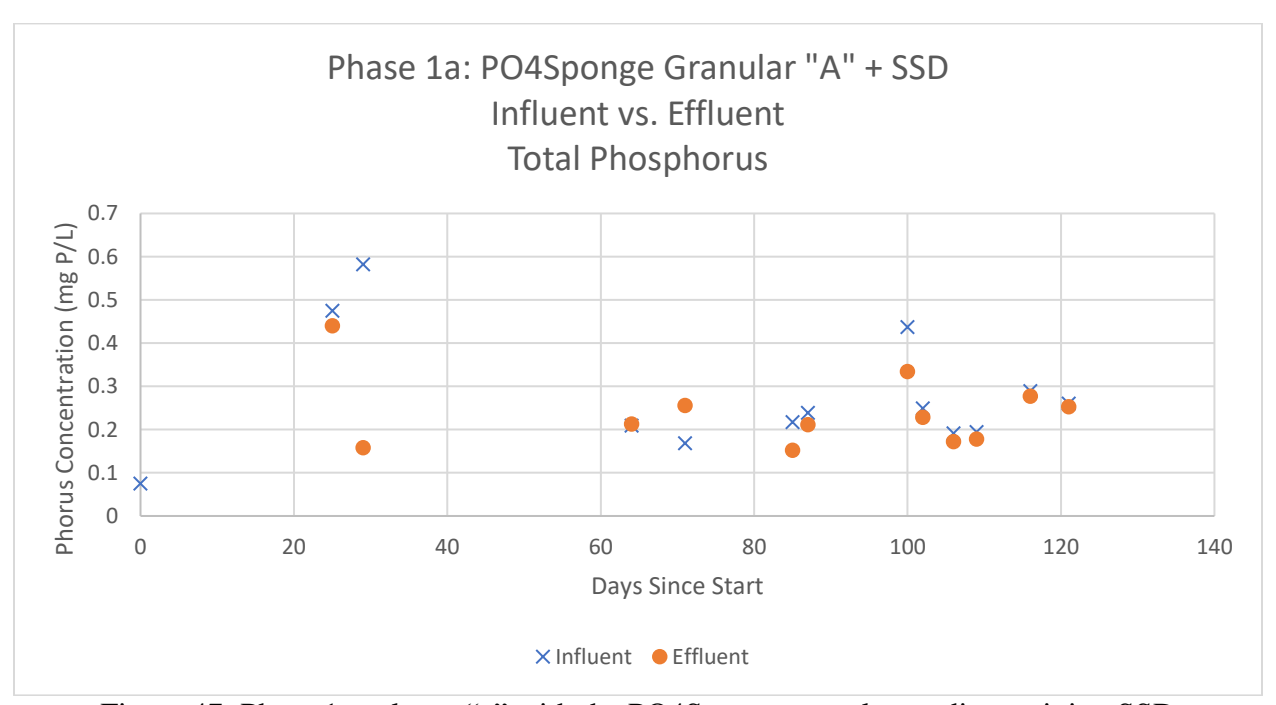


Figure 47: Phase 1a column "a" with the PO4Sponge granular media receiving SSD

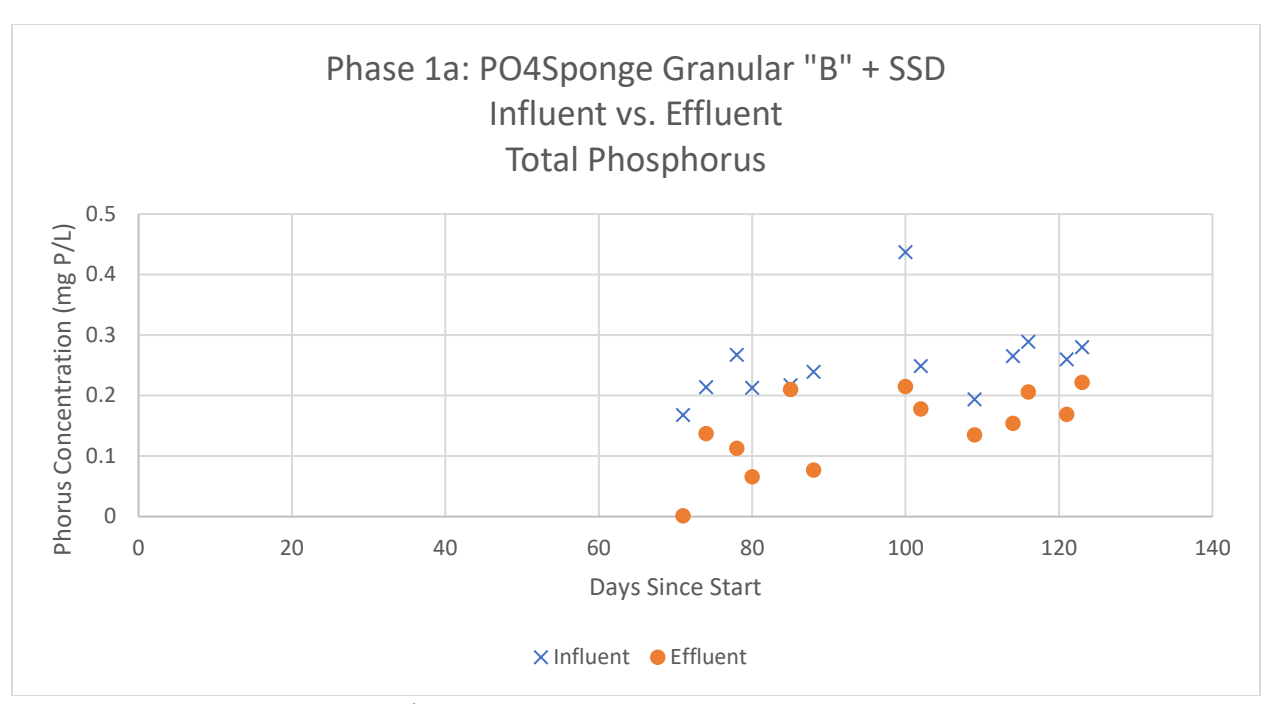


Figure 48: Phase 1a column "b" with the PO4Sponge granular media receiving SSD instead of RSD (day 71-124)

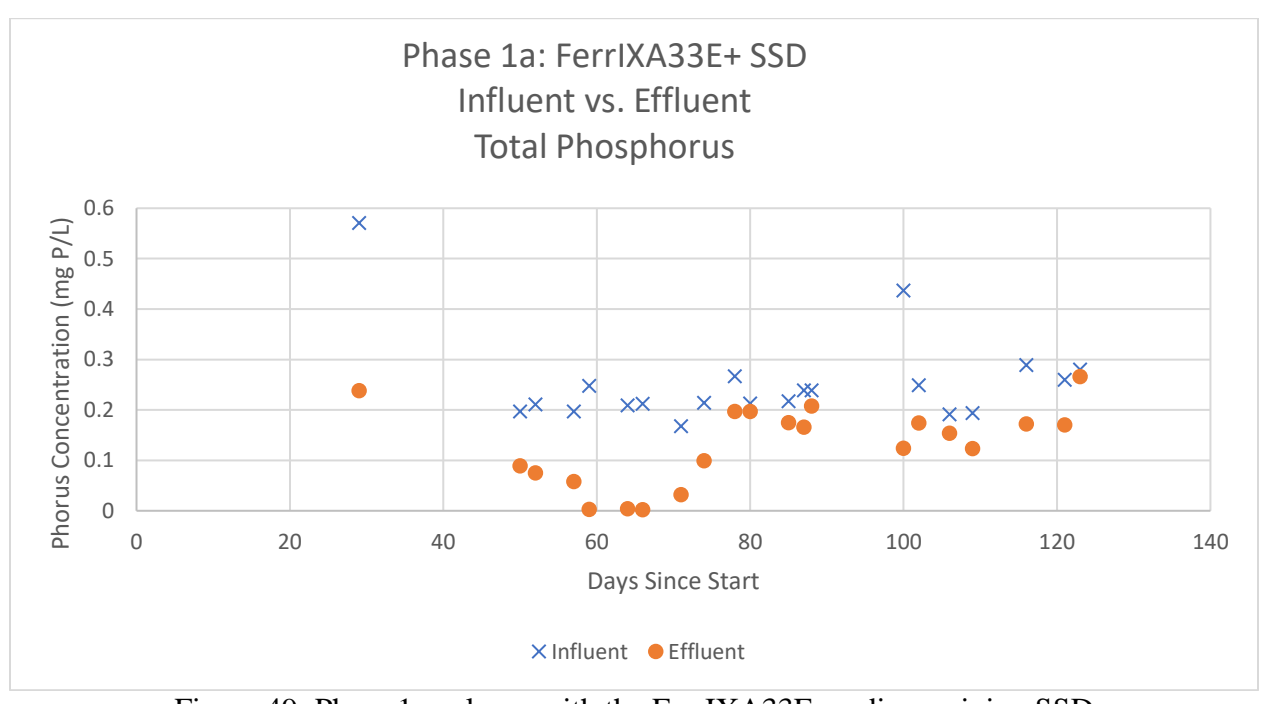


Figure 49: Phase 1a column with the FerrIXA33E media receiving SSD

C.2.2. Column experiments – Phase 1b (Total Phosphorus)

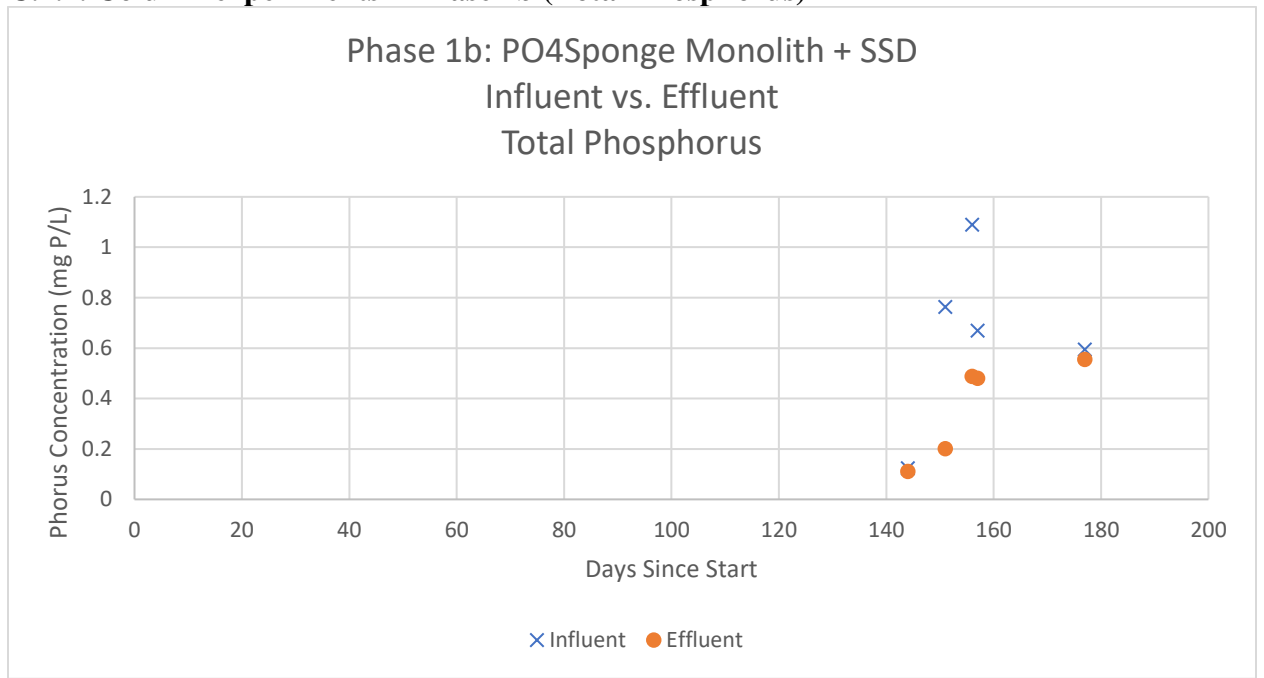


Figure 50: Phase 1b column with the PO4Sponge monolith media receiving SSD

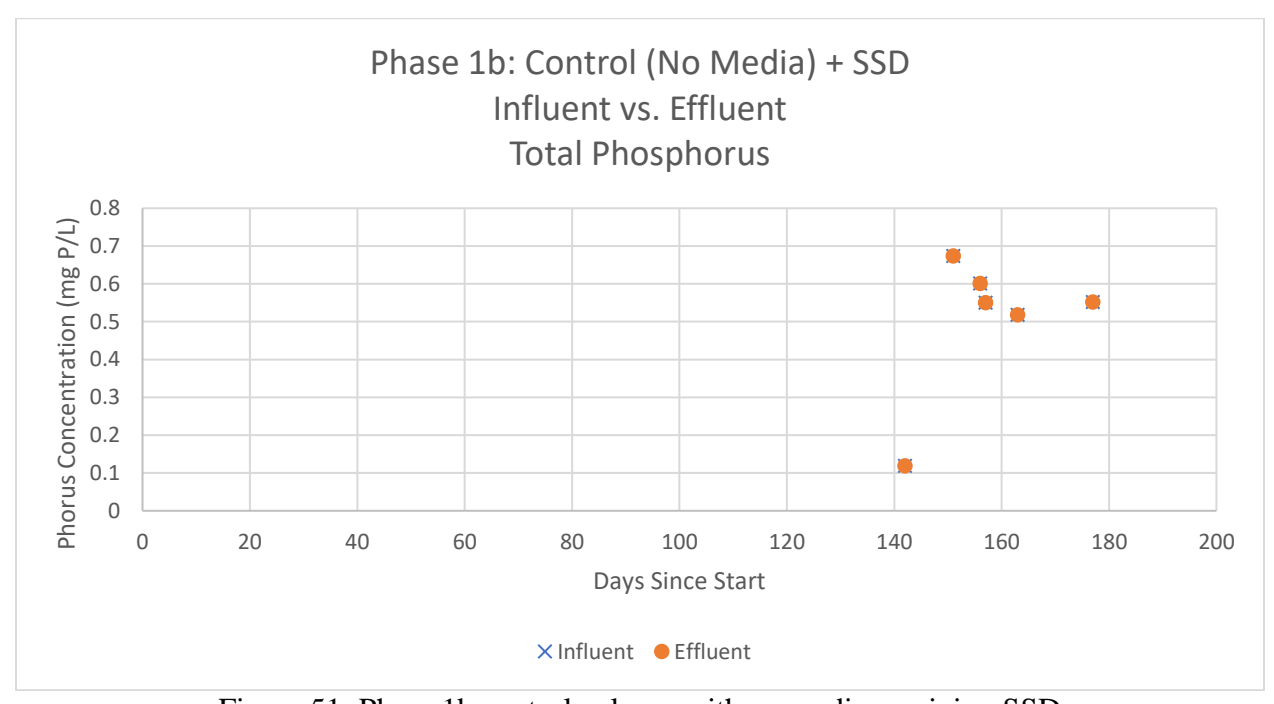


Figure 51: Phase 1b control column with no media receiving SSD

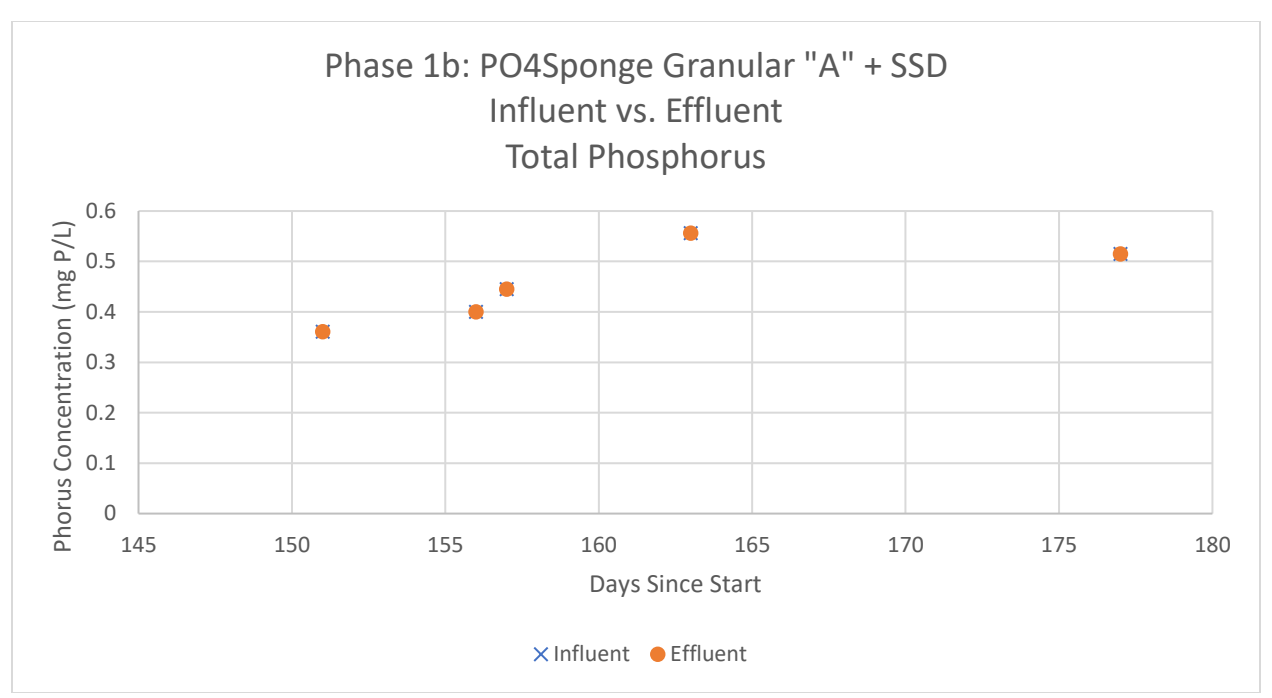


Figure 52: Phase 1b column "a" with the PO4Sponge granular media receiving SSD

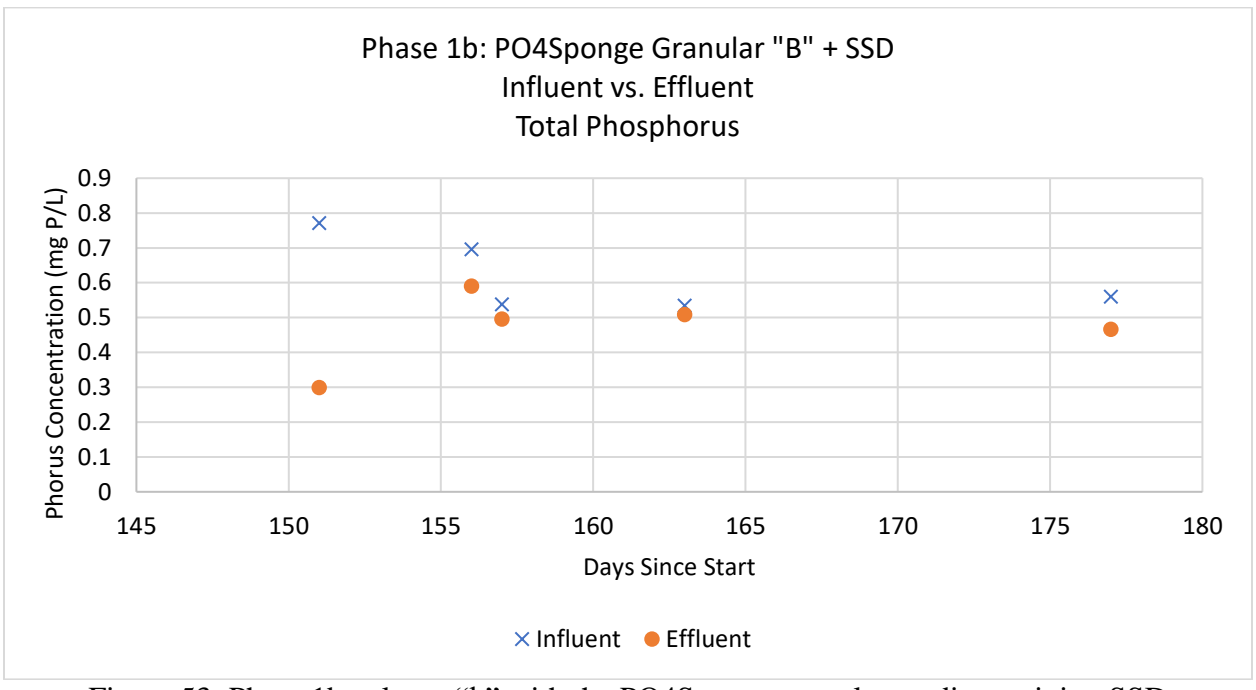


Figure 53: Phase 1b column "b" with the PO4Sponge granular media receiving SSD

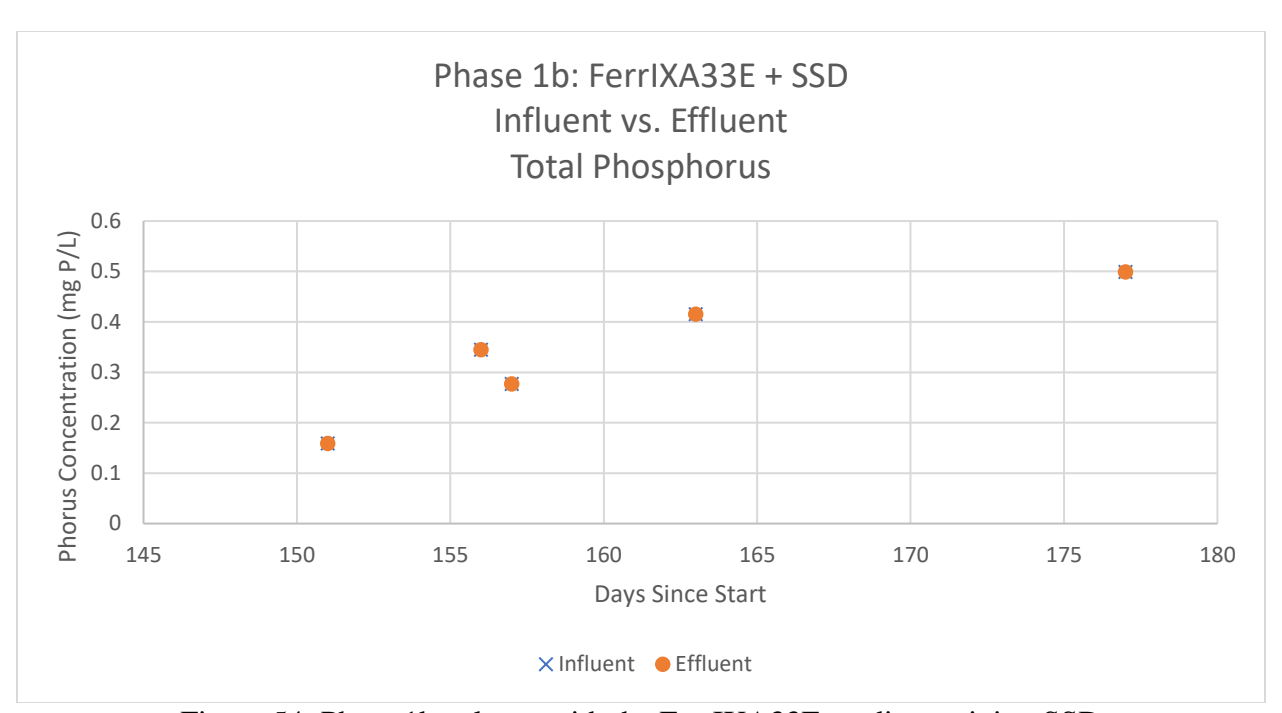


Figure 54: Phase 1b column with the FerrIXA33E media receiving SSD

C.2.3. Column experiments – Phase 1b (Soluble Reactive Phosphorus)

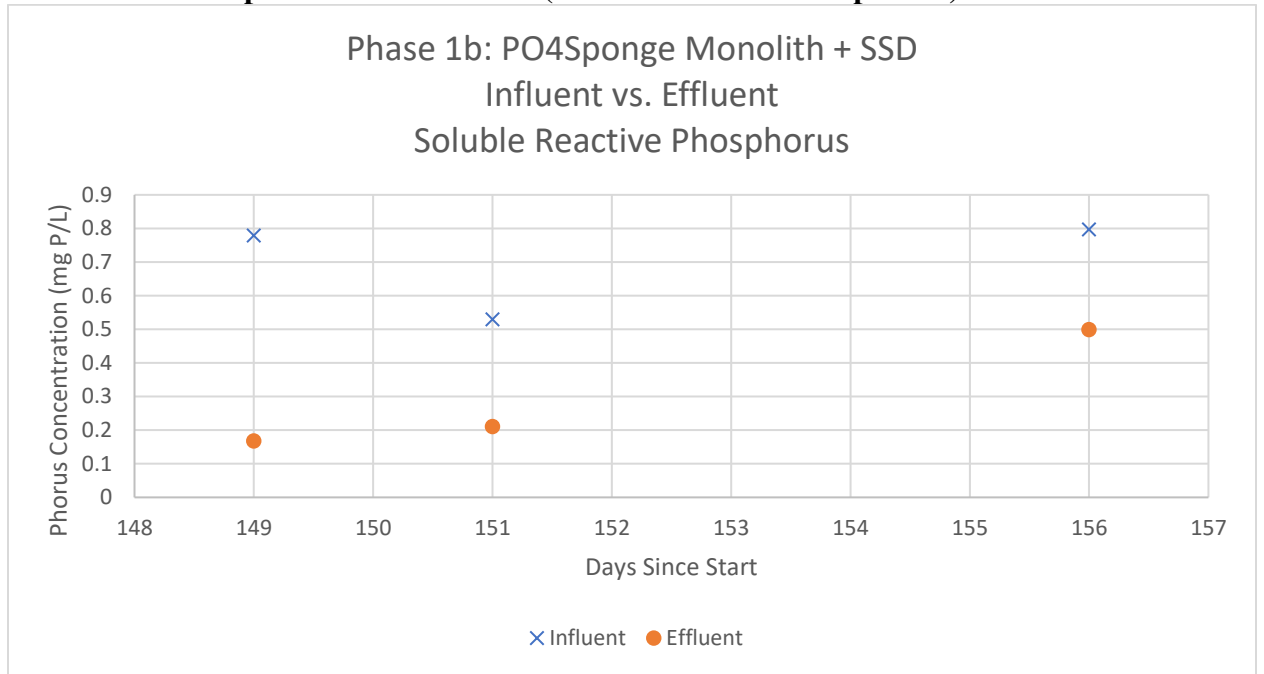


Figure 55: Phase 1b column with the PO4Sponge monolith media receiving SSD

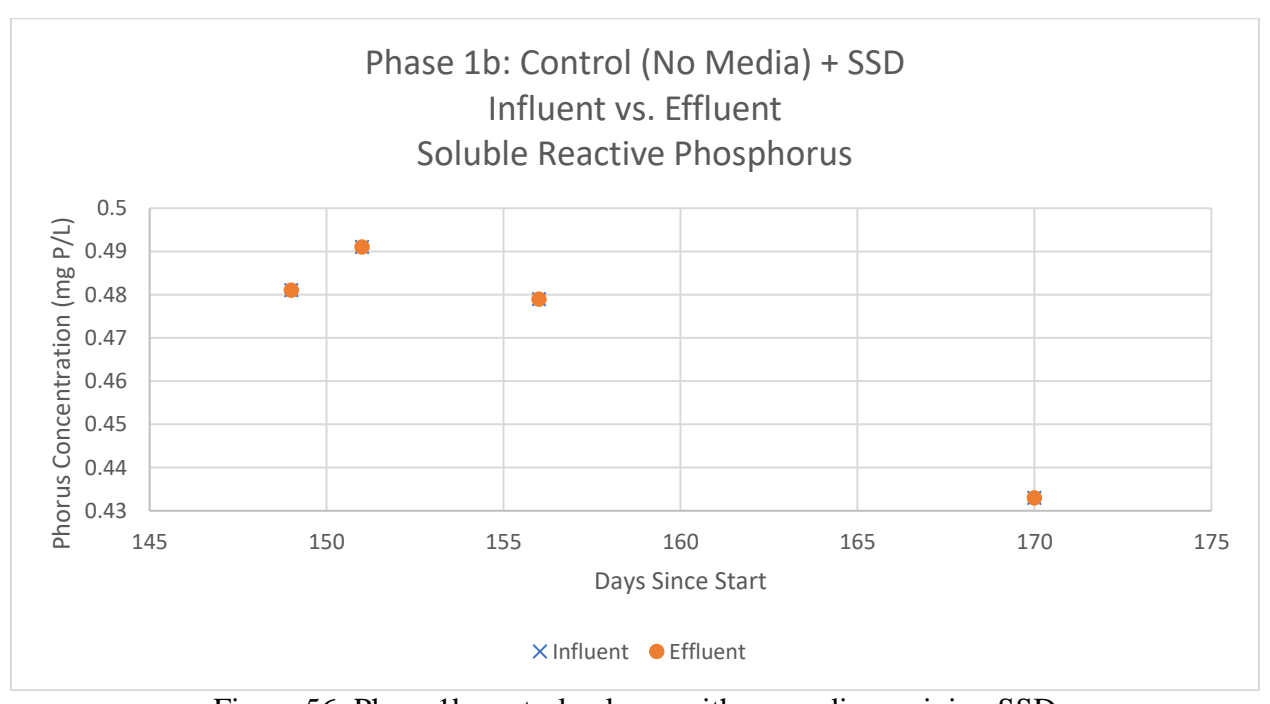


Figure 56: Phase 1b control column with no media receiving SSD

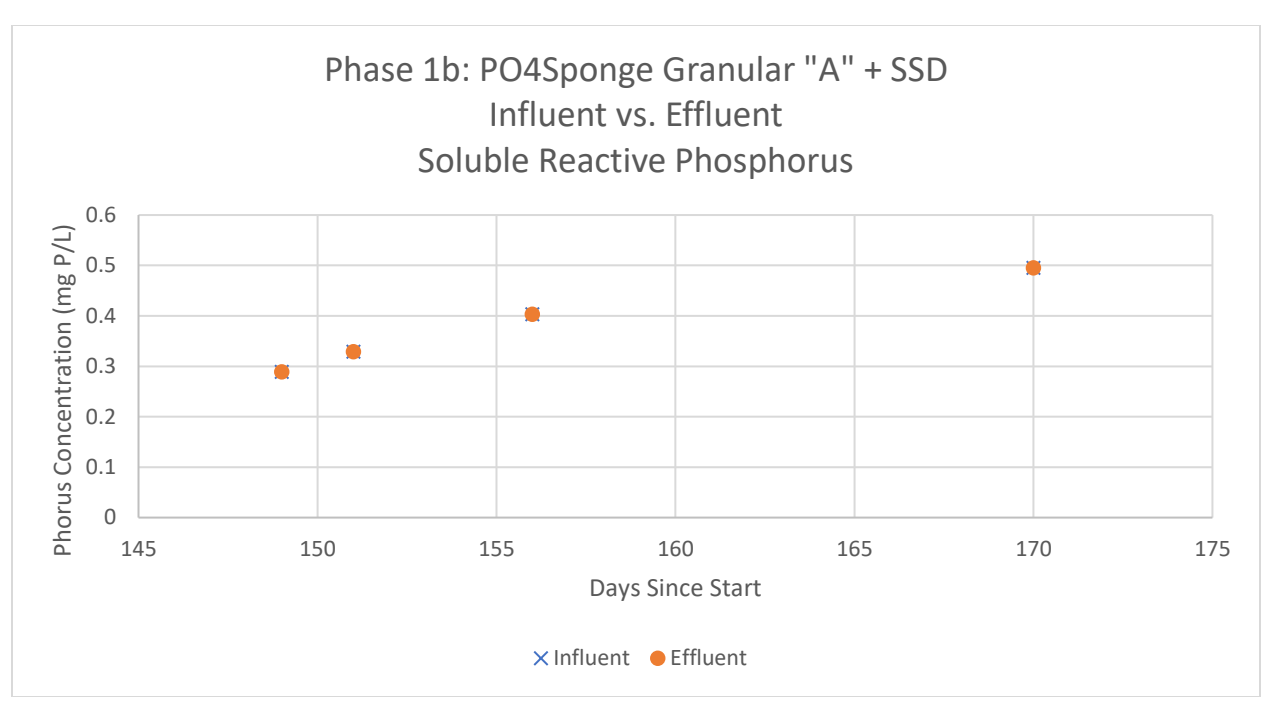


Figure 57: Phase 1b column "a" with the PO4Sponge granular media receiving SSD

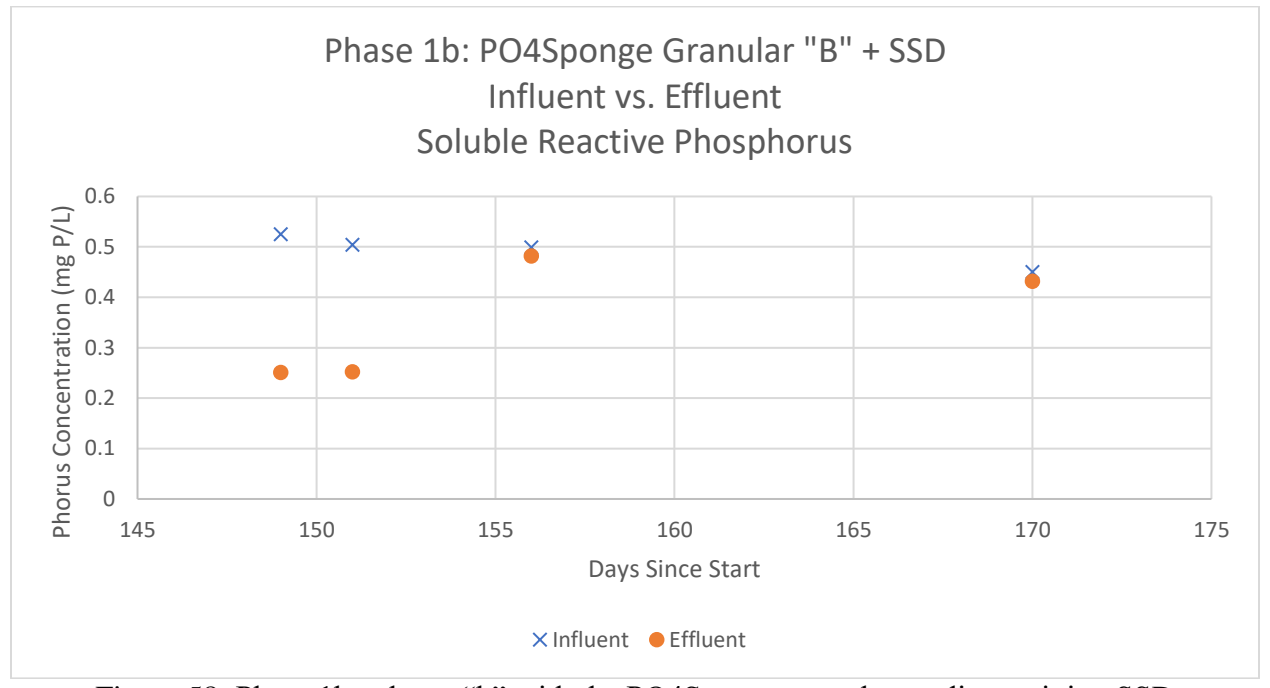


Figure 58: Phase 1b column "b" with the PO4Sponge granular media receiving SSD

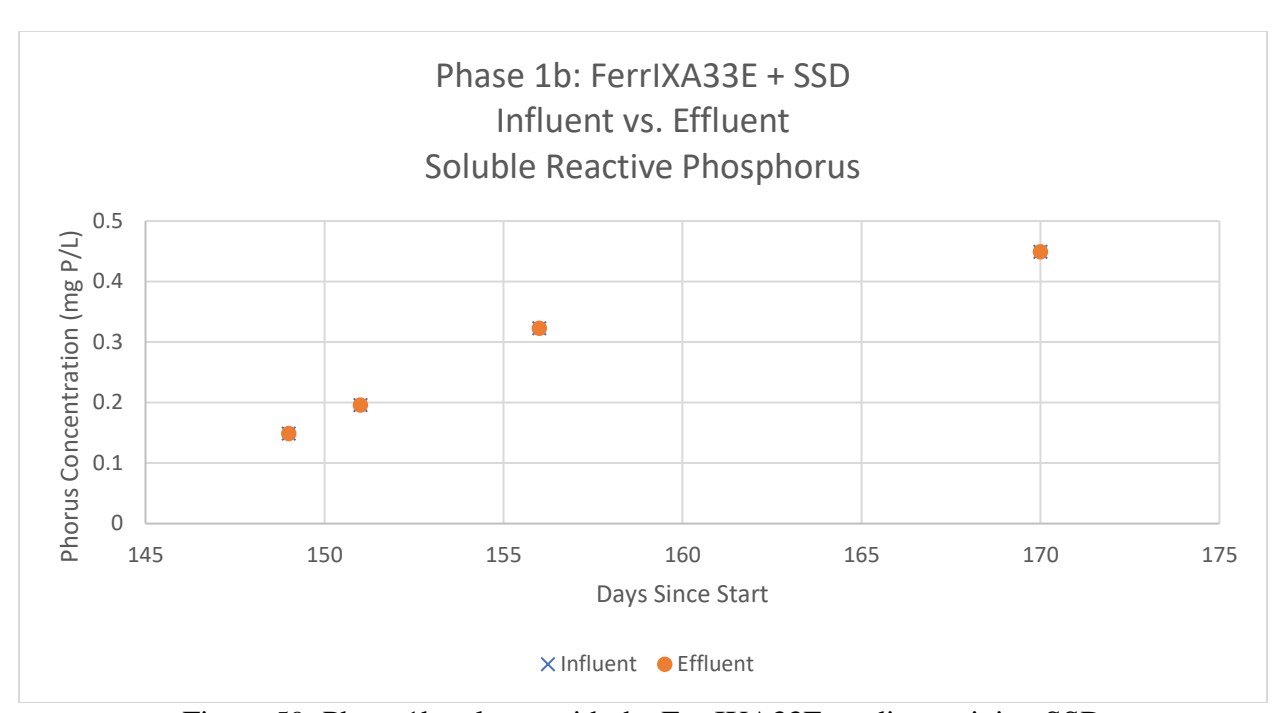


Figure 59: Phase 1b column with the FerrIXA33E media receiving SSD

C.2.4. Column experiments – Phase 1c (Total Phosphorus)

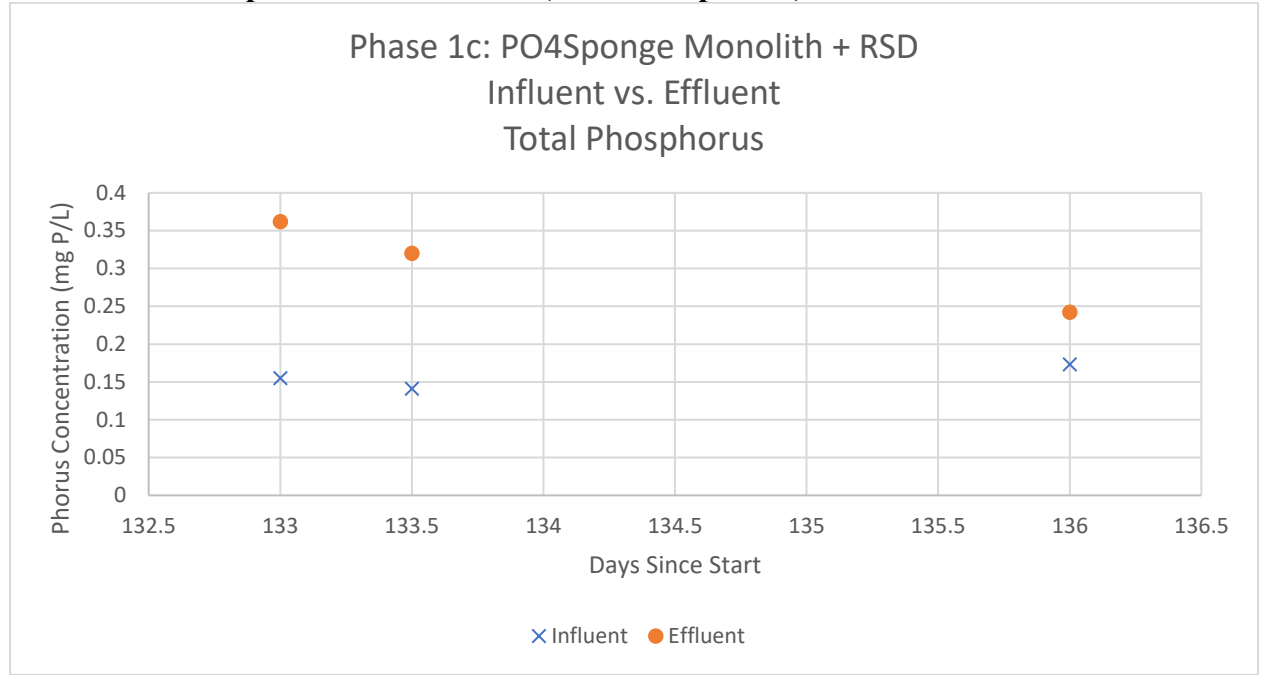


Figure 60: Phase 1c column with the PO4Sponge monolith media receiving RSD

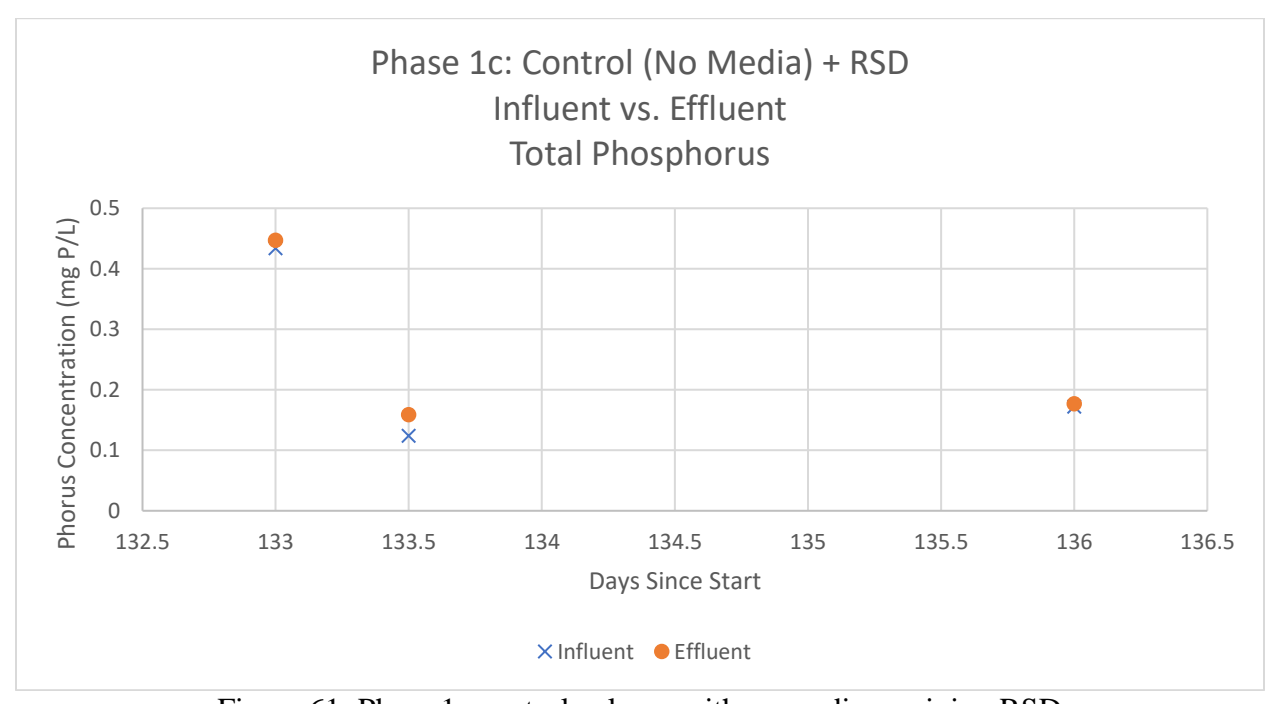


Figure 61: Phase 1c control column with no media receiving RSD

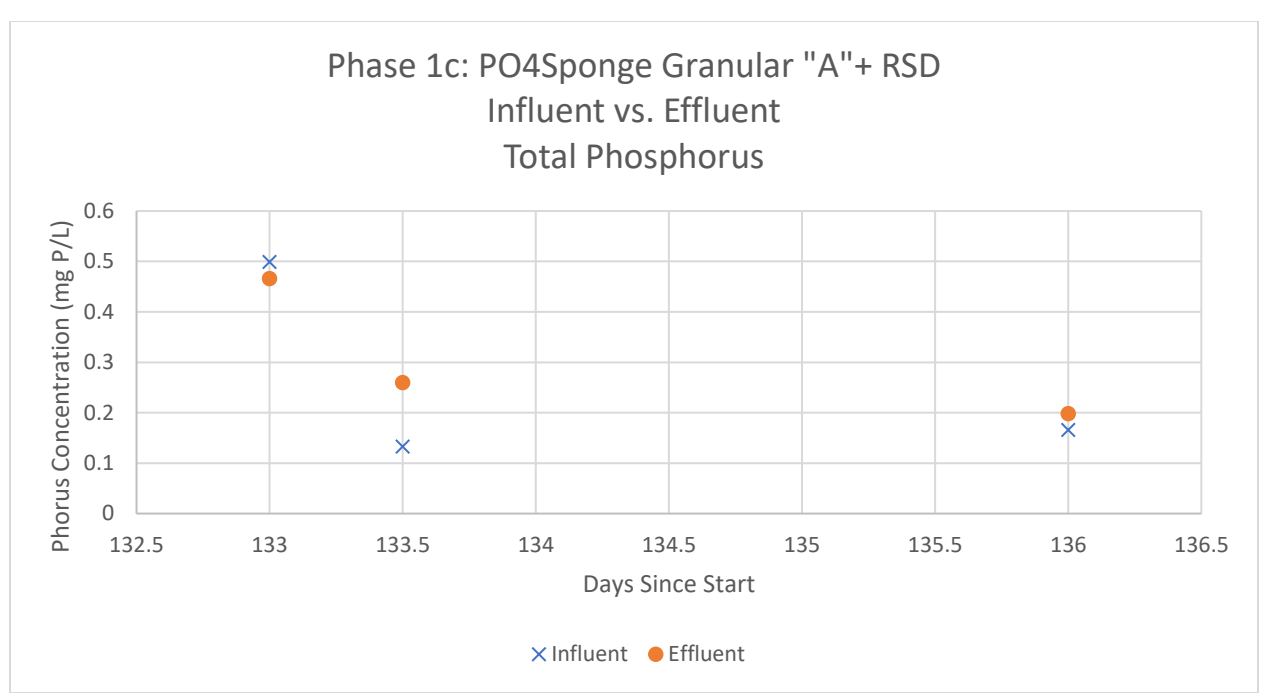


Figure 62: Phase 1c column "a" with the PO4Sponge granular media receiving RSD

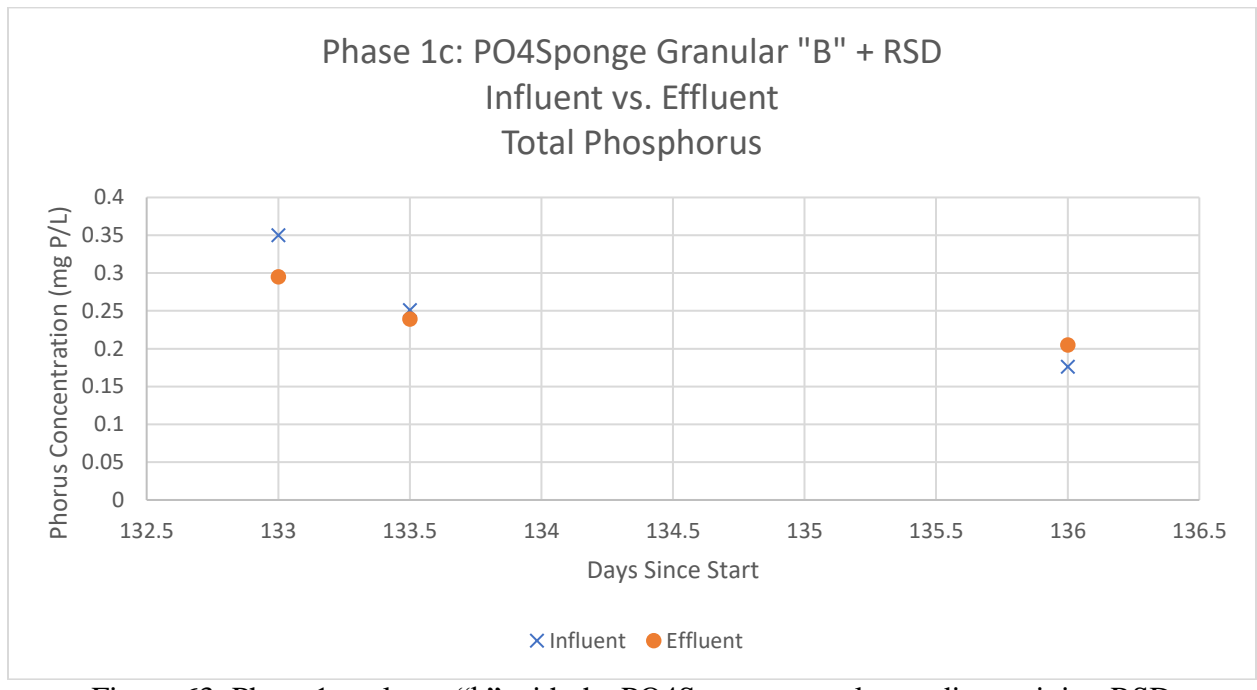


Figure 63: Phase 1c column "b" with the PO4Sponge granular media receiving RSD

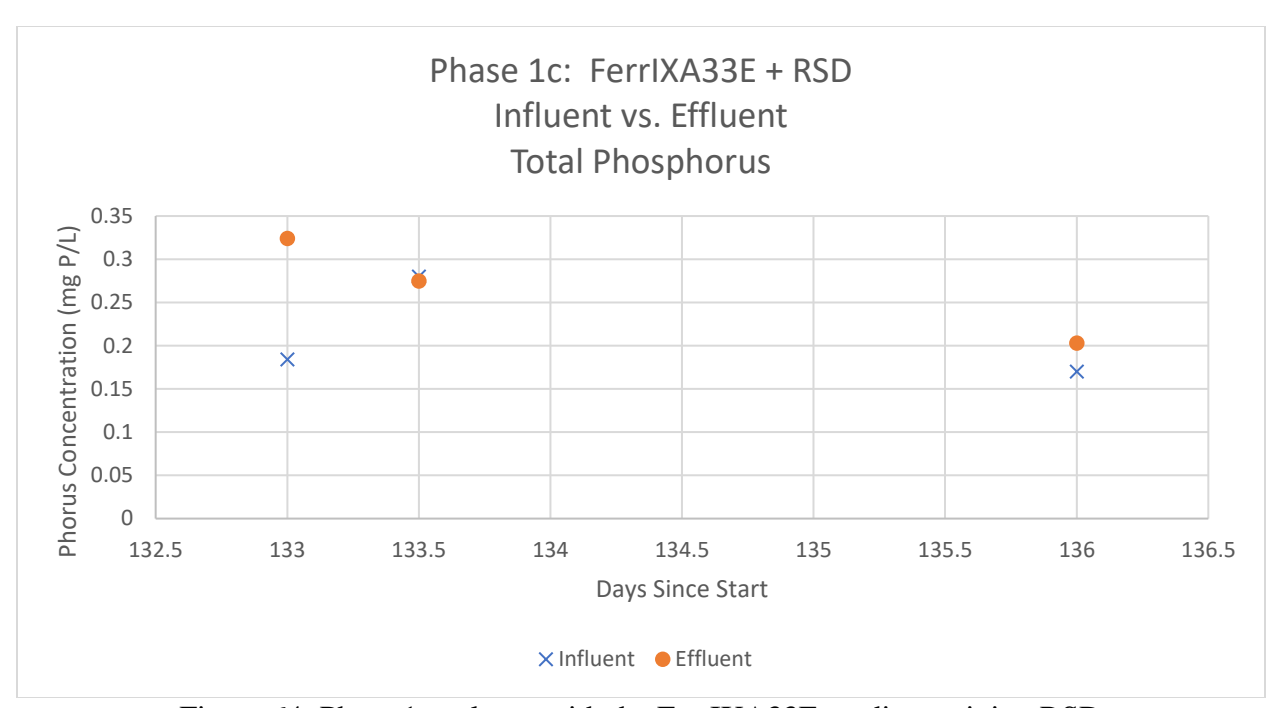


Figure 64: Phase 1c column with the FerrIXA33E media receiving RSD

C.2.5. Column experiments – Phase 1c (Soluble Reactive Phosphorus)

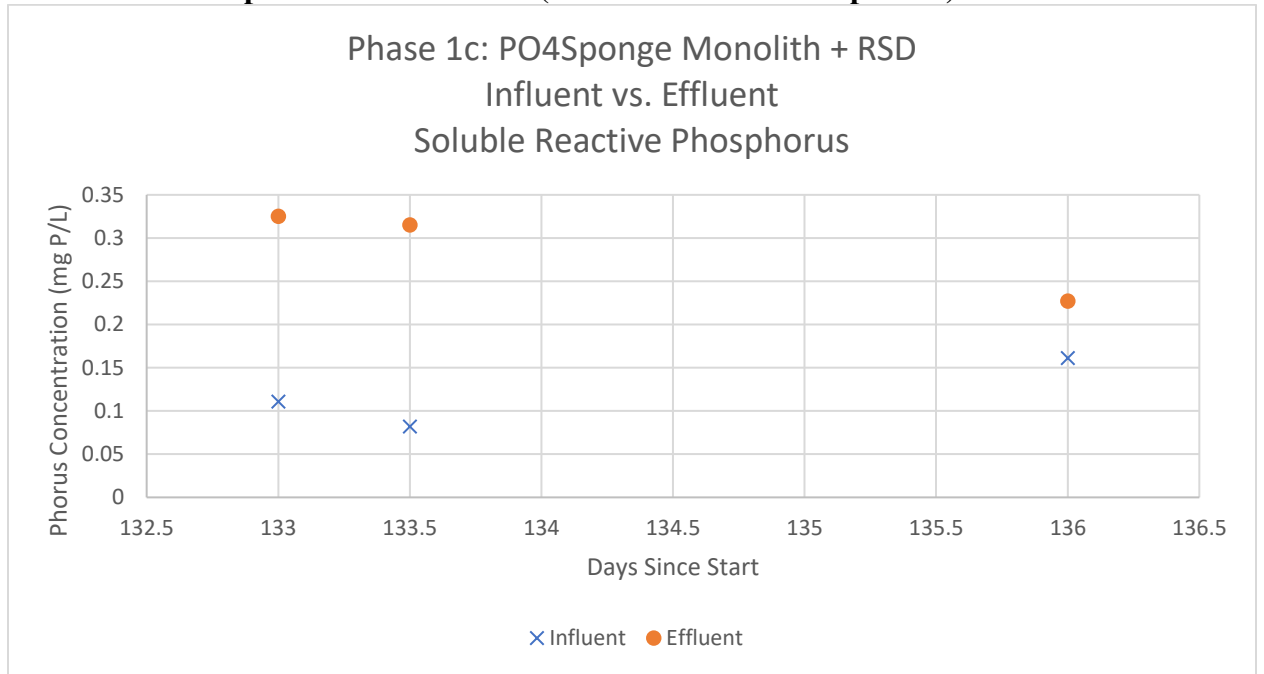


Figure 65: Phase 1c column with the PO4Sponge monolith media receiving RSD

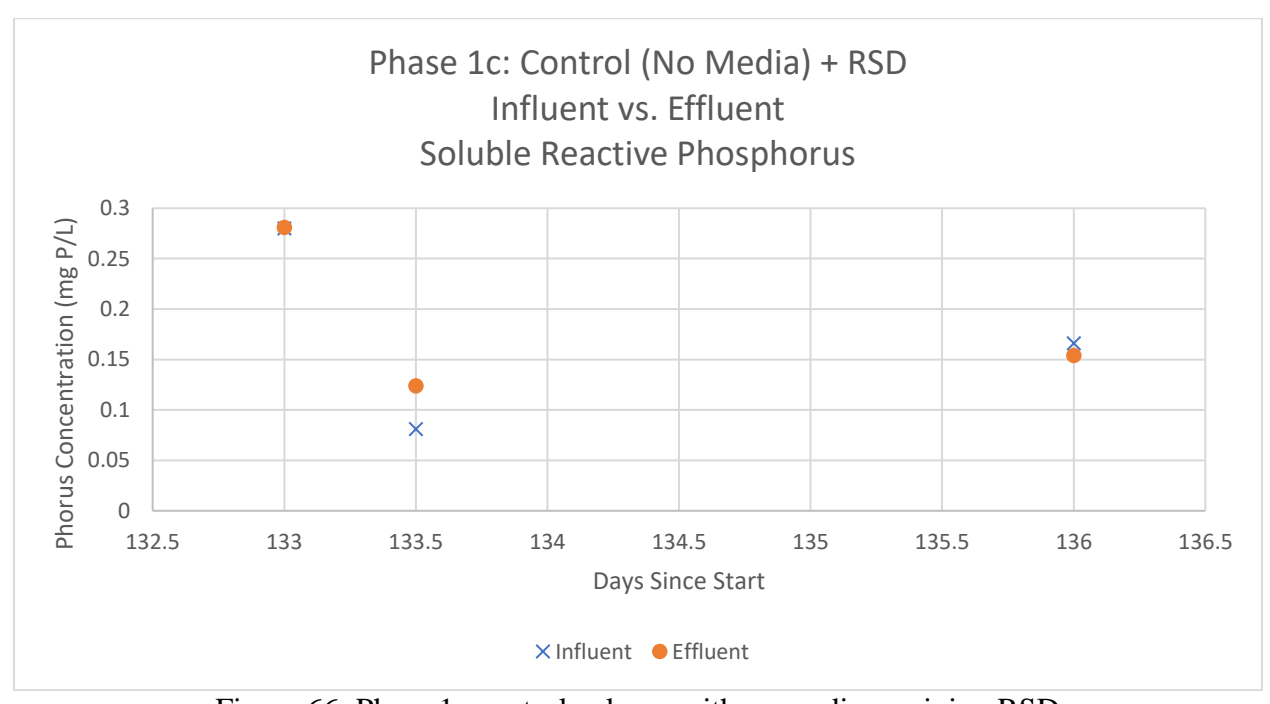


Figure 66: Phase 1c control column with no media receiving RSD

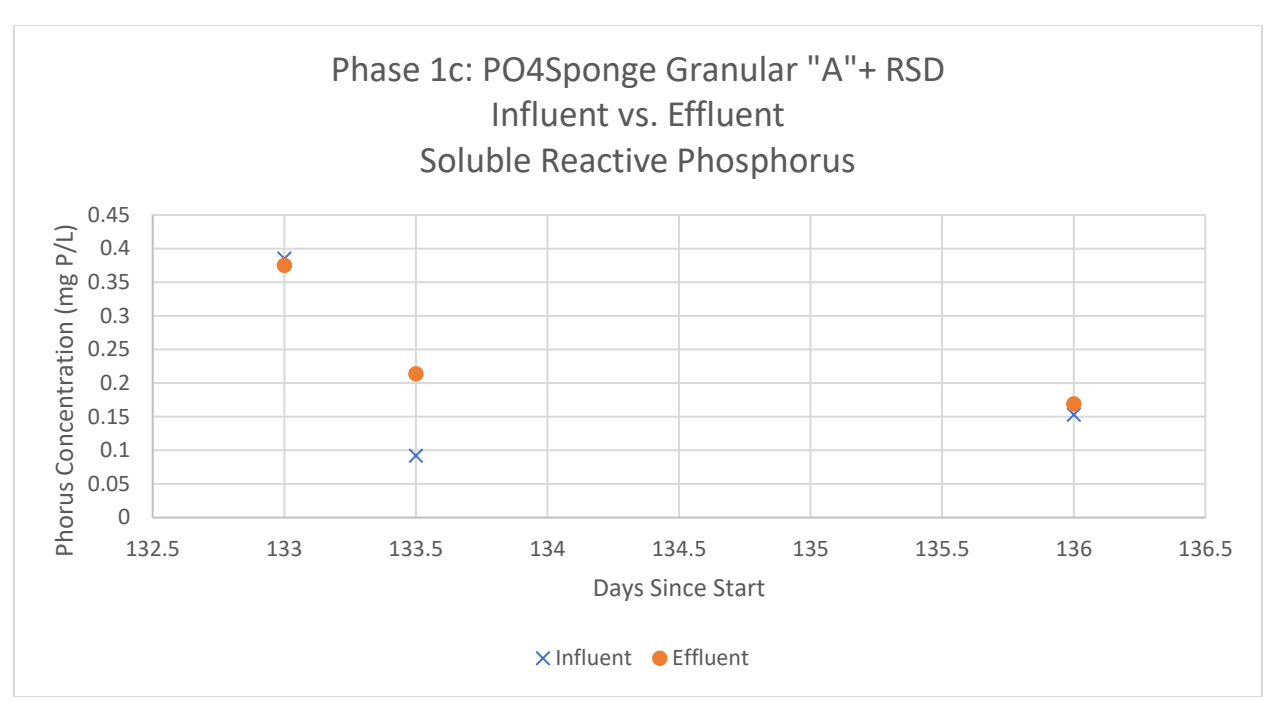


Figure 67: Phase 1c column "a" with the PO4Sponge granular media receiving RSD

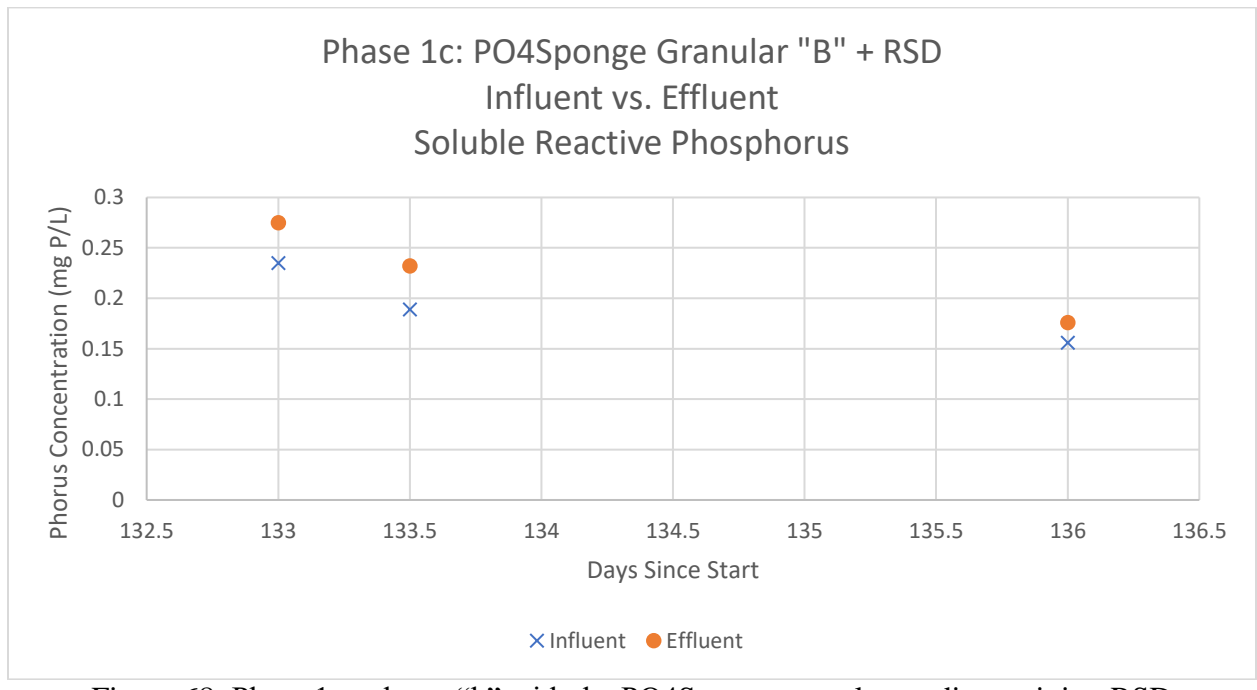


Figure 68: Phase 1c column "b" with the PO4Sponge granular media receiving RSD

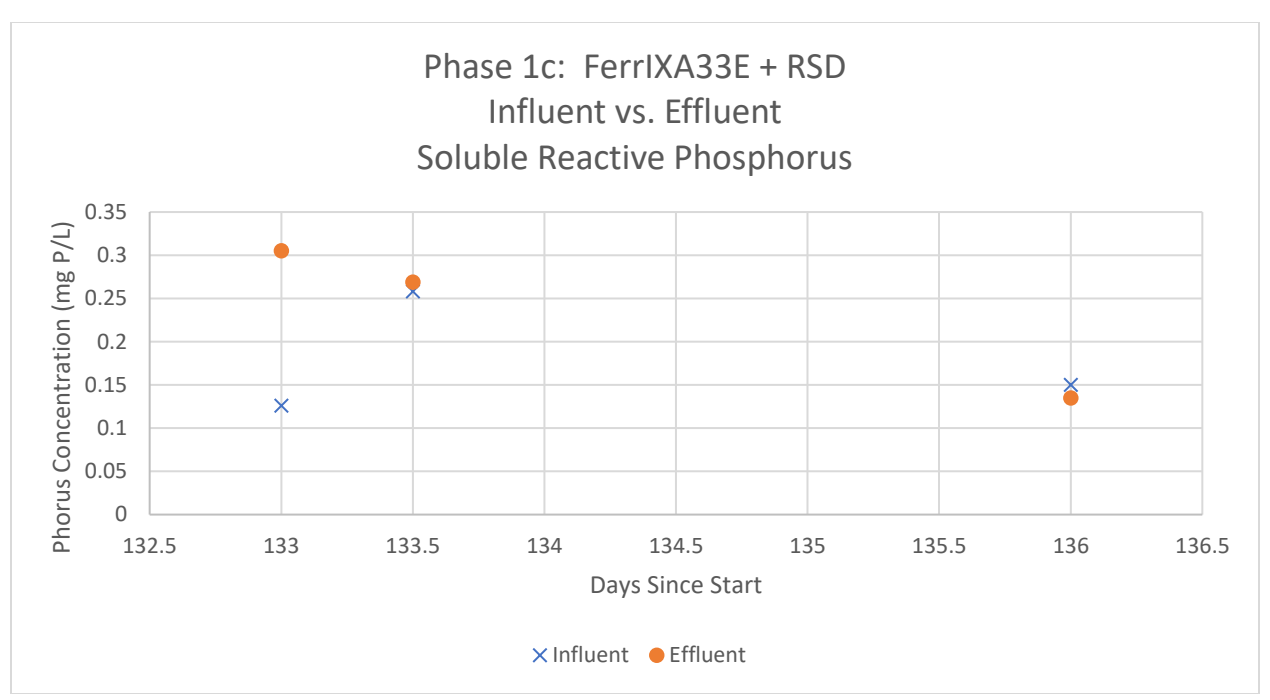


Figure 69: Phase 1c column with the FerrIXA33E media receiving RSD

C.2.6. Column experiments – Phase 1d (Total Phosphorus)

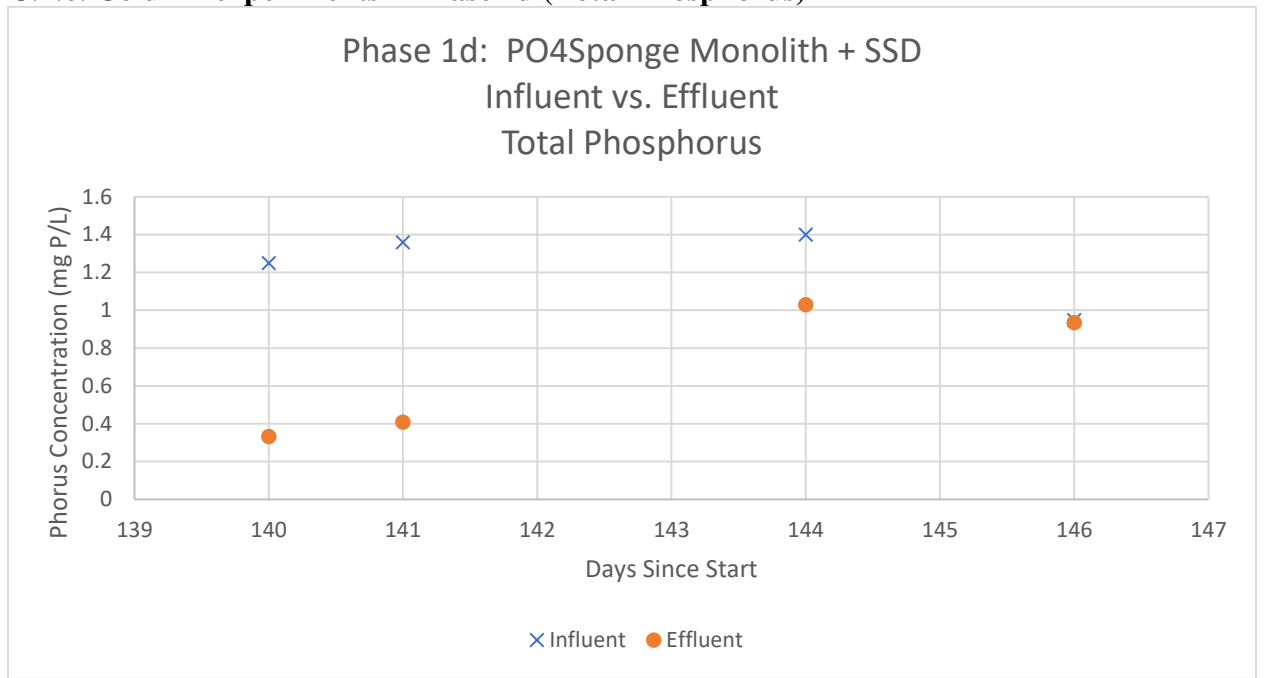


Figure 70: Phase 1d column with the PO4Sponge monolith media receiving SSD

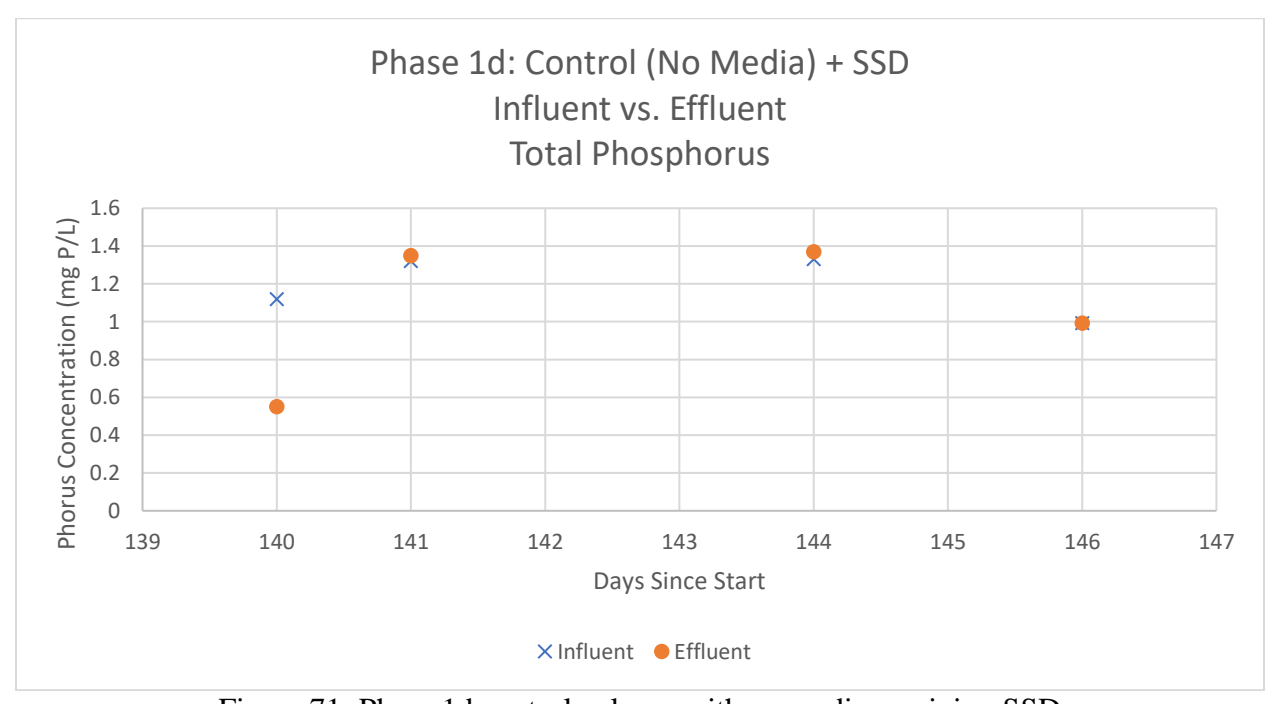


Figure 71: Phase 1d control column with no media receiving SSD

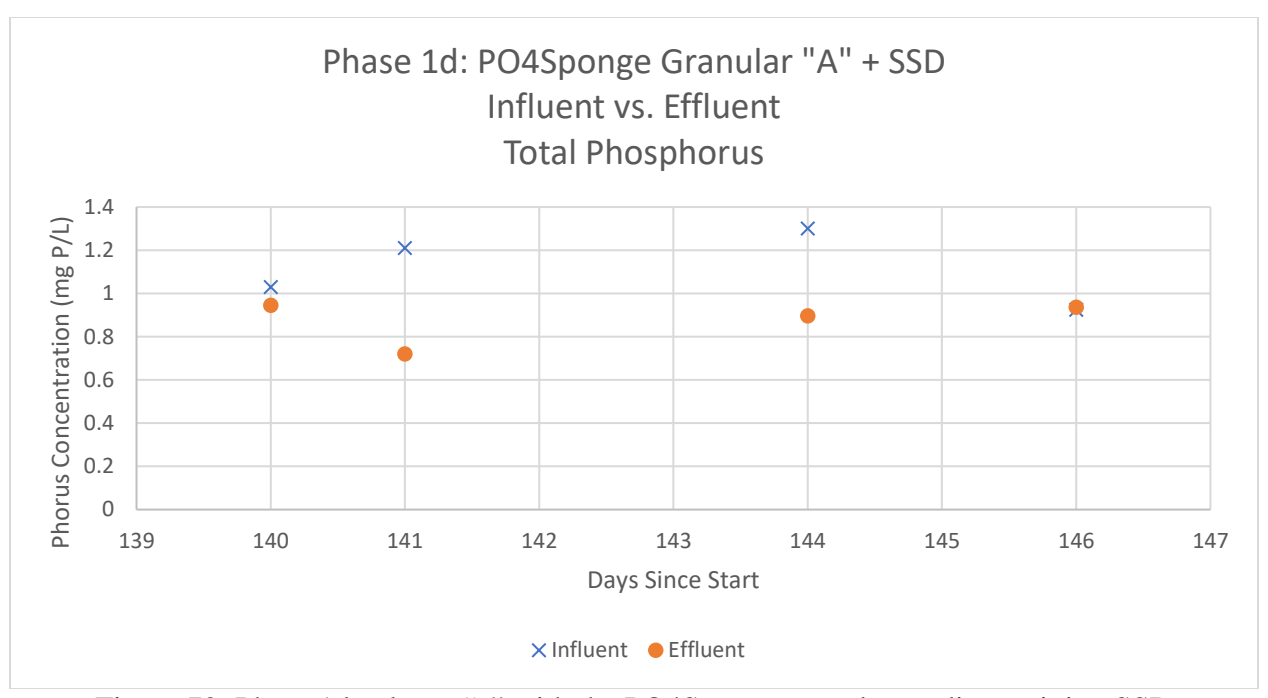


Figure 72: Phase 1d column "a" with the PO4Sponge granular media receiving SSD

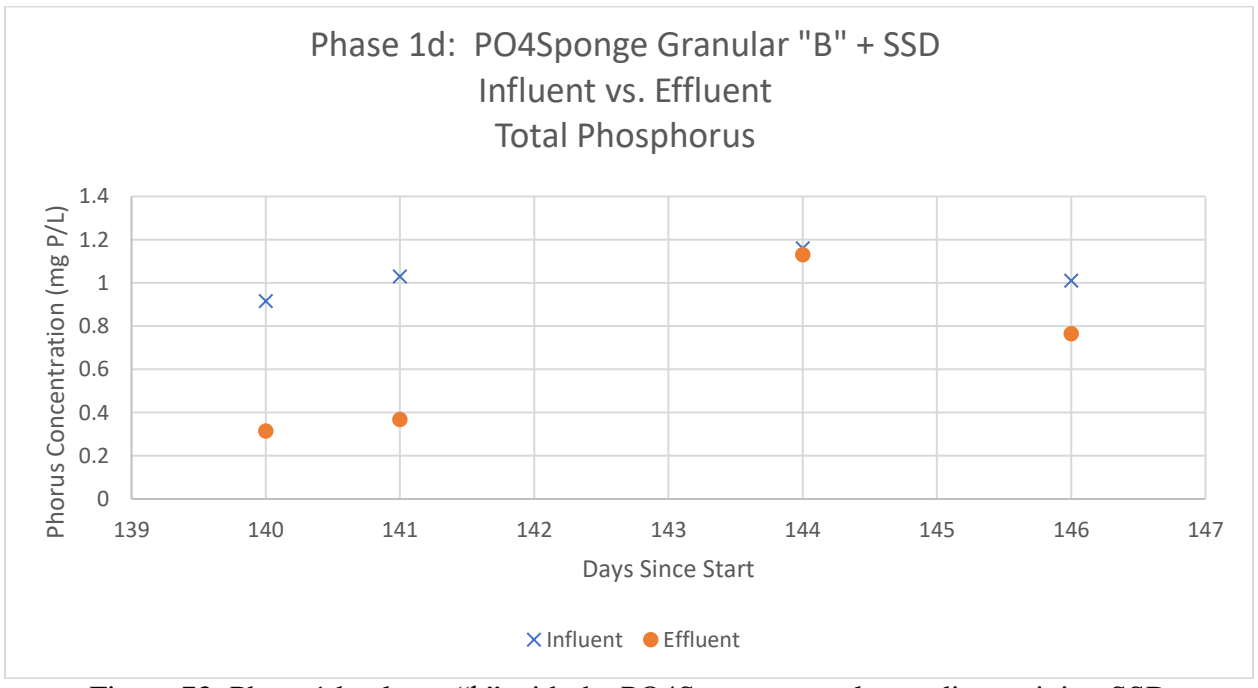


Figure 73: Phase 1d column "b" with the PO4Sponge granular media receiving SSD

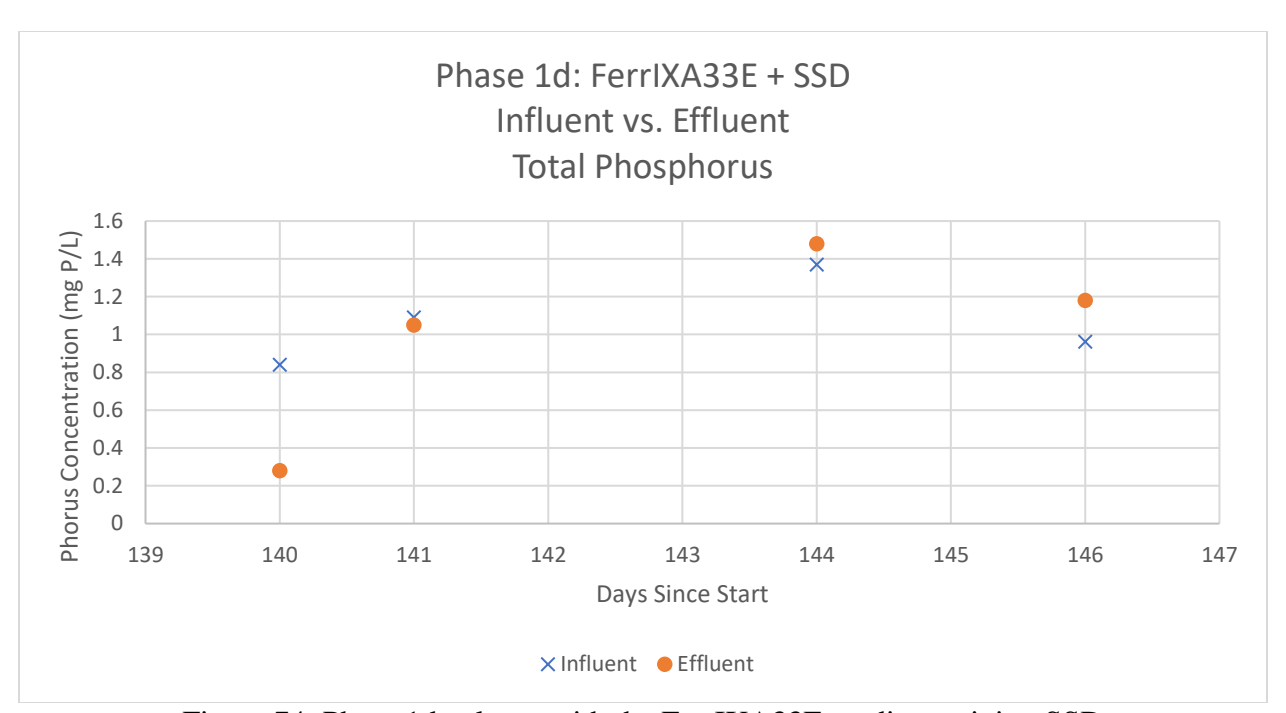


Figure 74: Phase 1d column with the FerrIXA33E media receiving SSD

C.2.7. Column experiments – Phase 1d (Soluble Reactive Phosphorus)

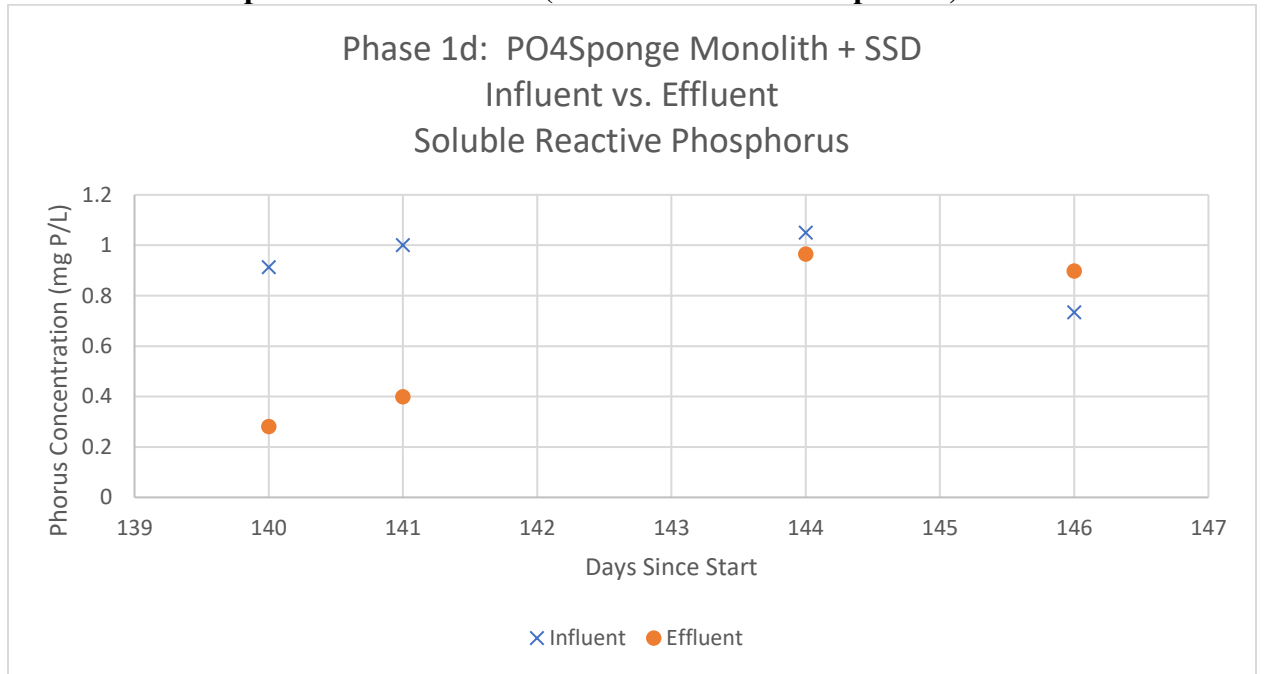


Figure 75: Phase 1d column with the PO4Sponge monolith media receiving SSD

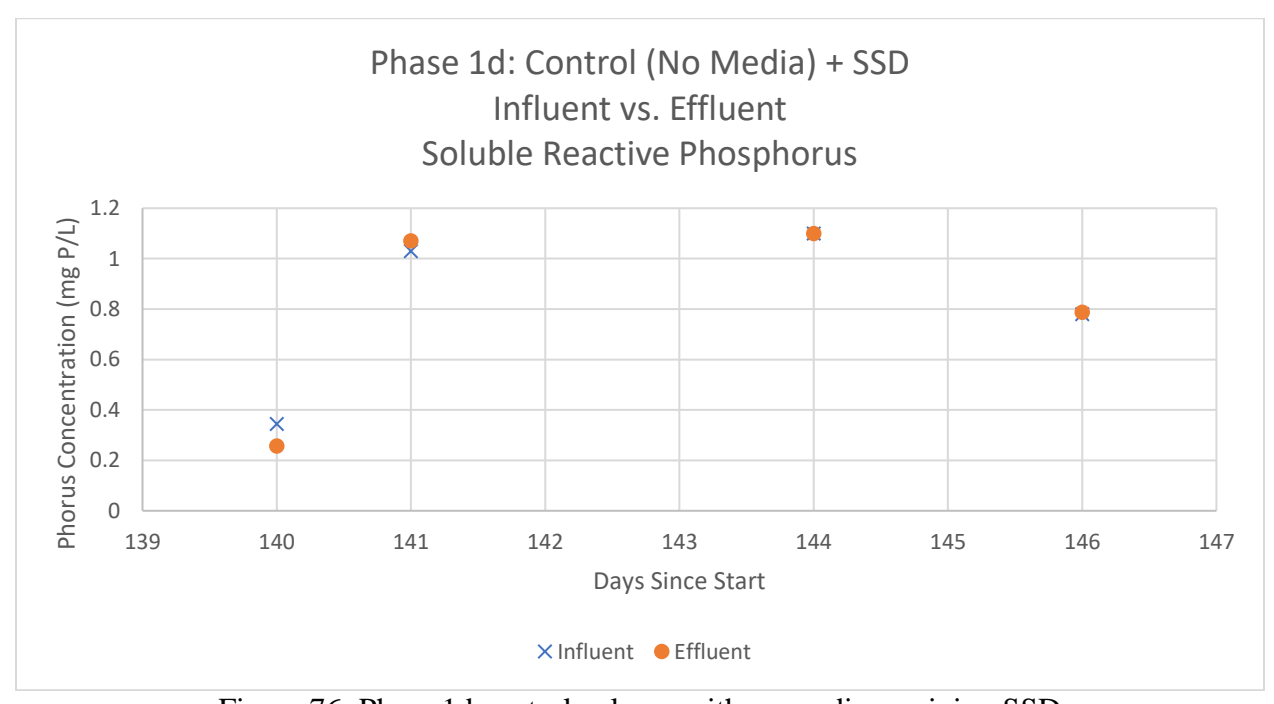


Figure 76: Phase 1d control column with no media receiving SSD

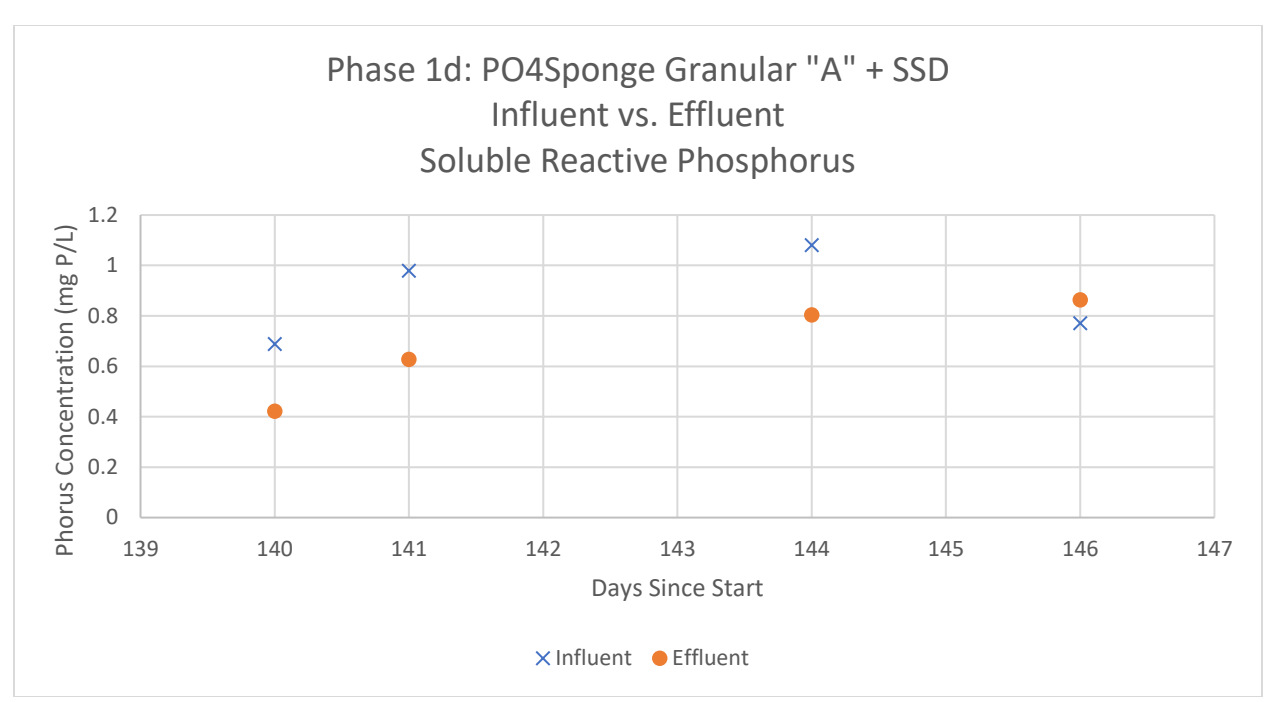


Figure 77: Phase 1d column "a" with the PO4Sponge granular media receiving SSD

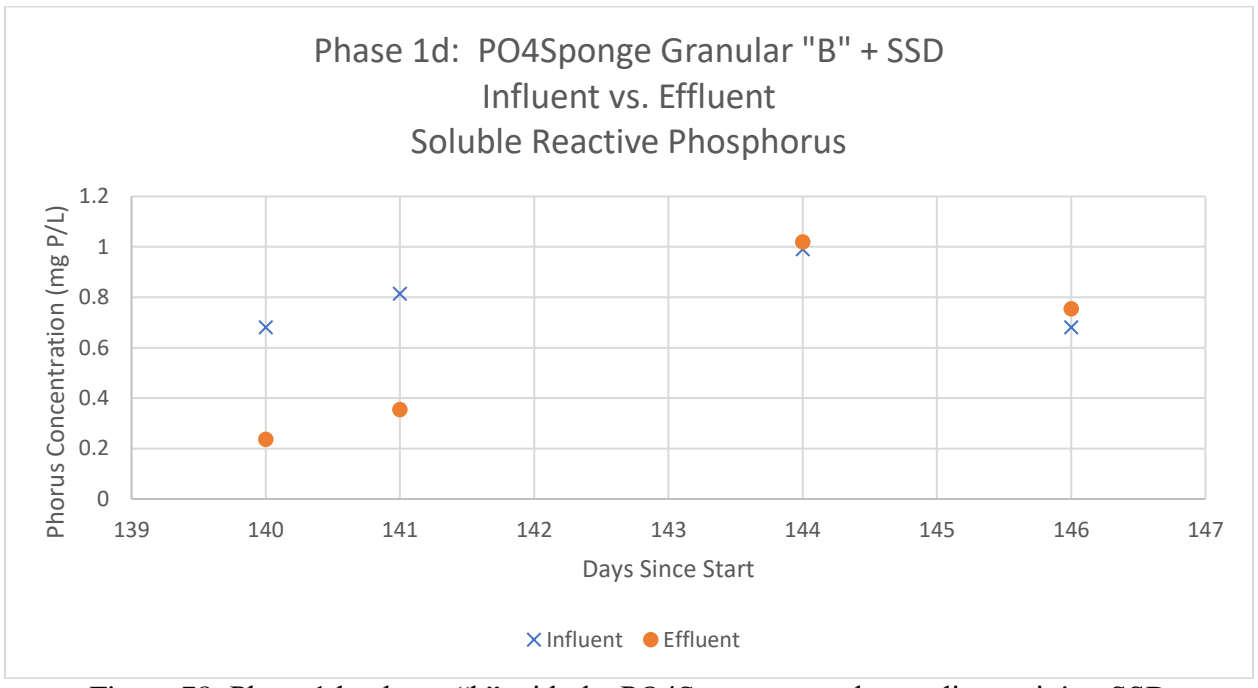


Figure 78: Phase 1d column "b" with the PO4Sponge granular media receiving SSD

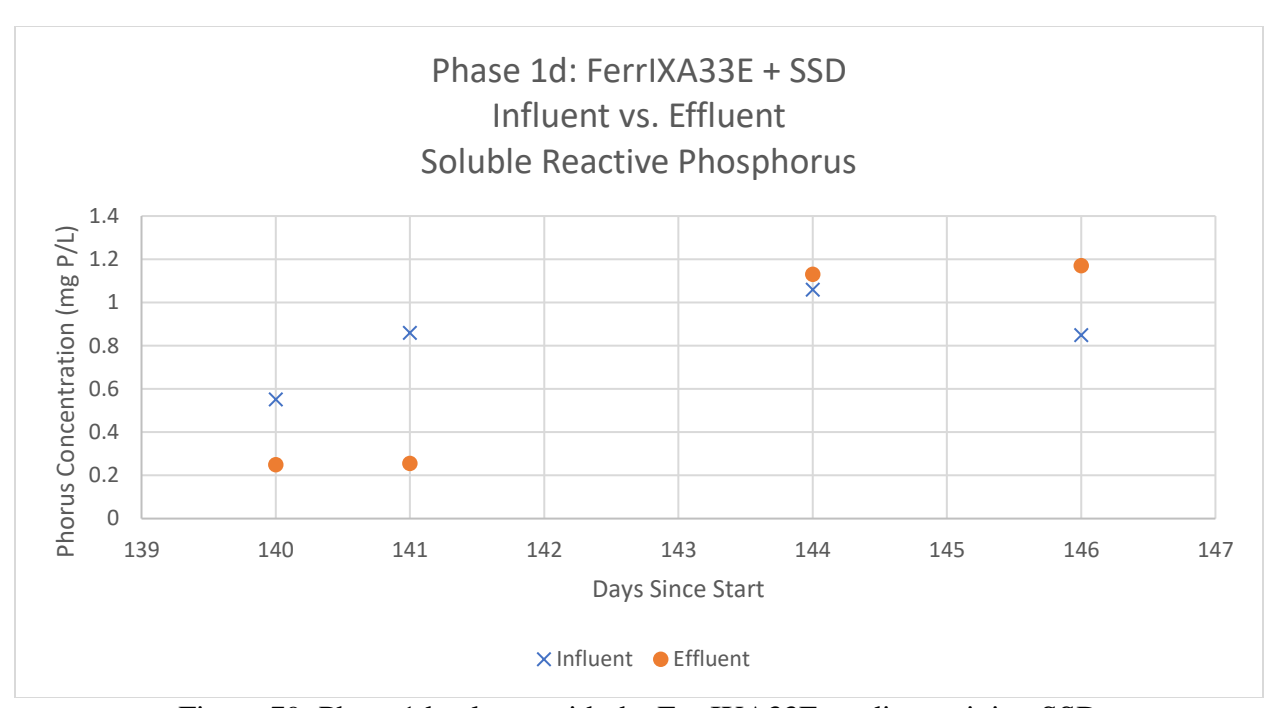


Figure 79: Phase 1d column with the FerrIXA33E media receiving SSD

C.2.8. Column experiments – Phase 2a (Total Phosphorus)

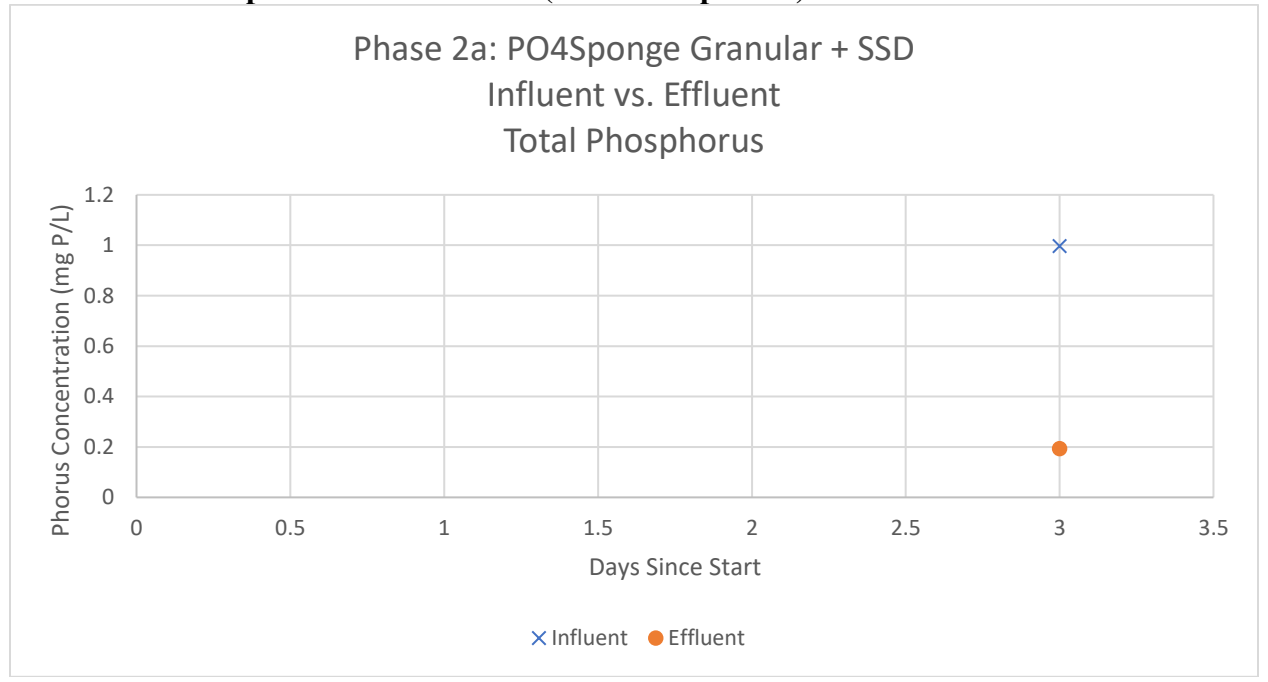


Figure 80: Phase 2a column with the PO4Spnge granular media receiving SSD

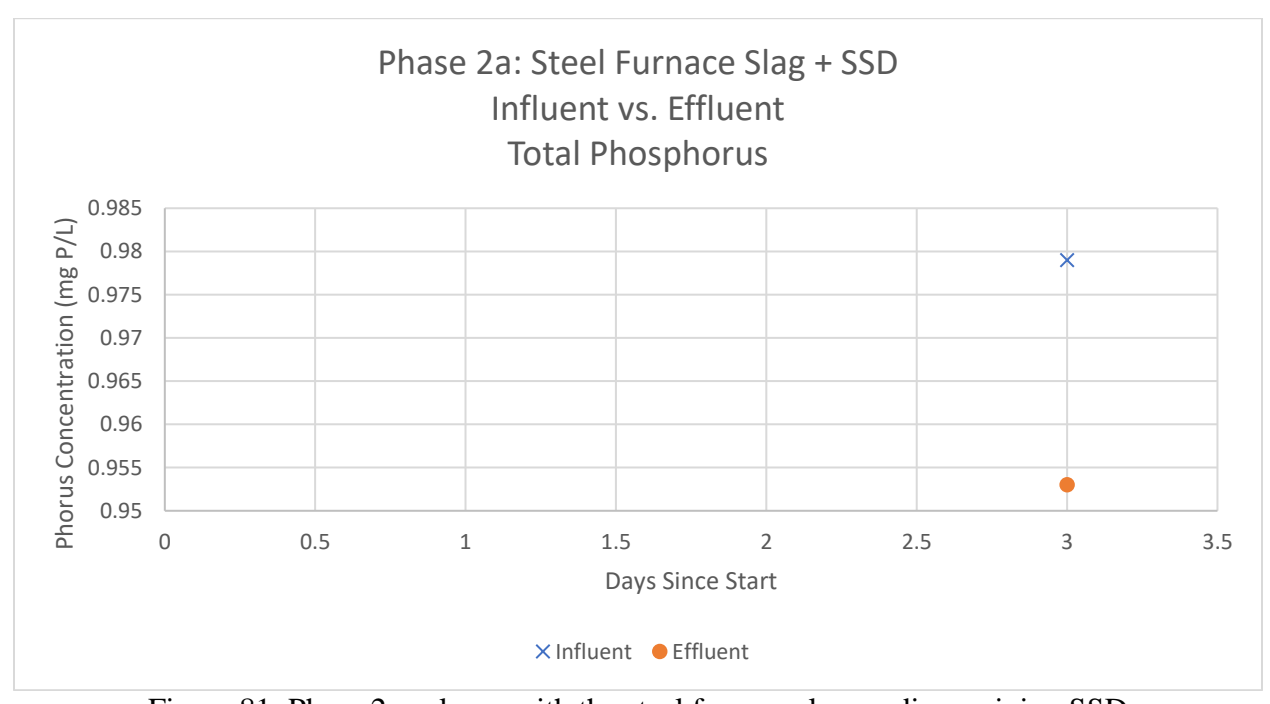


Figure 81: Phase 2a column with the steel furnace slag media receiving SSD

C.2.9. Column experiments – Phase 2a (Soluble Reactive Phosphorus)

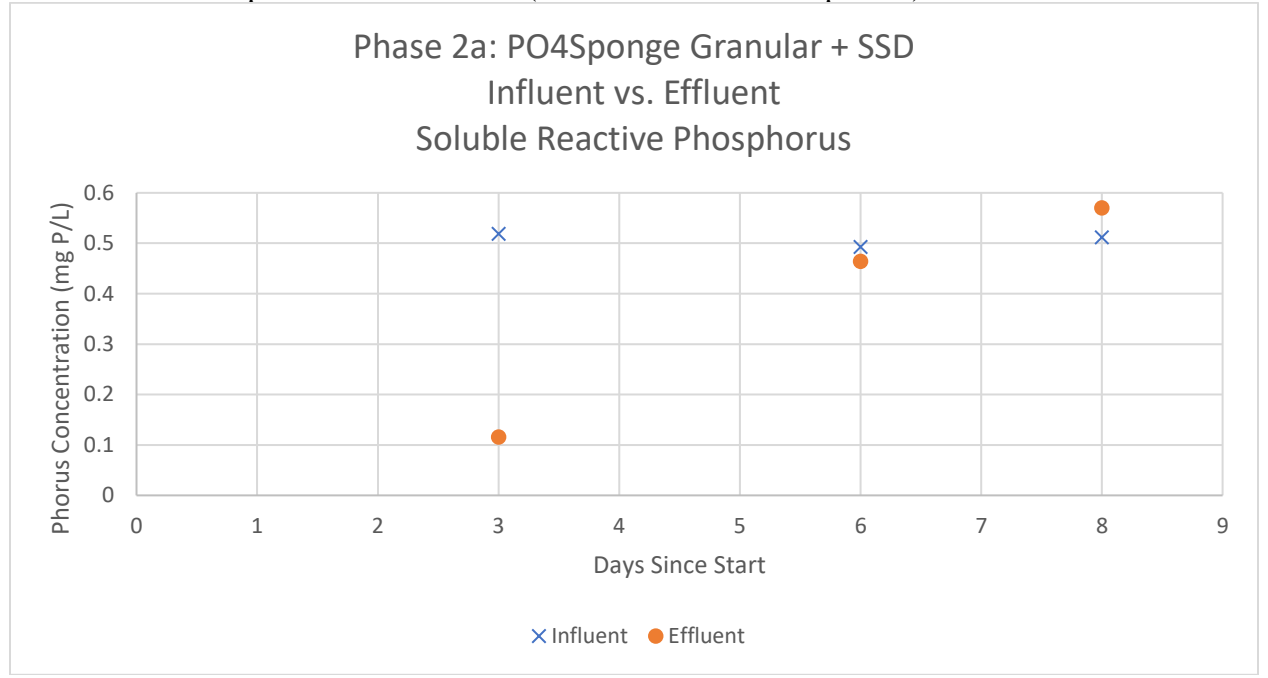


Figure 82: Phase 2a column with the PO4Spnge granular media receiving SSD

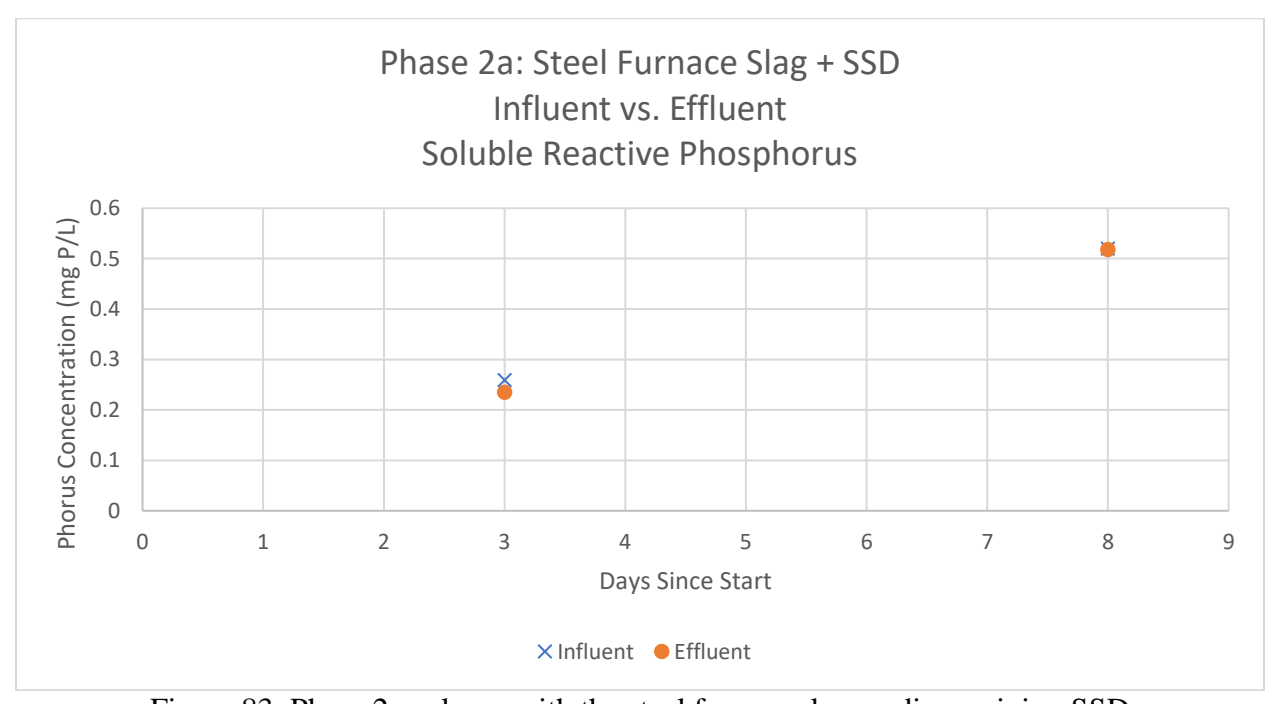


Figure 83: Phase 2a column with the steel furnace slag media receiving SSD

C.2.10. Column experiments – Phase 2b (Total Phosphorus)

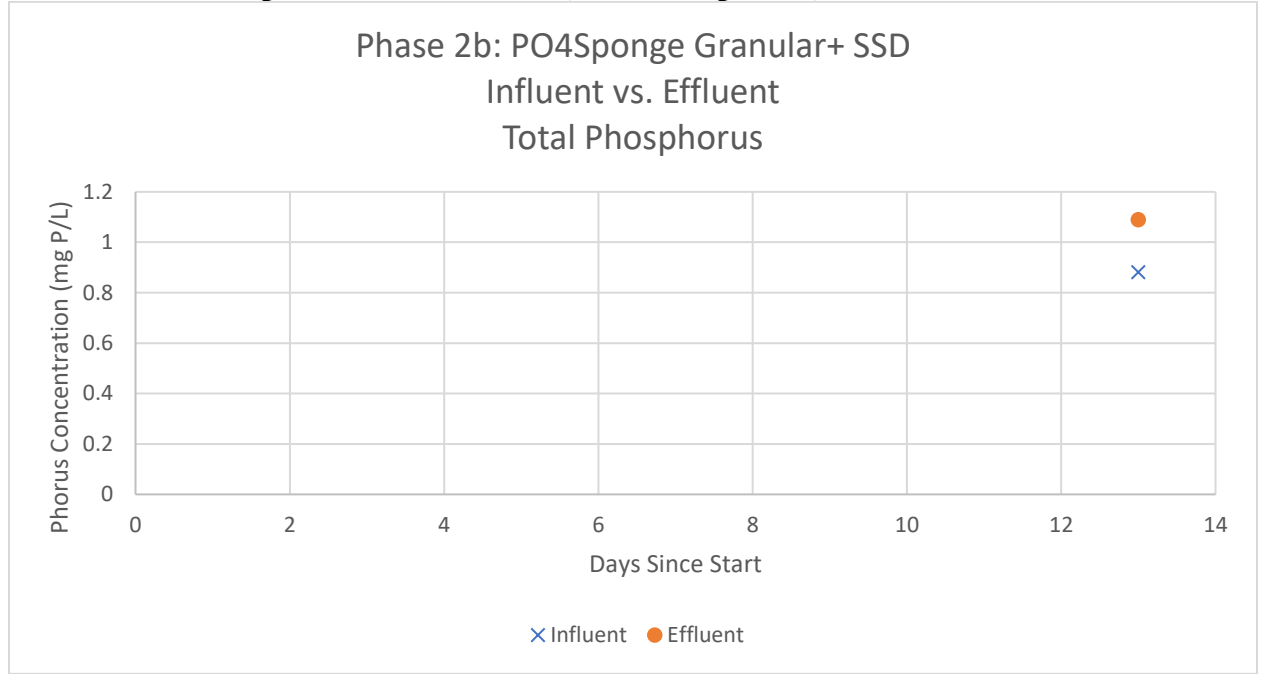


Figure 84: Phase 2b column with the PO4Spnge granular media receiving SSD

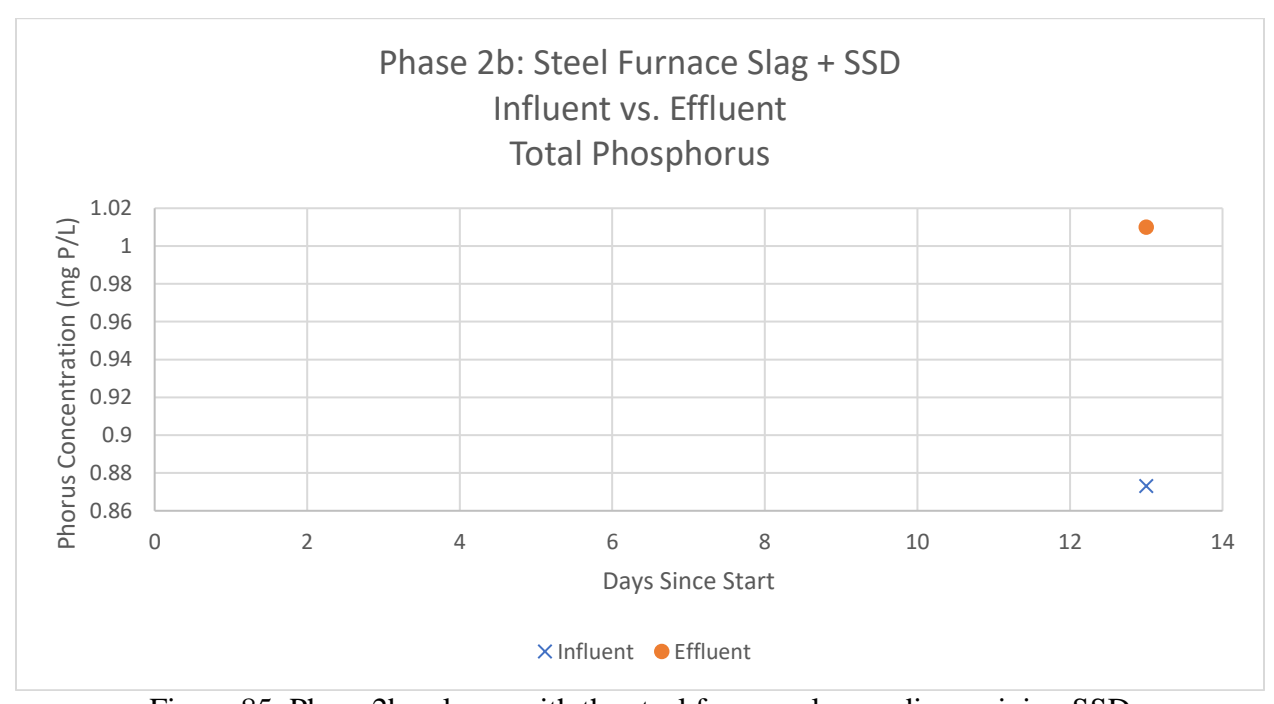


Figure 85: Phase 2b column with the steel furnace slag media receiving SSD

C.2.11. Column experiments – Phase 2b (Soluble Reactive Phosphorus)

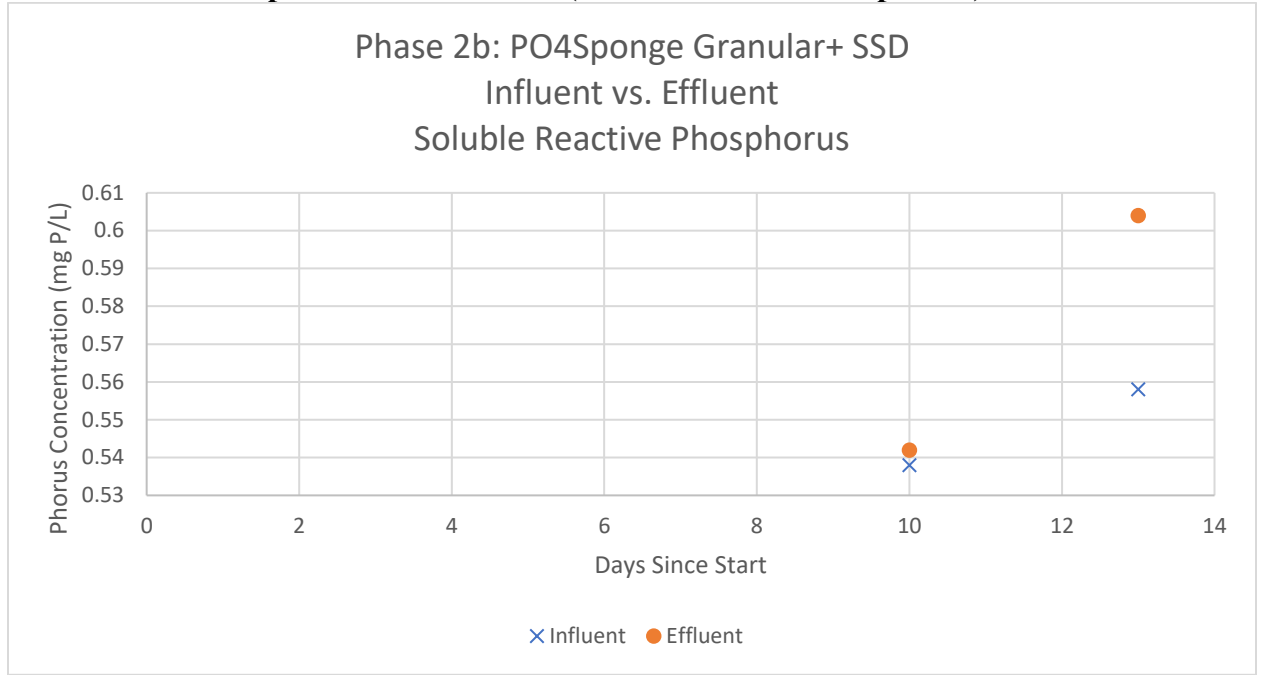


Figure 86: Phase 2b column with the PO4Spnge granular media receiving SSD

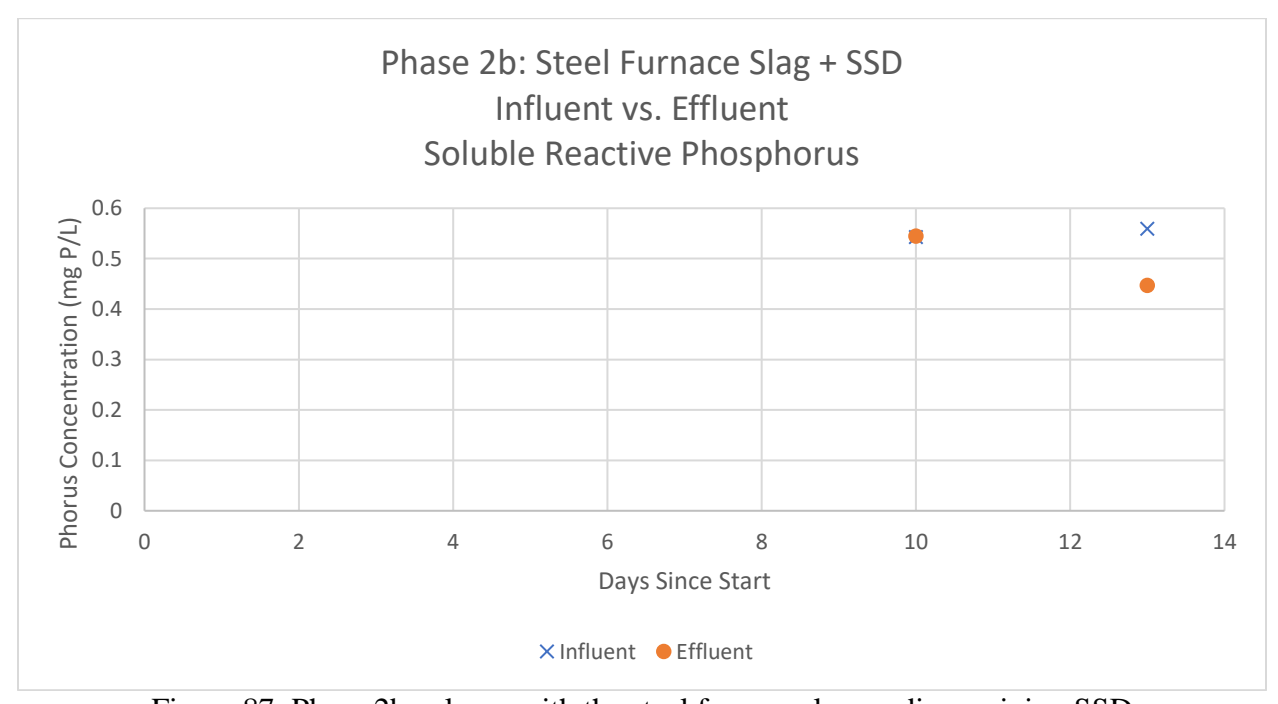


Figure 87: Phase 2b column with the steel furnace slag media receiving SSD

C.2.12. Column experiments – Phase 2c (Total Phosphorus)

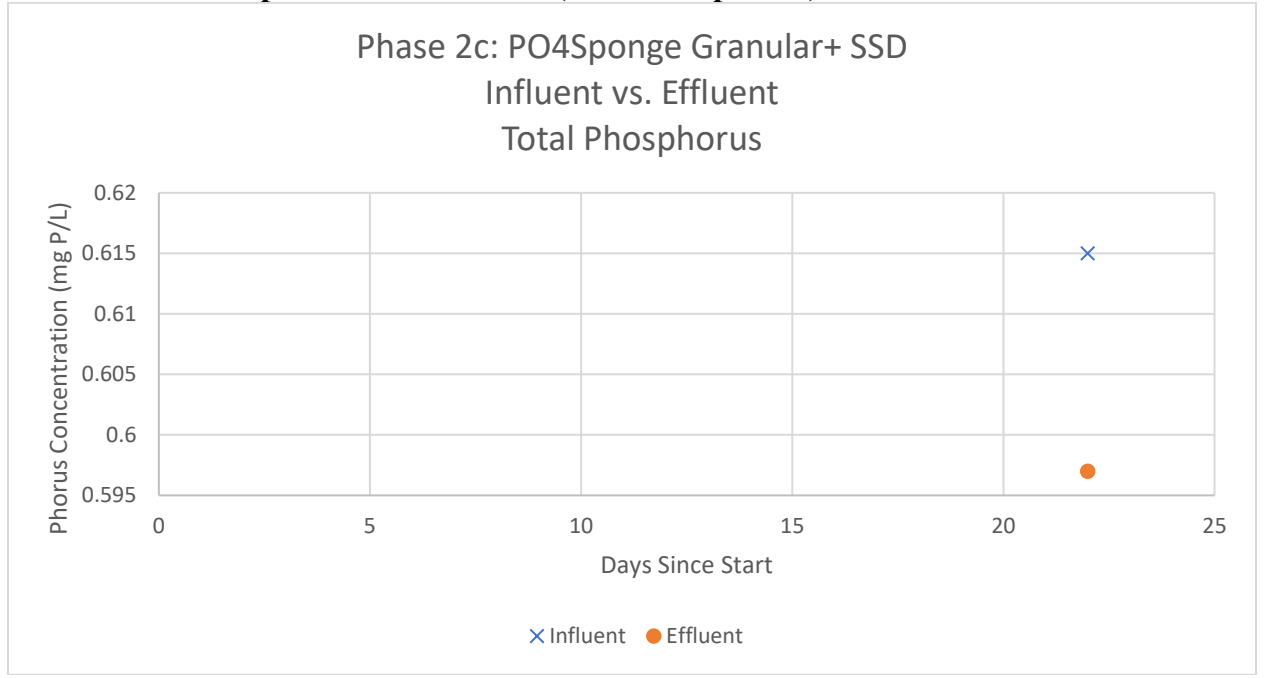


Figure 88: Phase 2c column with the PO4Spnge granular media receiving SSD

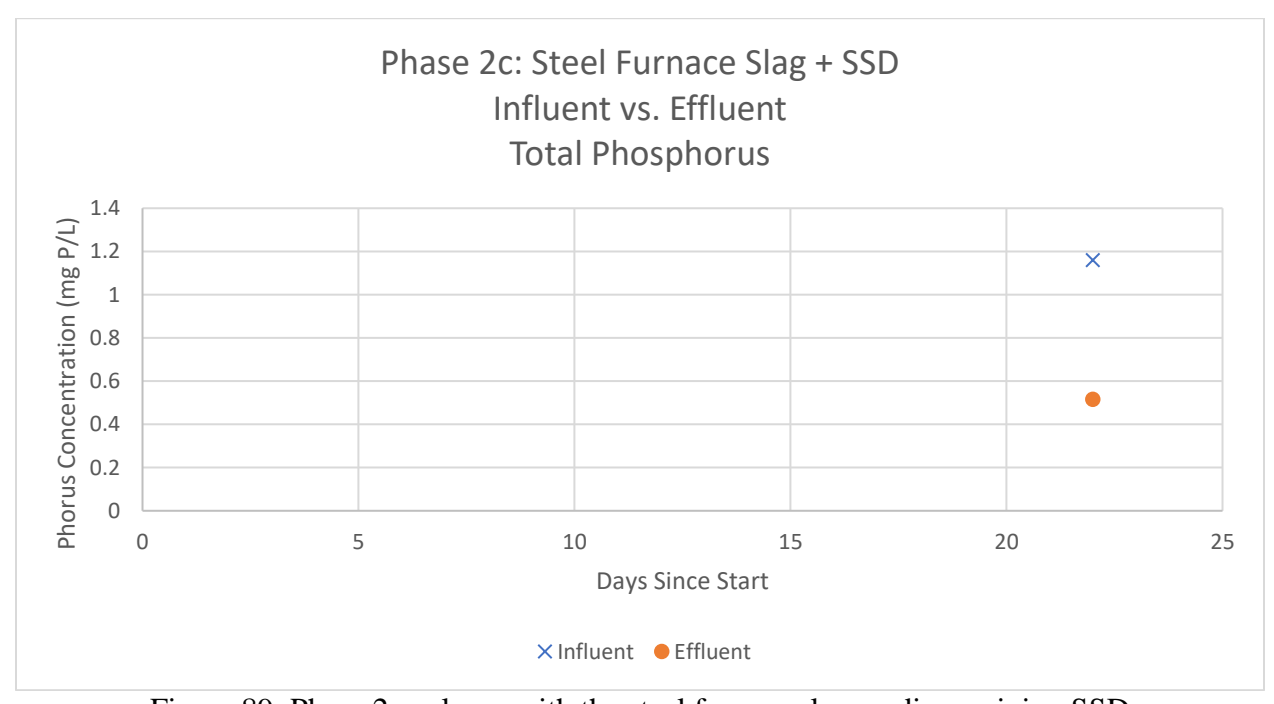


Figure 89: Phase 2c column with the steel furnace slag media receiving SSD

C.2.13. Column experiments – Phase 2c (Soluble Reactive Phosphorus)

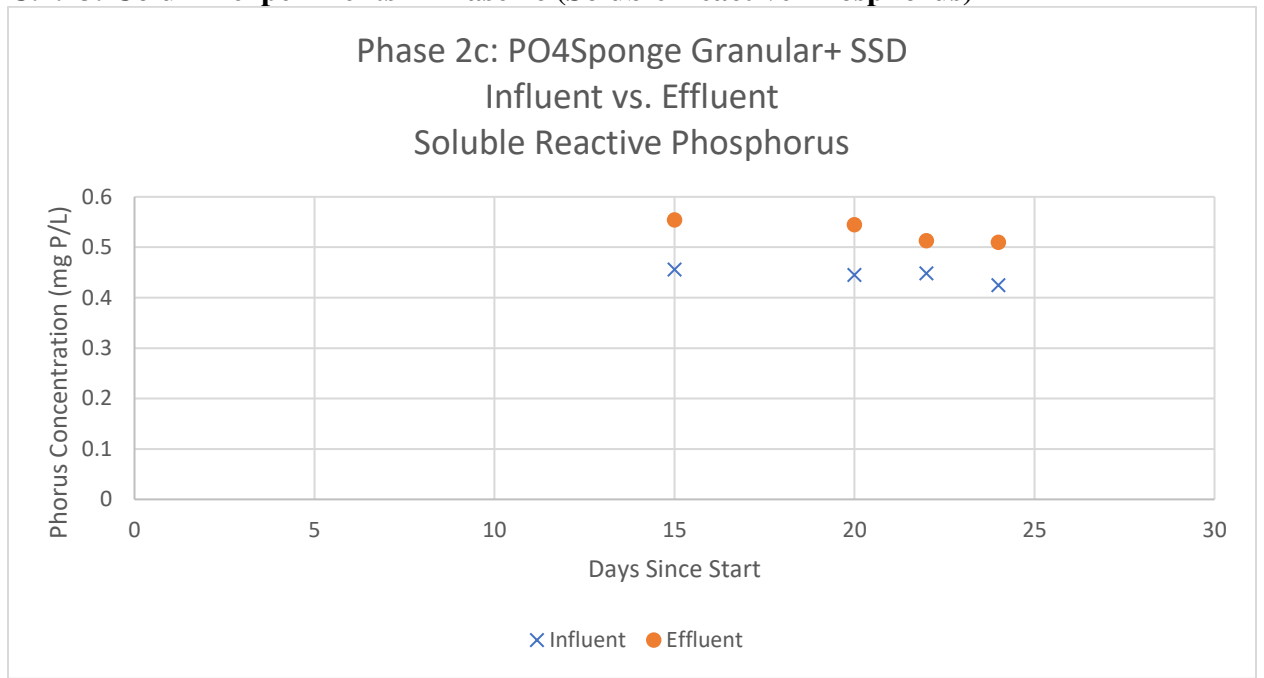


Figure 90: Phase 2c column with the PO4Spnge granular media receiving SSD

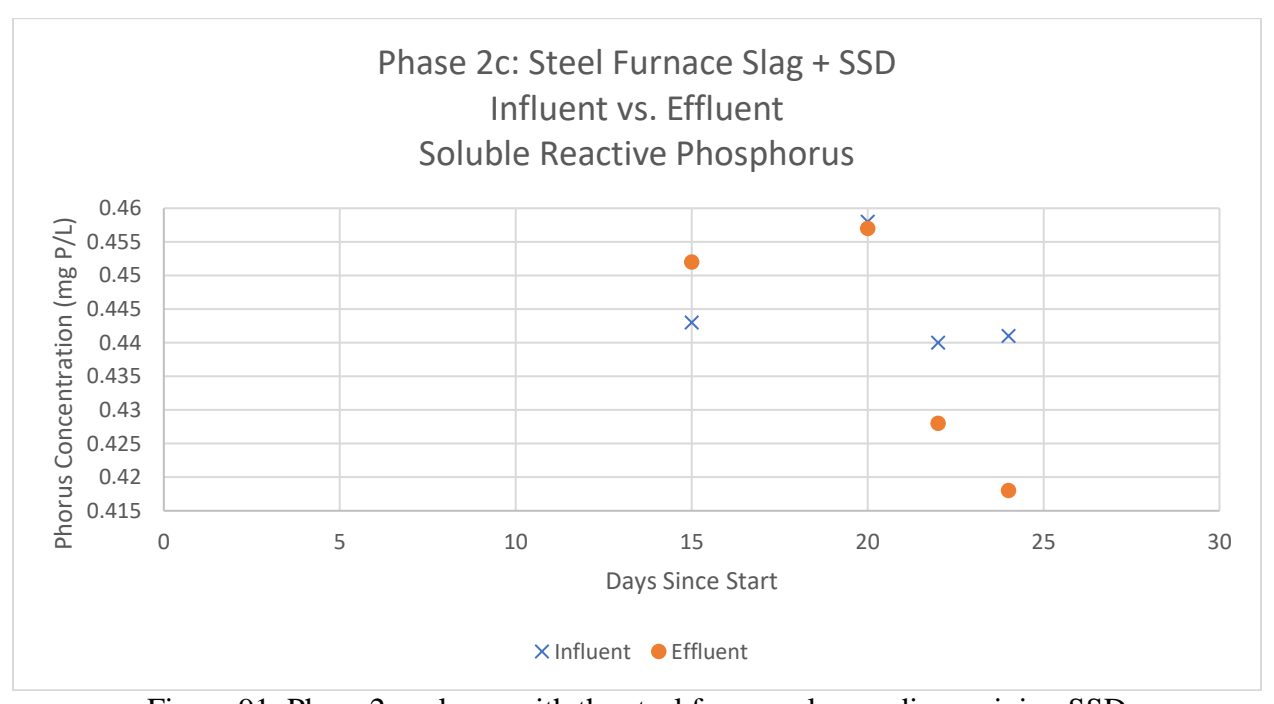


Figure 91: Phase 2c column with the steel furnace slag media receiving SSD

C.2.14. Column experiments – Phase 2d (Total Phosphorus)

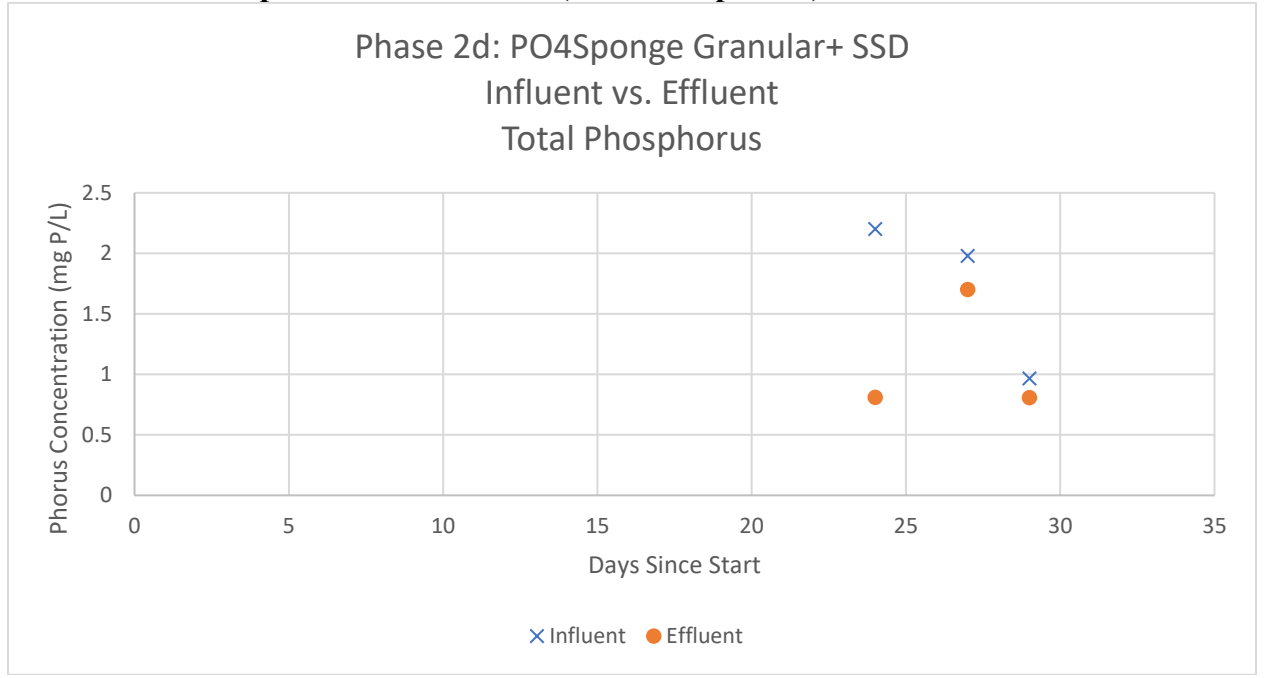


Figure 92: Phase 2d column with the PO4Spnge granular media receiving SSD

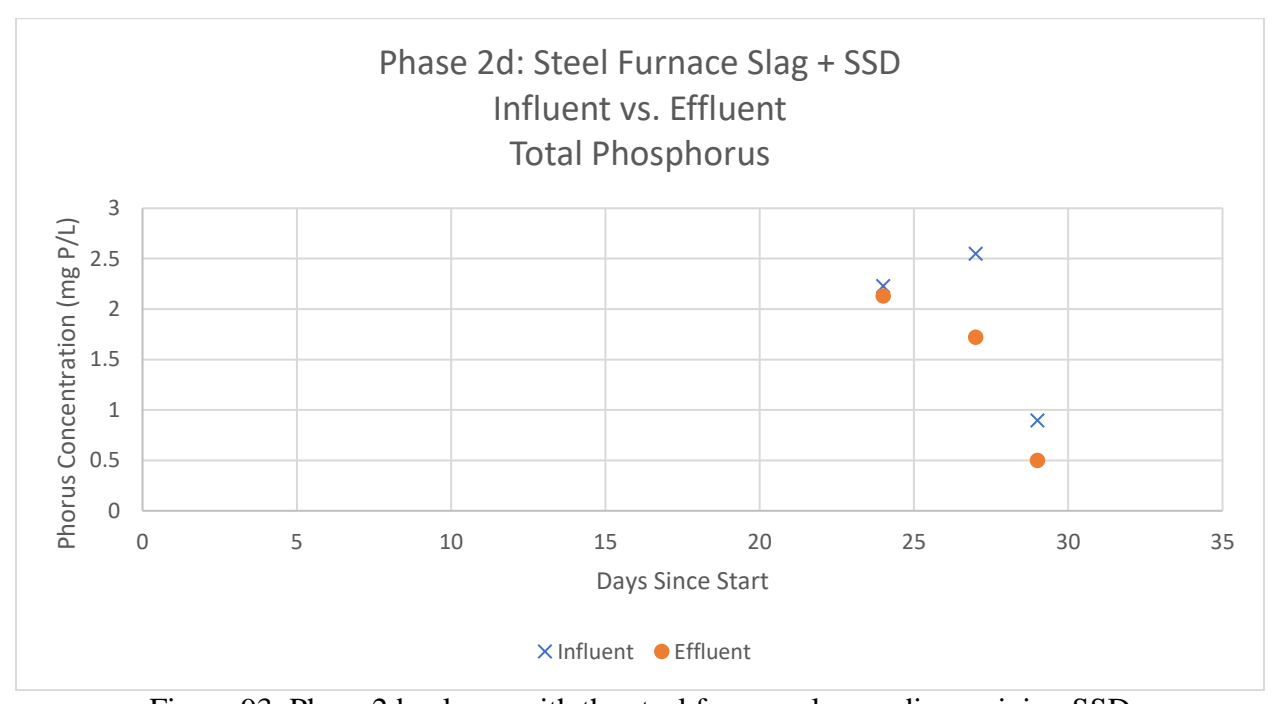


Figure 93: Phase 2d column with the steel furnace slag media receiving SSD

C.2.15. Column experiments – Phase 2d (Soluble Reactive Phosphorus)

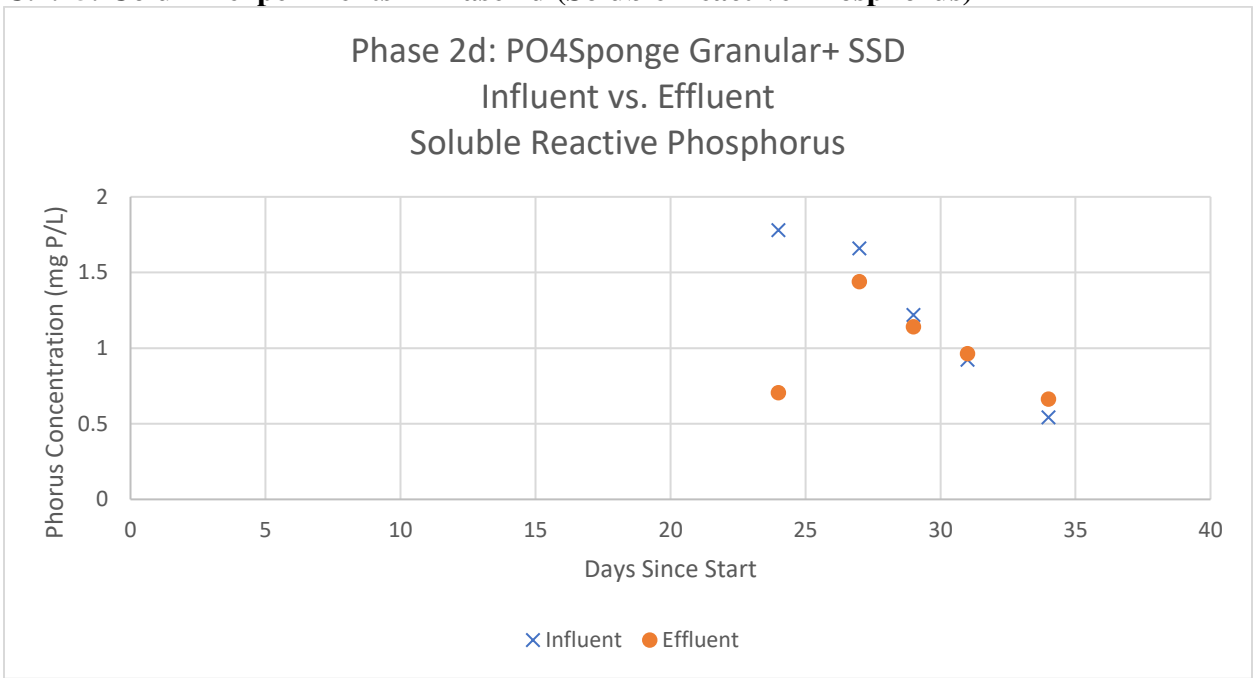


Figure 94: Phase 2d column with the PO4Spnge granular media receiving SSD

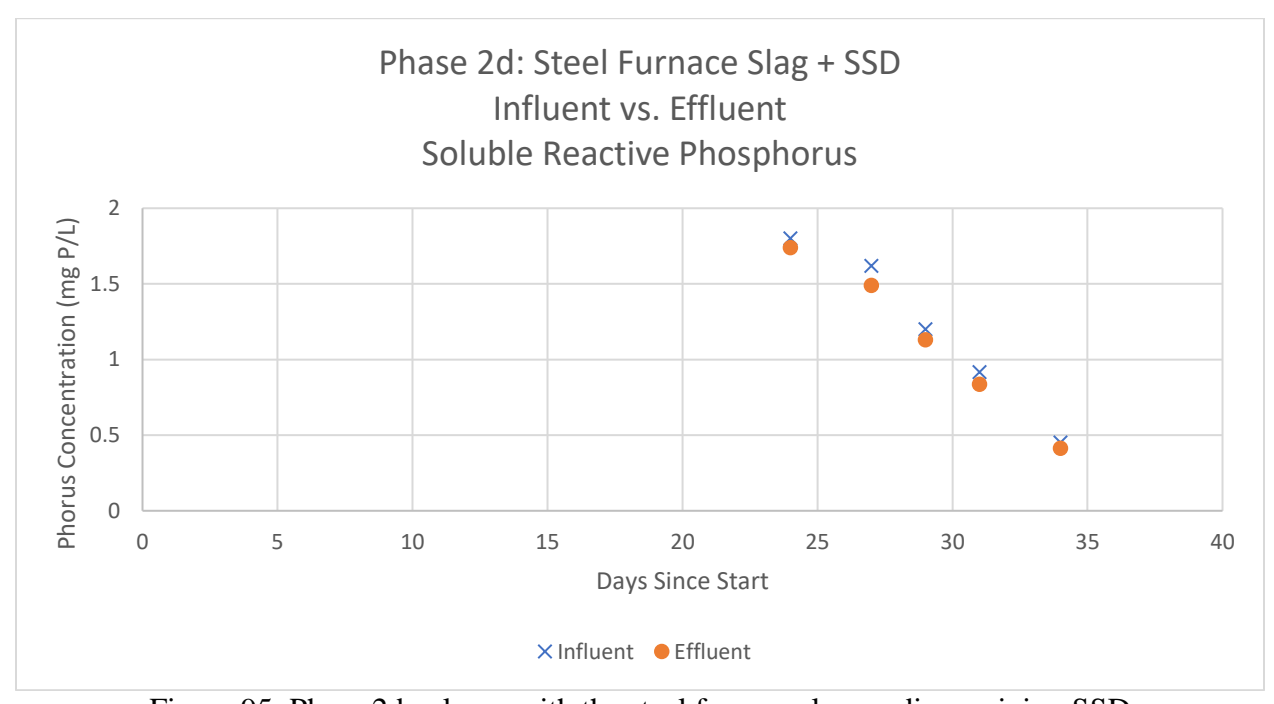


Figure 95: Phase 2d column with the steel furnace slag media receiving SSD

C.2.16. Column experiments – Phase 2e (Soluble Reactive Phosphorus – No Total Phosphorus Data)

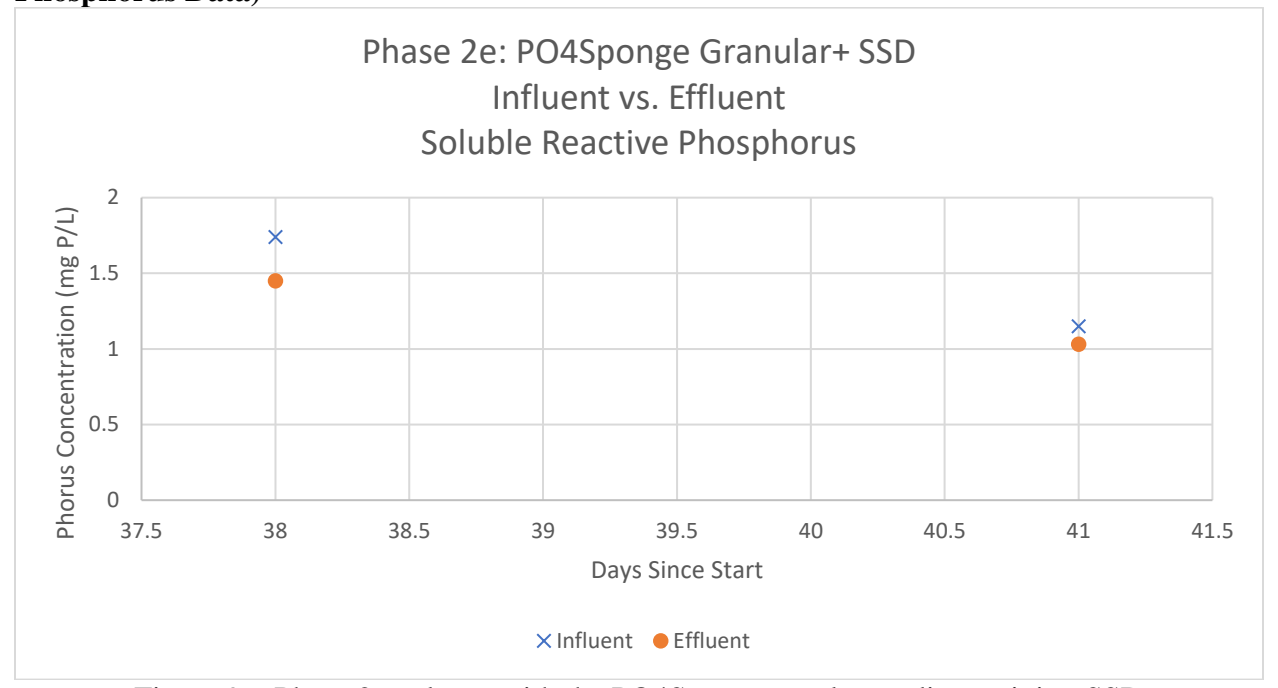


Figure 96: Phase 2e column with the PO4Spnge granular media receiving SSD

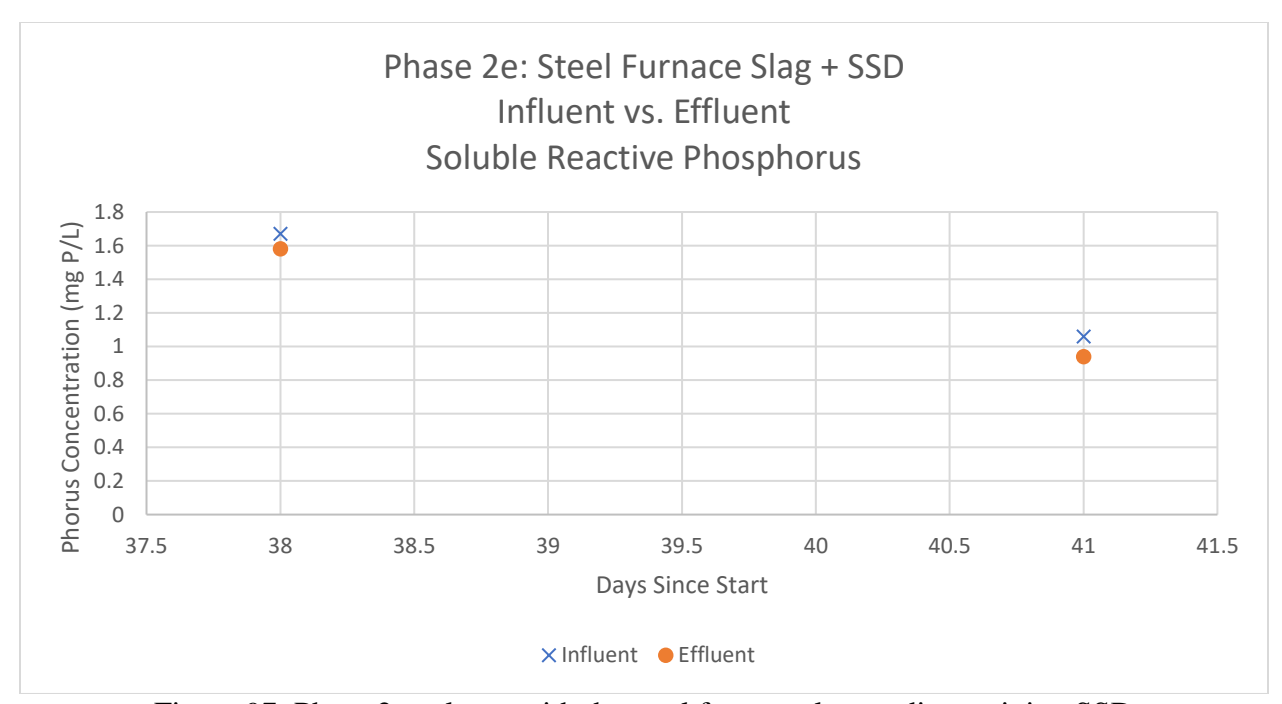


Figure 97: Phase 2e column with the steel furnace slag media receiving SSD

C.2.17. Column experiments – Phase 3 (Total Phosphorus)

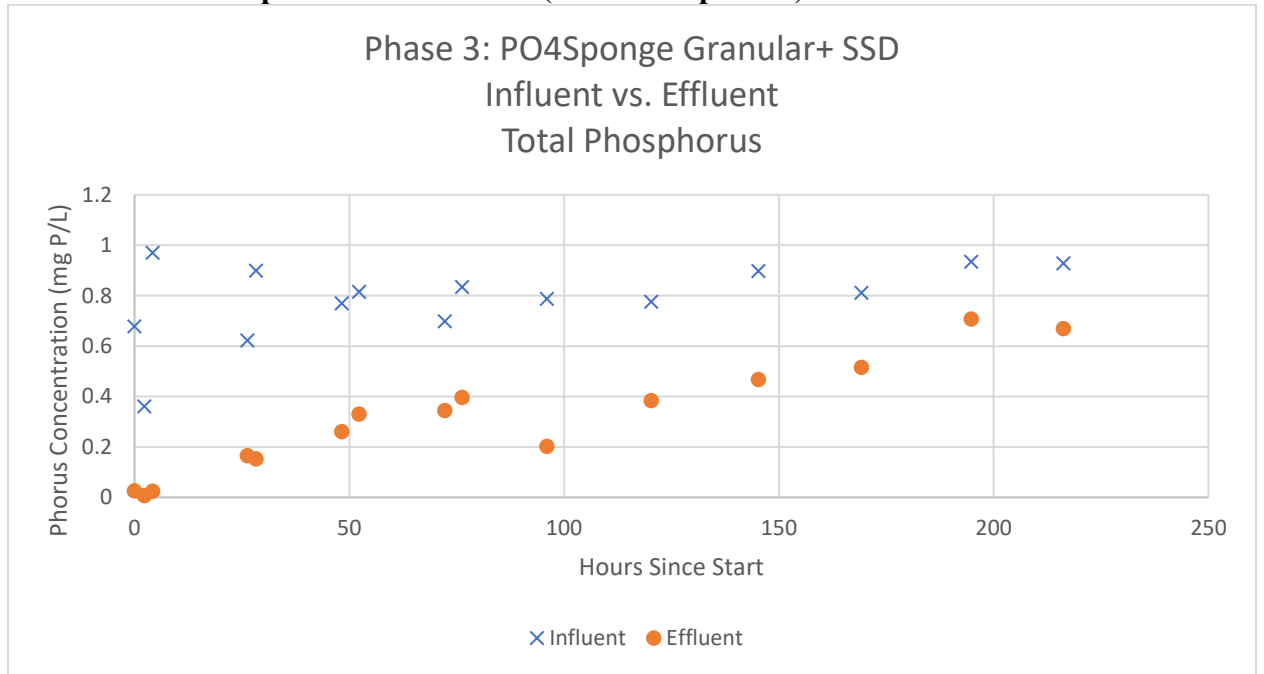


Figure 98: Phase 3 column with the PO4Spnge granular media receiving SSD

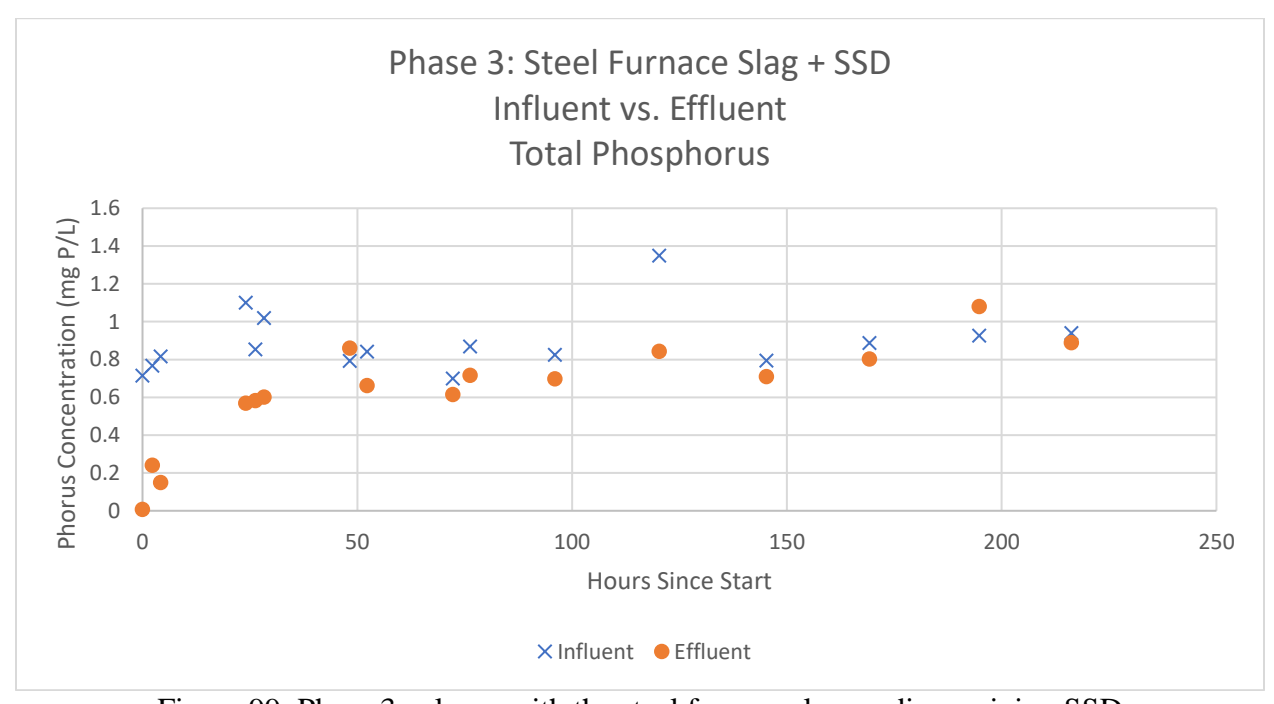


Figure 99: Phase 3 column with the steel furnace slag media receiving SSD

C.2.18. Column experiments – Phase 3 (Soluble Reactive Phosphorus)

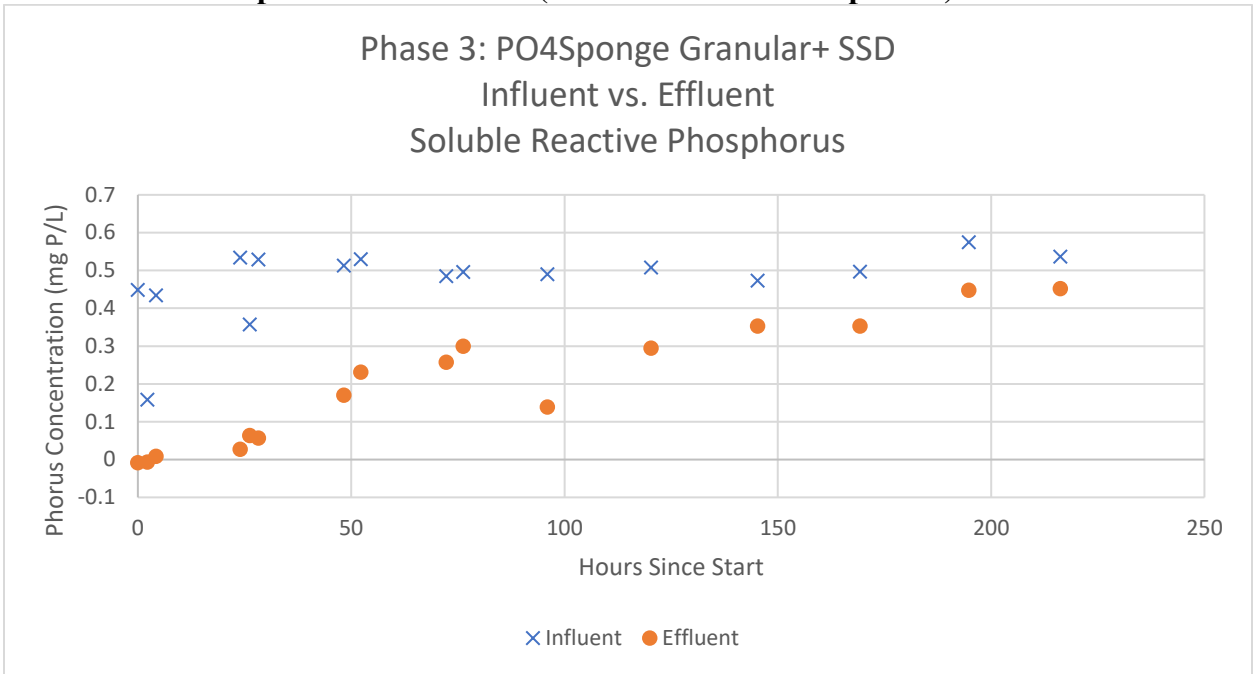


Figure 100: Phase 3 column with the PO4Spnge granular media receiving SSD

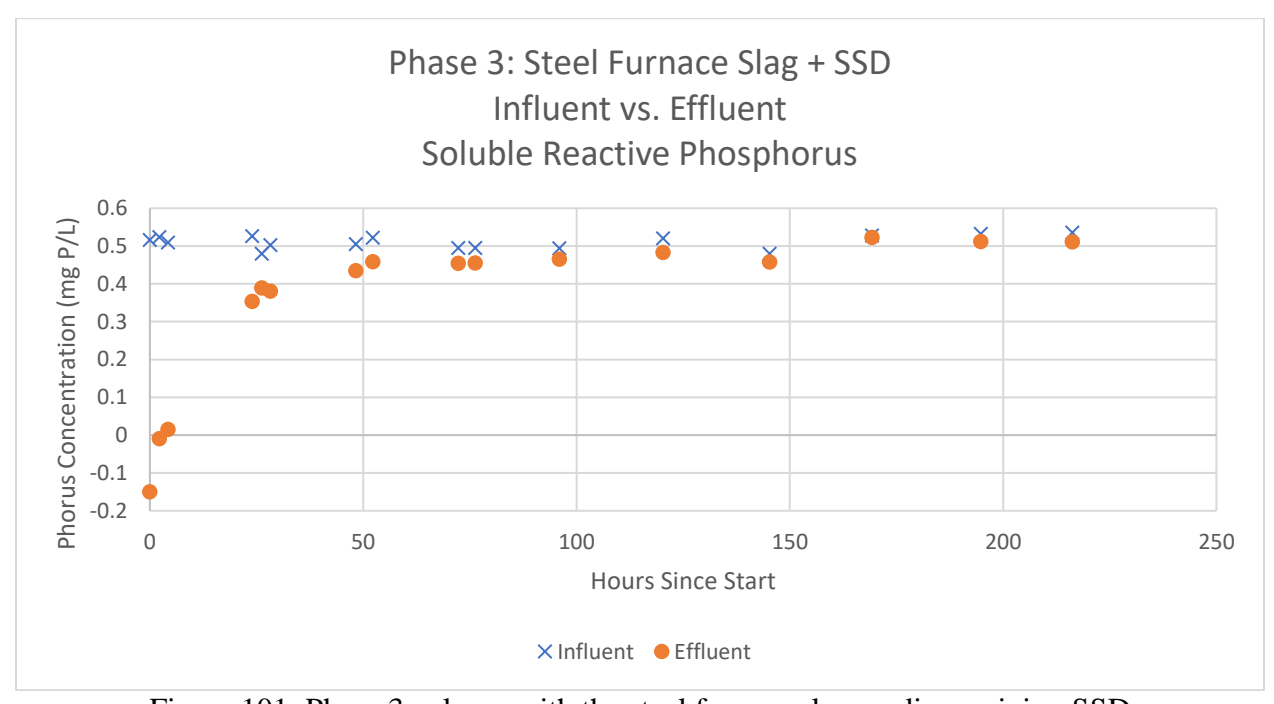


Figure 101: Phase 3 column with the steel furnace slag media receiving SSD

APPENDIX D – Sample Calculations

D.1. Synthetic Subsurface drainage Formulation Calculations

Calculation of Mass of Compounds for the SSD solution.

Equation 1: Molarity and concentration conversion of the same compound or ion:

$$M = \frac{C}{M_m}$$

Where: $M = \text{molarity (mol L}^{-1})$, $C = \text{concentration (mg L}^{-1})$, and $M_m = \text{molar mass of a compound or an ion (g mol}^{-1})$.

Equation 2: Molarity conversion between compound and ion:

$$r \cdot (X_a Y_b) = X \cdot \left(\frac{r}{r \cdot b}\right)$$

Where: r, a, and b = positive real numbers, and X_aY_b = compound that contains X_a and Y_b molecules or ions where X is a molecule or an ion of interests (mmol L⁻¹).

Example calculation of the mass of H_2KPO_4 ($m_{H_2KPO_4}$) for 100 gallons of SSD solution.

Given:

- Target SRP (C_P) = 0.2 mg L⁻¹ as PO₄-P
- Initial SRP in DI or tap water = 0.0 mg L^{-1} as PO₄-P
- Total volume of DI or tap water (V_{DI}). = 378.5 L =100 gallons
- Molar mass of P (M_{m_P}) = 30.97 (g mol⁻¹)
- Molar mass of $H_2KPO_4(M_{m_{H_2KPO_4}}) = 136.09 \text{ (g mol}^{-1})$

Calculate:

To calculate molarity of P (M_P) , input C_P and M_{m_P} values into Equation 1:

$$M_{\rm P} = \frac{C_{\rm P}}{M_{m_{\rm P}}} = \frac{0.2 \text{ (mg L}^{-1} as P)}{30.97 \text{ (g mol}^{-1})} = 0.00646 \text{ mmol L}^{-1}$$

To calculate molarity of H₂KPO₄, input P as an ion of interest into Equation 2:

$$1 \cdot (H_2KPO_4) = 0.00646 \ (mmol \ L^{-1}of \ P) \cdot$$

$$\left(\frac{1 \ mmol \ L^{-1} \ of \ H_2KPO_4}{1 \cdot 1 \ mmol \ L^{-1} \ of \ P}\right) = 0.00646 \ (mmol \ L^{-1} \ of \ H_2KPO_4)$$

To calculate $m_{\rm H_2KPO_4}$ to make around 378.5 L of SSD, input $M_{m_{\rm H_2KPO_4}}$ and $M_{\rm H_2KPO_4}$ values into Eq. B-1. Then multiply the result ($C_{\rm H_2KPO_4}$) by $V_{\rm DI}$ value:

$$m_{\text{H}_2\text{KPO}_4} = \left(M_{\text{H}_2\text{KPO}_4} \cdot M_{m_{\text{H}_2\text{KPO}_4}} \right) \cdot V_{DI}$$
$$= \left[0.00646 \ (mmol \ L^{-1} \) \cdot 136.09 \ (g \ mol^{-1}) \right] \cdot 378.5 \ (L) = 0.3327 \ (g)$$

End of example calculation

D.2. Feasibility Study Calculations

This section goes through how the cost comparisons in Table 17 were done for the selected media, PO4Sponge and steel furnace slag (SFS), based on the field data from "Site BN" (zip code: 49256). After analysis of the preliminary field data, 1.66 kg of SRP was lost through a tile drain responsible for draining 14.9 acres between January 2019 and June 2019. This timespan covers the period where the most phosphorus is lost through tile drains, which was determined using Table 14. The following cost of each scenario was calculated over a period of 15-years.

Step 1: Use the PO4Sponge and SFS data (

Table 27) from phase 3 of the column study to calculate the bulk density and media capacity (results summarized in Table 28). Assume that breakthrough capacity is when the media adsorbs 50% of the SRP required to exhaust the media.

Table 27: Column study phase 3 information for the PO4Sponge and steel furnace slag

	PO4Sponge	Steel Furnace Slag
Volume of Media (mL)	190	240
Mass of Media (g)	111.7	353.5
Amount of SRP Adsorbed to	131.4	57.32
Exhaust the Media (mg SRP)		

Equation 3: Bulk density of the PO4Sponge

$$\frac{111.7 \ g \ PO4Sponge}{190 \ mL \ PO4Sponge} = \frac{0.588 \ g \ PO4Sponge}{mL \ PO4Sponge}$$

Equation 4: Bulk density of the steel furnace slag

$$\frac{353.5 \text{ g SFS}}{240 \text{ mL SFS}} = \frac{1.473 \text{ g SFS}}{\text{mL SFS}}$$

Equation 5: Capacity for the PO4Sponge when exhaustion is reached

$$\frac{131.4 mg SRP}{111.7 g PO4Sponge} = \frac{1.176 mg SRP}{g PO4Sponge}$$

Equation 6: Capacity for the steel furnace slag when exhaustion is reached

$$\frac{57.32 mg SRP}{353.5 g SFS} = \frac{0.162 mg SRP}{g SFS}$$

Equation 7: Capacity for the PO4Sponge when breakthrough is reached

$$\frac{\left(\frac{1.176 \text{ mg SRP}}{g \text{ PO4Sponge}}\right)}{2} = \frac{0.588 \text{ mg SRP}}{g \text{ PO4Sponge}}$$

Equation 8: Capacity for the steel furnace slag when breakthrough is reached

$$\frac{\left(\frac{0.162 \ mg \ SRP}{g \ SFS}\right)}{2} = \frac{0.081 \ mg \ SRP}{g \ SFS}$$

Table 28: Summary of bulk density and capacity calculations for the PO4Sponge and steel furnace slag

	PO4Sponge	Steel Furnace Slag
Bulk Density (g/mL)	0.588	1.473
Capacity (mg SRP/g Media)	1.176	0.162
Breakthrough Capacity (mg	0.588	0.081
SRP/g Media)		

Step 2: Calculate the mass and volume of media required to treat 1.66 kg of SRP assuming breakthrough capacity and determine the estimated contactor cost for each option.

Equation 9: Mass of PO4Sponge required to treat 1.66 kg SRP assuming breakthrough capacity

$$1.66 \ kg \ SRP * \frac{g \ PO4Sponge}{0.588 \ mg \ SRP} * \frac{10^6 \ mg}{kg} * \frac{kg}{10^3 \ g} = 2,823 \ kg \ PO4Sponge$$

Equation 10: Mass of steel furnace slag required to treat 1.66 kg SRP assuming breakthrough capacity

$$1.66 \ kg \ SRP * \frac{g \ SFS}{0.081 \ mg \ SRP} * \frac{10^6 \ mg}{kg} * \frac{kg}{10^3 \ g} = 20,494 \ kg \ SFS$$

Equation 11: Volume of PO4Sponge required to treat 1.66 kg SRP assuming breakthrough capacity

2,823 kg PO4Sponge *
$$\frac{mL\ PO4Sponge}{0.588\ g\ PO4Sponge}$$
 * $\frac{10^3\ g}{kg}$ * $\frac{L}{10^3\ mL}$ * $\frac{m^3}{10^3\ L}$ = 4.80 $m^3\ PO4Sponge$

4.80
$$m^3$$
 PO4Sponge * $\frac{264 \ gallons}{m^3}$ = 1267 gallons of PO4Sponge

Equation 12: Volume of steel furnace slag required to treat 1.66 kg SRP assuming breakthrough capacity

20,494 kg SFS *
$$\frac{mL\ SFS}{1.473\ g\ SFS}$$
 * $\frac{10^3\ g}{kg}$ * $\frac{L}{10^3\ mL}$ * $\frac{m^3}{10^3\ L}$ = 13.91 $m^3\ SFS$

13.91
$$m^3 SFS * \frac{264 \ gallons}{m^3} = 3672 \ gallons \ of \ SFS$$

Table 29: Summary of calculations used to determine the mass and volume of PO4Sponge and steel furnace slag required to treat 1.66 kg of SRP assuming breakthrough capacity

	PO4Sponge	Steel Furnace Slag
Mass of Media (kg)	2,823	20,494
Volume of Media (m ³)	4.80	13.91

Step 3: Calculate the media contactor, labor, and installation costs

1. First, the cost of septic tanks was pulled from Table 30 below:

Table 30: Costs of the PO4PSonge and SFS contactors

Tank Size (Gallons)	Capital Cost (\$)	Shipping Cost from Hagerstown, MD to Site BN (Zip code: 49256) (\$)	Total Cost (\$)
PO4Sponge 1,500 (850 lbs)	\$6,271	\$414	\$6,685
SFS 4,000 (1,400 lbs)	\$10,503	\$366	\$10,869

^{*}https://www.rainharvest.com/xerxes-fiberglass-tanks.asp → used for weight

^{*}https://alternativesepticsystems.com/pdf/catalogs/Xerxes%20tanks%20and%20accessories%20 and%20price%20list.pdf → used for prices

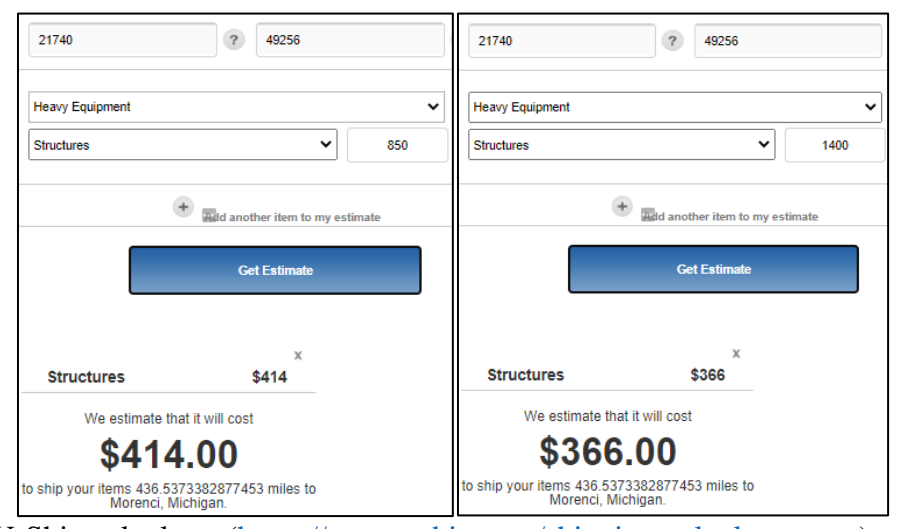


Figure 102: U-Ship calculator (https://www.uship.com/shipping-calculator.aspx) cost to ship the contactor for the PO4Sponge and SFS

- 2. Next, the cost of labor used the average hourly pay for a general contractor (from https://www.payscale.com/research/US/Job=General_Contractor/Hourly_Rate), which was \$30/hour. It was assumed that two contractors were required for one, 8-hour day to work on the installation of the contactor and/or media. This results in a total of 16 paid hours. The total cost for installation for the PO4Sponge and SFS was \$480.
- 3. Lastly, it was assumed that the installation required a backhoe. The average hourly backhoe rental with an operator costs between \$60 to \$100 per hour (from

https://www.thepricer.org/backhoe-price/
). This averages to \$80/hour. Assuming an 8-hour day and one backhoe, the contactor installation cost for the PO4Sponge and SFS was \$640.

Table 31: The cost of the media contactor, labor, and installation

	PO4Sponge	Steel Furnace Slag
Estimated Contactor Cost	\$6,685	\$10,869
Labor Cost	\$480	\$480
Contactor Installation Cost	\$640	\$640

Step 4: Calculate the annual cost of the PO4Sponge adsorption media to treat 1.66 kg of SRP, which includes the following tasks:

- Task A The PO4Sponge capital cost
- Task B The cost to ship the PO4Sponge from the manufacturer, MetaMateria (zip code: 43228) to "Site BN" (zip code: 49256)
- Task C The cost to ship the PO4Sponge from "Site BN" (zip code: 49256) back to
 MetaMateria (zip code: 43228) for regeneration
- Task D The cost to regenerate the PO4Sponge at the manufacturer, MetaMateria
- Task E The cost to regenerate the PO4Sponge on-site
- Task F The cost to ship the PO4Sponge from the manufacturer, MetaMateria (zip code: 43228) to "Site BN" (zip code: 49256) after regeneration
- Task G The value of regenerated, or recovered phosphorus from the PO4Sponge media as dicalcium phosphate
- Task H The estimated cost of the contactor, labor, and installation from Table 30
- Task I The cost to dispose the PO4Sponge after 15 years

And assumptions:

- a. That the farmer has the equipment and time to maintain and remove the media
- b. The PO4Sponge lasts 15 years with the proper regeneration
- c. Regeneration of the PO4Sponge is done once a year
- d. The cost to regenerate the PO4Sponge on-site is half the cost of regenerating the PO4Sponge at the manufacturer

- e. 100% of the SRP adsorbed onto the PO4Sponge media can be regenerated off as calcium phosphate (Ca₃(PO₄)₂)
- f. Calcium phosphate cost is \$322/500 grams (Fisher Scientific; catalog no. C133-500), or
 \$0.64/gram
- g. Scenario A: Assume that the cost to regenerate the PO4Sponge via MetaMateria includes only the cost of the regeneration and that the value of the recovered phosphorus as dicalcium phosphate is already included in the cost to regenerate by the manufacturer, MetaMateria. Also assume that the recovered calcium phosphate is not sent back to farmer because it would cost to ship back to farm & would cost time and money to get into a usable product after regeneration
- h. <u>Scenario B</u>: Assume that the cost to regenerate the PO4Sponge <u>on-site</u> includes the cost of the regeneration minus the value of the recovered phosphorus as dicalcium phosphate

Step 4-1: Calculate the capital cost of the total required mass of PO4Sponge (Task A)

Equation 13: Annual capital cost of the PO4Sponge when the PO4Sponge is assumed to last 15 years

$$\frac{\$19}{kg\ PO4Sponge} * 2,823\ kg\ PO4Sponge = \$53,637$$

$$\frac{\$53,637}{15 \ years} = \frac{\$3,580}{year}$$

<u>Step 4-2</u>: Calculate the total shipping cost (Task B, Task C, and Task F) using shipping estimates from U-ship (https://www.uship.com/shipping-calculator.aspx)

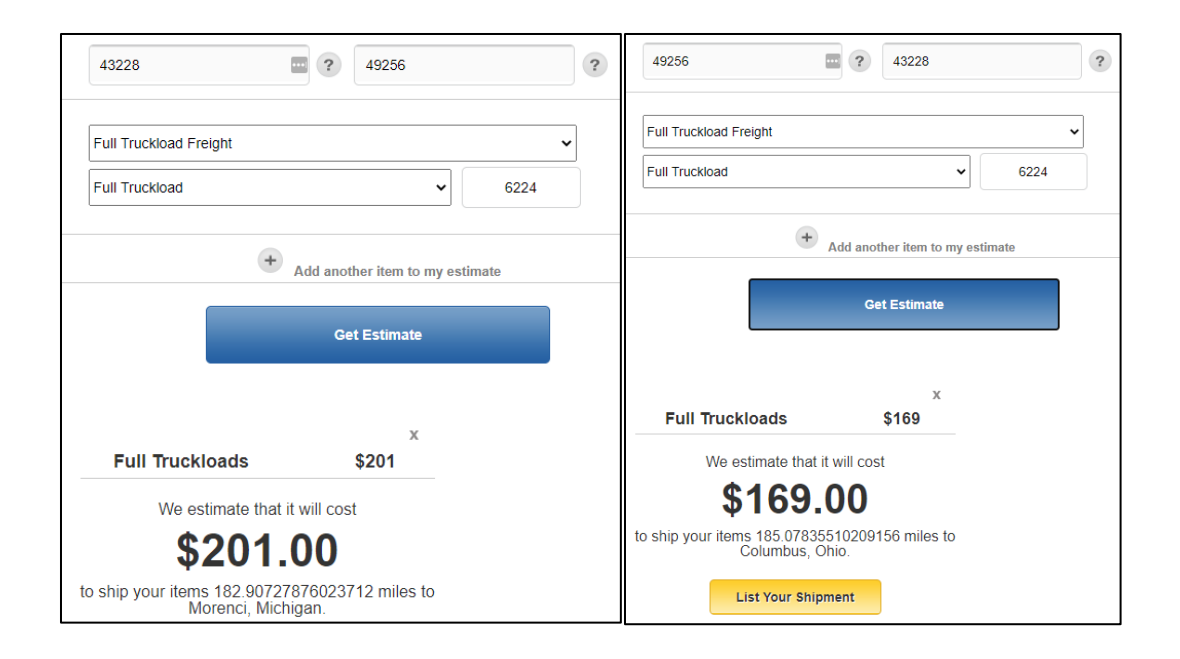


Figure 103: Uship.com cost estimates for shipping PO4Sponge (Left) from manufacturer to farm; (right) from farm to manufacturer

Task B: Shipping 2,823 kg (6224 lbs) of PO4Sponge from manufacturer (zip code: 43228) to farm (zip code: 49256)

- Full truckload freight; full truckload; mass: 6224 pounds
 - o Costs \$201; 183 miles

Task C: Shipping 2,823 kg (6224 lbs) of PO4Sponge from farm (zip code: 49256) to manufacturer (zip code: 43228) for regeneration

- Full truckload freight; full truckload; mass: 6224 pounds
 - o Costs \$169; 185 miles

Task F: Shipping 2,823 kg (6224 lbs) of PO4Sponge from manufacturer (zip code: 43228) to farm (zip code: 49256) after regeneration costs \$310

- Full truckload freight; full truckload; mass: 6224 pounds
 - Costs \$201; 183 miles

Scenario A: Total annual shipping cost for 2,823 kg of PO4Sponge is \$571/year (\$1/mile)

Scenario B: Total annual shipping cost for 2,823 kg of PO4Sponge is \$201/year (\$1.10/mile)

Step 4-3: Calculate the cost to regenerate the PO4Sponge at MetaMateria (Task D)

Equation 14: Cost of regeneration for 2,823 kg of PO4Sponge

$$\frac{\$2}{kg \ PO4Sponge \ regenerated} * 2,823 \ kg \ PO4Sponge = \frac{\$5,650}{regeneration}$$

Step 4-4: Calculate the value of recovered dicalcium phosphate produced during regeneration (Task G)

Equation 15: Amount of soluble reactive phosphorus, PO₄³⁻ adsorbed to 2,823 kg of PO4Sponge assuming breakthrough capacity for the media

2,823 kg PO4Sponge *
$$\frac{0.588 \, mg \, SRP}{g \, PO4Sponge}$$
 * $\frac{10^3 \, g}{kg}$ * $\frac{g}{10^3 \, mg}$ = 1,660 g SRP

According to MetaMateria, the manufacturer of the PO4Sponge, states in the regeneration instructions that 6-7 regeneration cycles remove more than 99% of the SRP on the media, so assume that 100% of the SRP can be removed and recovered as calcium phosphate [139].

Equation 16: Amount and cost of calcium phosphate produced from 1,660 g of PO₄³⁻ if all 1,660 g of PO₄³⁻ react

$$1,660 \ g \ PO_4^{\ 3-} * \frac{mol \ PO_4^{\ 3-}}{94.971 \ g \ PO_4^{\ 3-}} * \frac{1 \ mol \ Ca_3(PO_4)_2}{2 \ mol \ PO_4^{\ 3-}} * \frac{310.2 \ g \ Ca_3(PO_4)_2}{mol \ Ca_3(PO_4)_2}$$
$$= 2,711 \ g \ Ca_3(PO_4)_2$$

$$2,711 g Ca_3(PO_4)_2 * \frac{\$0.64}{g Ca_3(PO_4)_2} = \$1735$$

Step 4-5: Calculate the cost to regenerate the PO4Sponge on-site assuming that this costs half as much as regenerating the PO4Sponge by the manufacturer and that the value of calcium phosphate is subtracted from the final regeneration cost (Task E)

Equation 17: Cost to regenerate 2,823 kg of PO4Sponge on-site

$$\frac{\$1}{kg\ PO4Sponge\ regenerated} * 2,823\ kg\ PO4Sponge = \$2,823 - \$1,735 = \frac{\$1,088}{Regeneration}$$

• <u>Step 4-6:</u> Calculate the cost of disposal for the PO4Sponge using the disposal cost information in Table 32 (

Task I)

Equation 18: Convert volume of PO4Sponge from m³ to yd³

$$4.80 \ m^3 PO4Sponge * \frac{1.308 \ yd^3}{m^3} = 6.28 \ yd^3 \ PO4Sponge$$

Equation 19: Calculate the total disposal cost including the entrance fee for one day and general waste disposal cost

Entrance Fee
$$\rightarrow \frac{\$12}{day} * 1 day = \$12$$

General Waste Disposal Cost
$$\rightarrow \frac{\$28}{yd^3} * 6.28 \ yd^3 \ PO4Sponge = \$176$$

Total Cost of Disposal
$$\rightarrow$$
 \$12 + \$176 = \$188

<u>Step 5</u>: Calculate the annual cost of the steel furnace slag adsorption media to treat 1.66 kg of SRP, which includes the following tasks:

 Task J - The steel furnace slag capital cost and the cost to ship the steel furnace slag from the manufacturer, Edward Levy (zip code: 48120; shipped from Levy Plant #6 in Dearborn, MI) to "Site BN" (zip code: 49256)

- Task K The cost of the vacuum truck rental (<u>www.vactruckrental.com</u>; (888)-955-2087;
 13075 Newburgh Rd, Livonia, MI 48150; customer service representative recommends
 "vac-all jet combo") used to remove the steel furnace slag
- Task L The cost of the vacuum truck fuel when it drives from (1) the rental site to "Site BN" (2) "Site BN" to the Ann Arbor Recycling Center (3) from the Ann Arbor Recycling Center to the rental site <u>AND</u> the cost of additional fuel used for operation <u>AND</u> the cost to fill the fuel tank back to full after the rental period is over
- Task M The cost of disposal for the used steel furnace slag at the Ann Arbor Recycling
 Center (2950 E. Ellsworth Rd, Ann Arbor, MI 48108)
- Task N: The estimated cost of the contactor, labor, and installation from Table 30

And Assumptions:

- a. The capital and shipping cost for the steel furnace slag is \$49.92/ton (given by Edward Levy Company)
- b. The farmer has the necessary equipment to maintain the media
- c. The farmer does not have the necessary equipment to install and remove the media
- d. The vacuum truck can access the Ann Arbor Recycling Center categorized as a "large vehicle"
- e. The vacuum truck rental is for 2 days where the first half of the media is removed and disposed on the first day, and the second half of the media is removed and disposed on the second day
 - a. The vacuum truck drives from the rental site → "Site BN" → Ann Arbor
 Recycling Center → "Site BN" on day 1

- b. The vacuum truck drives from "Site BN" → Ann Arbor Recycling Center → rental site on day 2
- f. The fuel required to operate the vacuum truck while idle and removing the media totals to half the volume of one full tank of diesel fuel. This occurs during each media removal at the farm and each time media is disposed at the recycling center (4 times total).
- g. The diesel fuel cost for the Midwest region in June 2019 is \$2.978/gallon (https://www.eia.gov/petroleum/gasdiesel/)
- h. The vacuum truck has a full tank of fuel at the start of the rental period

Table 32: Vacuum truck costs, transport information, and fees for recycling center

Vacuum Truck Rental Cost	\$725/truck/day
Vacuum Truck Holding Capacity	$3,000 \text{ gallons} = 11 \text{ m}^3$
Vacuum Truck Diesel Fuel Tank Volume	113 gallons
Vacuum Truck Mileage	7.5 MPG
Vacuum Truck Rental Zip Code	48150
Ann Arbor Recycling Center Zip Code	48108
"Site BN" / Farm Zip Code	49256
Distance between Vacuum Truck Rental and Farm	86 miles
Distance between Farm and Recycling Center	65 miles
Distance between Recycling Center and Vacuum Truck Rental	28 miles
Cost of Diesel Fuel in Midwest	\$2.978/gallon
Entrance Fee for Large Vehicle to Recycling Center	\$12/vehicle/day
General Waste Disposal Cost at Recycling Center	\$28/yd ³

<u>Step 5-1</u>: Calculate the capital and shipping cost of the total required mass of steel furnace slag based on the cost estimate given by the Edward Levy Company in Dearborn, MI (Task J)

Equation 20: Capital and shipping cost of 20,494 kg of steel furnace slag

$$\frac{\$49.92}{ton\ SFS} * 20,494\ kg\ SFS * \frac{lb}{0.454\ kg} * \frac{ton}{2000\ lb} = \$1,130$$

Step 5-2: Calculate the cost of the vacuum truck rental and fuel required for the vacuum truck operation (Task K and Task L)

Equation 21: Cost to rent one vacuum truck for two days

$$\frac{\left(\frac{\$725}{truck}\right)}{day} * 2 days = \$1,450$$

Equation 22: Total distance (miles) required for vacuum truck

Day 1 =
$$86 \text{ miles} + 65 \text{ miles} + 65 \text{ miles} = 216 \text{ miles}$$

$$Day 2 = 65 \text{ miles} + 28 \text{ miles} = 93 \text{ miles}$$

 $Total \ Distance = 93 \ miles + 216 \ miles = 309 \ miles$

Equation 23: Total fuel costs for vacuum truck

Distance Traveled
$$\rightarrow$$
 309 miles * $\frac{gallons}{7.5 \text{ miles}} = 42 \text{ gallons of diesel fuel}$

$$\textbf{Operation} \rightarrow \frac{113 \ gallons}{fuel \ tank} * \frac{1}{2} = \frac{57 \ gallons}{removal \ period} * 4 \ removal \ periods$$

= 228 gallons of diesel fuel

Tank Full Upon Return

 \rightarrow |113 gallons starting - 42 gallons driving - 228 gallons operation|

= 157 gallons of fuel required to have a full tank after use

Total Cost of Fuel
$$\rightarrow$$
 157 gallons * $\frac{$2.978}{gallon}$ = \$470

Total Cost of Vacuum Truck \rightarrow \$1,450 + \$470 = \$1920/year

Step 5-3: Calculate the cost of disposing the steel furnace slag at the Ann Arbor Recycling Center (Task M)

Equation 24: Convert volume of steel furnace slag from m³ to yd³

$$13.91 \ m^3 SFS * \frac{1.308 \ yd^3}{m^3} = 19 \ yd^3 \ SFS$$

Equation 25: Calculate the volume of steel furnace slag to be removed and disposed per day

$$\frac{19 \ yd^3 \ SFS}{2 \ days} = \frac{9.5 \ yd^3 \ SFS}{day}$$

Equation 26: Calculate the total disposal cost including the entrance fee for two days and general waste disposal cost

Entrance Fee
$$\rightarrow \frac{\$12}{day} * 2 days = \$24$$

General Waste Disposal Cost
$$\rightarrow \frac{\$28}{yd^3} * \frac{9.5 \ yd^3 \ SFS}{day} * 2 \ days = \$532$$

Total Cost of Disposal \rightarrow \$24 + \$532 = \$556

Step 6: Calculate the cost for each scenario for a 15-year period

Table 33: Cost of Scenario A for 15-years

	Year 0	Year 1 to 14	Year 15
Media Capital Cost	\$53,623	N/A	N/A
Contactor Capital Cost	\$6,685	N/A	N/A
Contactor Installation	\$640	N/A	N/A
Cost			
Labor to Install/Re-Install	\$480	\$480	N/A
Media in Contactor			
Shipping Cost	\$201	\$370	N/A
Regeneration Cost	N/A	\$5,645	N/A
Labor to Remove Media	N/A	\$480	\$480
from Contactor			
Removal Cost via	N/A	N/A	N/A
Vacuum Truck			
Disposal Cost	N/A	N/A	\$188
Annual Cost (Separate)	\$61,215/year	\$6,975/year	\$668/year
Total Cost (Separate)	\$61,215	\$97,643	\$668
Total Cost (Together)	\$159,526 for 15 years		
Annual Cost	\$10,635/year		

- Assume that year 14 is the last time the media is shipped back to the farm after regeneration and that there is no shipping or regeneration after year 15, just the cost of labor to remove the media and disposal costs
- Assume that the farmer can transport the PO4Sponge to the disposal site without the use of a vacuum truck

Table 34: Cost of Scenario B for 15-years

	Year 0	Year 1 to 14	Year 15
Media Capital Cost	\$53,623	N/A	N/A
Contactor Capital Cost	\$6,685	N/A	N/A
Contactor Installation	\$640	N/A	N/A
Cost			
Labor to Install/Re-Install	\$480	\$480	N/A
Media in Contactor			
Shipping Cost	\$201	N/A	N/A
Regeneration Cost	N/A	\$1,088	N/A
Labor to Remove Media	N/A	\$480	\$480
from Contactor			

Table 31 (cont'd)

Removal Cost via	N/A	N/A	N/A
Vacuum Truck			
Disposal Cost	N/A	N/A	\$188
Annual Cost (Separate)	\$61,215/year	\$2,047/year	\$668/year
Total Cost (Separate)	\$61,215	\$28,661	\$668
Total Cost (Together)	\$90,554 for 15 years		
Annual Cost	\$6,036/year		

- Assume that year 14 is the last time the media is regenerated, and there is no regeneration after year 15, just the cost of labor to remove the media and disposal costs
- Assume that the farmer can transport the PO4Sponge to the disposal site without the use of a vacuum truck

Table 35: Cost of Scenario C for 15-years

	Year 0	Year 1 to 14	Year 15
Media Shipping & Capital	\$1,130	\$1,130	N/A
Cost			
Contactor Capital Cost	\$10,869	N/A	N/A
Contactor Installation	\$640	N/A	N/A
Cost			
Labor to Install/Re-Install	\$480	\$480	N/A
Media in Contactor			
Regeneration Cost	N/A	N/A	N/A
Labor to Remove Media	N/A	\$480	\$480
from Contactor			
Removal Cost via	N/A	\$1,909	\$1,909
Vacuum Truck			
Disposal Cost	N/A	\$556	\$556
Annual Cost (Separate)	\$13,119/year	\$4,529/year	\$2,922 /year
Total Cost (Separate)	\$13,119	\$63,406	\$2,922
Total Cost (Together)	\$79,078 for 15 years		
Annual Cost	\$5,272/year	·	

 Assume that no new SFS media is purchased at the start of year 15, there are only removal and disposal costs REFERENCES

REFERENCES

- 1. Paytan, A. and K. McLaughlin, *The Oceanic Phosphorus Cycle*. Chemical Reviews, 2007. **107**(2): p. 563-576.
- 2. Beegle, D., *Comparing Fertilizer Materials*, in *Agronomy Facts 6*. 1985, Pennsylvania State University: College of Agricultural Sciences.
- 3. Cordell, D., et al., *The story of phosphorus: Global food security and food for thought.* Global Environmental Change, 2009. **19**(2): p. 292-305.
- 4. Reijnders, L., *Phosphorus resources, their depletion and conservation, a review.* Resources, Conservation & Recycling, 2014. **93**: p. 32-49.
- 5. Gérard, F., *Clay minerals, iron/aluminum oxides, and their contribution to phosphate sorption in soils A myth revisited.* Geoderma, 2016. **262**: p. 213-226.
- 6. Lake Erie Algae, *Different Types of Phosphorus*. Heidelberg University.
- 7. Murphy, S. *General Information on Phosphorus*. 2007 Monday April 23, 2007; Available from: http://bcn.boulder.co.us/basin/data/NEW/info/TP.html.
- 8. HACH. What is the difference between reactive, acid hydrolyzable, and total phosphorus? 2018; Available from: https://support.hach.com/app/answers/answer_view/a_id/1000294/~/what-is-the-difference-between-reactive%2C-acid-hydrolyzable%2C-and-total.
- 9. Zeckoski, R.W., *Hydrologic and Water Quality Terminology as Applied to Modeling.* Transactions of the ASABE, 2015. **58**(6): p. 1619-1635.
- 10. US EPA. *The Sources and Solutions: Agriculture*. Nutrient Pollution n.d.; Available from: https://www.epa.gov/nutrientpollution/sources-and-solutions-agriculture.
- 11. Warncke, D., J. Dahl, and L. Jacobs, *Nutrient Recommendations for Field Crops in Michigan*. 2009, Michigan State University: Department of Crop and Soil Sciences.
- 12. Carmichael, W.W. and G.L. Boyer, *Health impacts from cyanobacteria harmful algae blooms: Implications for the North American Great Lakes.* Harmful Algae, 2016. **54**: p. 194-212.
- 13. Carpenter, S.R., *Eutrophication of Aquatic Ecosystems: Bistability and Soil Phosphorus.* Proceedings of the National Academy of Sciences of the United States of America, 2005. **102**(29): p. 10002-10005.
- 14. Sharpley, A.R., Seppo, *PHOSPHORUS IN AGRICULTURE AND ITS ENVIRONMENTAL IMPLICATIONS*. Centre for Agriculture and Biosciences International, 1996.
- 15. Hartig, J., Great Lakes Moment: Harmful algal blooms negatively impact the Lake Erie economy, in GreatLakesNow. 2019.

- 16. Kerr, J.M., et al., Sustainable management of Great Lakes watersheds dominated by agricultural land use. Journal of Great Lakes Research, 2016. **42**(6): p. 1252-1259.
- 17. Clement, D.R. and A.D. Steinman, *Phosphorus loading and ecological impacts from agricultural tile drains in a west Michigan watershed.* Journal of Great Lakes Research, 2017. **43**(1): p. 50-58.
- 18. Frankenburger, J., *Ag 101 Drainage*, in *Ag 101*, U.S.E.P. Agency, Editor. 2002, EPA & Purdue Research Foundation: West Lafayette, Indiana. p. 141-144.
- 19. Easton, Z.M.B., Emily; Collick, Amy S., *Factors When Considering an Agricultural Drainage System*, V.S.U. Virginia Tech, Virginia Cooperative Extension, Editor. 2017. p. 9.
- 20. USDA NRCS, CHAPTER 5. Open Ditches for Drainage Design, Construction, and Maintenance. 1971.
- 21. Tanji, K.K.K., Neeltje C., Chapter 4. Water quality concerns in drainage water management, in Agricultural Drainage Water Management in Arid and Semi-Arid Areas. 2003.
- 22. King, K.W., et al., *Phosphorus Transport in Agricultural Subsurface Drainage: A Review.* Journal of environmental quality, 2015. **44**(2): p. 467-485.
- 23. King, K.W., M.R. Williams, and N.R. Fausey, *Contributions of Systematic Tile Drainage to Watershed-Scale Phosphorus Transport*. Journal of Environmental Quality, 2015. **44**(2): p. 486-494.
- 24. Zimmer, D., P. Kahle, and C. Baum, *Loss of soil phosphorus by tile drains during storm events*. Agricultural Water Management, 2016. **167**: p. 21-28.
- 25. Southwest Michigan Planning Commission, *Chapter 3: LID in Michigan: The Key Determinants*, in *Low Impact Development Manual for Michigan*. 2008.
- 26. Hemwall, J.B., *The Fixation of Phosphorus by Soils*. 1957, Elsevier Science & Technology. p. 95-112.
- 27. Williams, M.R., et al., *Effect of tillage on macropore flow and phosphorus transport to tile drains*. Water Resources Research, 2016. **52**(4): p. 2868-2882.
- 28. Shen, J., et al., *Phosphorus Dynamics: From Soil to Plant*. Plant Physiology, 2011. **156**(3): p. 997-1005.
- 29. Kaiser, D. and P. Pagliari, *Understanding phosphorus fertilizers*. 2018, University of Minnesota: UM Extension.
- 30. HACH, What is the conversion factor from orthophosphate (PO4) to phosphorus pentoxide (P2O5)? 2018.
- 31. MacDonald, G.K., et al., *Agronomic phosphorus imbalances across the world's croplands*. Proceedings of the National Academy of Sciences of the United States of America, 2011. **108**(7): p. 3086-3091.

- 32. Bouwman, L., et al., Exploring global changes in nitrogen and phosphorus cycles in agriculture induced by livestock production over the 1900-2050 period. Proceedings of the National Academy of Sciences of the United States of America, 2013. **110**(52): p. 20882-20887.
- 33. Sharpley, A. and B. Moyer, *Phosphorus Forms in Manure and Compost and Their Release during Simulated Rainfall*. Journal of Environmental Quality, 2000. **29**(5): p. 1462-1469.
- 34. Al-Kaisi, M., M. Hanna, and M. Tidman, *Frequent tillage and its impact on soil quality*. 2004, Iowa State University: ISU Extension and Outreach.
- 35. Al-Kaisi, M., M. Hanna, and M. Tidman, *Think before you till*. 2002, Iowa State University: ISU Extension and Outreach.
- 36. Geohring, L.D., et al., *PHOSPHORUS TRANSPORT INTO SUBSURFACE DRAINS BY MACROPORES AFTER MANURE APPLICATIONS: IMPLICATIONS FOR BEST MANURE MANAGEMENT PRACTICES.* Soil Science, 2001. **166**(12): p. 896-909.
- 37. Lachnicht, S.L., et al., *Characteristics of macroporosity in a reduced tillage agroecosystem with manipulated earthworm populations: Implications for infiltration and nutrient transport.* Soil Biology and Biochemistry, 1997. **29**(3): p. 493-498.
- 38. White, R.E. *The Influence of Macropores on the Transport of Dissolved and Suspended Matter Through Soil.* 1985. New York, NY: Springer New York.
- 39. Kazemi, H.V., et al., *Atrazine and Alachlor Transport in Claypan Soils as Influenced by Differential Antecedent Soil Water Content.* Journal of Environmental Quality, 2008. **37**(4): p. 1599-1607.
- 40. Wang, Z., et al., Simulating crop yield, surface runoff, tile drainage and phosphorus loss in a clay loam soil of the Lake Erie region using EPIC. Agricultural Water Management, 2018. **204**: p. 212-221.
- 41. Maltais-Landry, G. and E. Frossard, *Similar phosphorus transfer from cover crop residues and water-soluble mineral fertilizer to soils and a subsequent crop.* Plant and Soil, 2015. **393**(1/2): p. 193-205.
- 42. Kleinman, P.J.A., et al., *Effect of cover crops established at time of corn planting on phosphorus runoff from soils before and after dairy manure application*. Journal of Soil and Water Conservation, 2005. **60**(6): p. 311.
- 43. Bechmann, M.E., et al., *Freeze-Thaw Effects on Phosphorus Loss in Runoff from Manured and Catch-Cropped Soils*. Journal of Environmental Quality, 2005. **34**(6): p. 2301-9.
- 44. Elliott, J., Evaluating the potential contribution of vegetation as a nutrient source in snowmelt runoff. Canadian Journal of Soil Science, 2013. **93**(4): p. 435-443.
- 45. Riddle, M.U. and L. Bergström, *Phosphorus Leaching from Two Soils with Catch Crops Exposed to Freeze–Thaw Cycles*. Agronomy Journal, 2013. **105**(3): p. 803-811.
- 46. Liu, J., et al., *Freezing–thawing effects on phosphorus leaching from catch crops*. Nutrient Cycling in Agroecosystems, 2014. **99**(1): p. 17-30.

- 47. Onwuka, B., *Effects of soil temperature on Some Soil properties and plant growth.* Journal of Agricultural Science and Technology, 2016.
- 48. Jarvie, H.P., et al., *Increased Soluble Phosphorus Loads to Lake Erie: Unintended Consequences of Conservation Practices?* Journal of Environmental Quality, 2017. **46**(1): p. 123-132.
- 49. Zheng, X., et al., Soil Degradation and the Decline of Available Nitrogen and Phosphorus in Soils of the Main Forest Types in the Qinling Mountains of China. Forests, 2017. **8**(11): p. 460.
- 50. Stone, M. and B.G. Krishnappan, *Transport Characteristics of Tile-Drain Sediments from an Agricultural Watershed*. Water, Air, and Soil Pollution, 1997. **99**(1): p. 89-103.
- 51. Zimmerman, B.A., *Dissolved Constituents in Agricultural Drainage Waters*. Transactions of the ASABE, 2017. **60**(3): p. 847-859.
- 52. Zhang, T.Q., et al., *Impacts of Soil Conditioners and Water Table Management on Phosphorus Loss in Tile Drainage from a Clay Loam Soil.* Journal of Environmental Quality, 2015. **44**(2): p. 572-584.
- 53. Xue, Y., et al., *Kinetics and Modeling of Dissolved Phosphorus Export from a Tile-Drained Agricultural Watershed.* Journal of Environmental Quality, 1998. **27**(4): p. 917-922.
- 54. Baker, J.L., et al., *Nitrate, Phosphorus, and Sulfate in Subsurface Drainage Water.* Journal of environmental quality, 1975. **4**(3): p. 406-412.
- 55. Sawhney, B.L., *Leaching of phosphate from agricultural soils to groundwater*. Water, Air, and Soil Pollution, 1978. **9**(4): p. 499-505.
- 56. Kinley, R.D., et al., *Phosphorus Losses through Agricultural Tile Drainage in Nova Scotia, Canada.* Journal of Environmental Quality, 2007. **36**(2): p. 469-477.
- 57. Tao, et al., Study on Characteristics of Nitrogen and Phosphorus Loss under an Improved Subsurface Drainage. Water (Basel), 2019. **11**(7): p. 1467.
- 58. Hupfer, M. and S. Hilt, Lake Restoration. 2008. p. 2080-2093.
- 59. Dodds, W.K., *Nutrients and the "Dead Zone": The Link between Nutrient Ratios and Dissolved Oxygen in the Northern Gulf of Mexico*. Frontiers in Ecology and the Environment, 2006. **4**(4): p. 211-217.
- 60. Rabalais, N.N., et al., *Dynamics and distribution of natural and human-caused hypoxia*. Biogeosciences, 2010. **7**(2): p. 585-619.
- 61. Diaz, R.J., et al., *Spreading Dead Zones and Consequences for Marine Ecosystems*. Science, 2008. **321**(5891): p. 926-929.
- 62. Metcalf, J.S. and N.R. Souza, *Chapter 6 Cyanobacteria and Their Toxins*, in *Separation Science and Technology*, S. Ahuja, Editor. 2019, Academic Press. p. 125-148.
- 63. Carmichael, W.W., The toxins of cyanobacteria. Sci Am, 1994. 270(1): p. 78-86.

- 64. Ohtani, I., R.E. Moore, and M.T.C. Runnegar, *Cylindrospermopsin: a potent hepatotoxin from the blue-green alga Cylindrospermopsis raciborskii*. Journal of the American Chemical Society, 1992. **114**(20): p. 7941-7942.
- 65. Codd G.A., L.J., Young F.M., Morrison L.F., Metcalf J.S., *Harmful Cyanobacteria*, in *Harmful Cyanobacteria*. *Aquatic Ecology Series*. 2005, Springer, Dordrecht.
- 66. Falconer, I.R. and A.R. Humpage, *Preliminary evidence for in vivo tumour initiation by oral administration of extracts of the blue-green algaCylindrospermopsis raciborskii containing the toxin cylindrospermopsin*. Environmental Toxicology, 2001. **16**(2): p. 192-195.
- 67. Bruno, M., et al., *Anatoxin-a, Homoanatoxin-a, and Natural Analogues*, in *Handbook of Cyanobacterial Monitoring and Cyanotoxin Analysis*. 2016, John Wiley & Sons, Ltd: Chichester, UK. p. 138-147.
- 68. Islam, M.S., et al., *Role of phytoplankton in maintaining endemicity and seasonality of cholera in Bangladesh*. Transactions of The Royal Society of Tropical Medicine and Hygiene, 2015. **109**(9): p. 572-578.
- 69. Pablo, J., et al., *Cyanobacterial neurotoxin BMAA in ALS and Alzheimers disease*. Acta Neurologica Scandinavica, 2009. **120**(4): p. 216-225.
- 70. Fujiki, H., et al., *Indole Alkaloids: Dihydroteleocidin B, Teleocidin, and Lyngbyatoxin A as Members of a New Class of Tumor Promoters.* Proceedings of the National Academy of Sciences of the United States of America, 1981. **78**(6): p. 3872-3876.
- 71. Rahal, S., NOAA predicts harmful Lake Erie algae bloom, in The Detroit News. 2018.
- 72. Briscoe, T. *Lake Erie provides drinking water for more people than any other, but algae blooms are making it toxic*. 2019; Available from: https://phys.org/news/2019-11-lake-erie-people-algae-blooms.html.
- 73. US EPA, GREAT LAKES RESTORATION INITIATIVE Action Plan III. 2019.
- 74. US EPA, *QUALITY CRITERIA for WATER*, O.o.W.R.a. Standards, Editor. 1986: Washington D.C.
- 75. Rittmann, B.E., et al., *Capturing the lost phosphorus*. Chemosphere, 2011. **84**(6): p. 846-853.
- 76. Schorr, R., et al., *Phosphorous Removal and Recovery Using Nano Technology*, in *Aquananotechnology: Global Prospects*. 2014, CRC Press Taylor & Francis Group.
- 77. George, T., et al., *Wastewater Engineering: Treatment and Resource Recovery*. 5th ed. 2014: Metcalf & Eddy, Inc.
- 78. Domagalski, J.L. and H.M. Johnson, *Subsurface transport of orthophosphate in five agricultural watersheds, USA*. Journal of Hydrology, 2011. **409**(1): p. 157-171.
- 79. Pan, B., et al., *Development of polymer-based nanosized hydrated ferric oxides (HFOs) for enhanced phosphate removal from waste effluents.* Water Research, 2009. **43**(17): p. 4421-4429.

- 80. Sengupta, S. and A. Pandit, *Selective removal of phosphorus from wastewater combined with its recovery as a solid-phase fertilizer.* Water Research, 2011. **45**(11): p. 3318-3330.
- 81. Office of Water Programs. *empty bed contact time (EBCT)*. Water and Wastewater Terms Beginning E 2019; Available from: http://www.owp.csus.edu/glossary/empty-bed-contact-time.php.
- 82. Water Quality Association, *Granular Activated Carbon [Fact sheet]*. 2013.
- 83. Hua, G., et al., *Influence of clogging and resting processes on flow patterns in vertical flow constructed wetlands.* The Science of the total environment, 2018. **621**: p. 1142-1150.
- 84. Sims, I., J. Lay, and J. Ferrari, 15 Concrete Aggregates, in Lea's Chemistry of Cement and Concrete (Fifth Edition), P.C. Hewlett and M. Liska, Editors. 2019, Butterworth-Heinemann. p. 699-778.
- 85. Mann, R. and H.J. Bavor, *Phosphorus Removal in Constructed Wetlands Using Gravel and Industrial Waste Substrata.* Water Science and Technology, 1993. **27**: p. 107-113.
- 86. Blanco, I., et al., *Basic Oxygen Furnace steel slag aggregates for phosphorus treatment.*Evaluation of its potential use as a substrate in constructed wetlands. Water Research, 2016. 89: p. 355-365.
- 87. Sheng-gao, L.U.S.-q.B.A.I.H.-d.S., *Mechanisms of phosphate removal from aqueous solution by blast furnace slag and steel furnace slag.* 浙江大学学报: A卷英文版, 2008. **9**(1): p. 125-132.
- 88. US EPA, Specifications and Guidance for Contaminant-Free Sample Containers, O.o.S.W.a.E. Response, Editor. 1992.
- 89. Jiang, D., et al., *Removal and recovery of phosphate from water by Mg-laden biochar: Batch and column studies.* Colloids and Surfaces A: Physicochemical and Engineering Aspects, 2018. **558**: p. 429-437.
- 90. Fang, C., et al., *Application of magnesium modified corn biochar for phosphorus removal and recovery from swine wastewater*. International journal of environmental research and public health, 2014. **11**(9): p. 9217-9237.
- 91. MetaMateria, R. Schorr, and T. Marth, *Use of PO4 Sponge*. n.d.: Columbus, OH.
- 92. Cumbal, L., et al., *Polymer supported inorganic nanoparticles: characterization and environmental applications.* Reactive and Functional Polymers, 2003. **54**(1): p. 167-180.
- 93. Chouyyok, W., et al., *Phosphate Removal by Anion Binding on Functionalized Nanoporous Sorbents*. Environmental Science & Technology, 2010. **44**(8): p. 3073-3078.
- 94. Fenglin, L.I.U.J.Z.U.O.T.C.H.I.P.W.B.Y., Removing phosphorus from aqueous solutions by using iron-modified corn straw biochar. 中国环境科学与工程前沿: 英文版, 2015. **9**(6): p. 1066-1075.

- 95. Jiang, Y.-H., et al., *Characteristics of nitrogen and phosphorus adsorption by Mg-loaded biochar from different feedstocks.* Bioresource Technology, 2019. **276**: p. 183-189.
- 96. Drizo, A., et al., *Physico-chemical screening of phosphate-removing substrates for use in constructed wetland systems.* Water Research, 1999. **33**(17): p. 3595-3602.
- 97. MetaMateria, R. Schorr, and T. Marth, *Remove Soluble Phosphorus: Tile Drain and Field Runoff*, in *Drain Tile & Field Runoff*. n.d.: Columbus, OH.
- 98. Blaney, L.M., S. Cinar, and A.K. SenGupta, *Hybrid anion exchanger for trace phosphate removal from water and wastewater.* Water Research, 2007. **41**(7): p. 1603-1613.
- 99. Drizo, A., et al., *Phosphorus removal by electric arc furnace steel slag and serpentinite*. Water Research, 2006. **40**(8): p. 1547-1554.
- 100. Baker, M.J., D.W. Blowes, and C.J. Ptacek, *Laboratory Development of Permeable Reactive Mixtures for the Removal of Phosphorus from Onsite Wastewater Disposal Systems*. Environmental Science & Technology, 1998. **32**(15): p. 2308-2316.
- 101. Vohla, C., et al., *Filter materials for phosphorus removal from wastewater in treatment wetlands—A review.* Ecological Engineering, 2011. **37**(1): p. 70-89.
- 102. Oguz, E., *Removal of phosphate from aqueous solution with blast furnace slag.* Journal of Hazardous Materials, 2004. **114**(1): p. 131-137.
- 103. Ádám, K., et al., *Phosphorus retention in the filter materials shellsand and Filtralite P* ®—Batch and column experiment with synthetic P solution and secondary wastewater. Ecological engineering, 2007. **29**(2): p. 200-208.
- 104. Mohammadi, A., et al., *Life cycle assessment of combination of anaerobic digestion and pyrolysis: focusing on different options for biogas use.* Advances in Geosciences, 2019. **49**: p. 57.
- 105. HACH, ULTRA LOW RANGE TOTAL AND REACTIVE PHOSPHORUS (FOR USE WITH DR 2700, DR 2800, DR 3800, DR 3900 AND DR 5000 HACH SPECTROPHOTOMETER). 2011.
- 106. HACH, *ULR Phosphorus, Reactive (Orthophosphate) and Tota, Ascorbic Acid Method 10209 Reactive and 10210 Total, TNTplus*TM*l.* 2015.
- 107. HACH, Phosphorus, Reactive (Orthophosphate) Method 10209 and Total Phosphorus Method 10210, LR Ascorbic Acid Method using TNTplusTM 843. 2016.
- 108. HACH, Phosphorus, Reactive (Orthophosphate) Method 10209 and Total Phosphorus Method 10210, HR Ascorbic Acid Method using TNTplusTM 844. 2016.
- 109. USEPA, *Methods for chemical analysis of water and wastes*, E.M.a.S.L. Office of Research and Development, Editor. 1983.
- 110. Fang, C., et al., *Phosphorus recovery from biogas fermentation liquid by Ca–Mg loaded biochar.* Journal of Environmental Sciences, 2015. **29**: p. 106-114.

- 111. MetaMateria. *Phosphorus Capture and Recovery*. n.d.; Available from: http://metamateria.com/phosphorus-capture-and-recovery.
- 112. Safferman, S.I., et al. *PHOSPHORUS REMOVAL FROM DOMESTIC WASTEWATER USING ENGINEERED NANO-MEDIA*. in *Onsite Wastewater Mega-Conference*. 2015. Virginia Beach, Virginia: Virginia: National Onsite Wastewater Recycling Association.
- 113. Hauda, J. and MetaMateria, MetaMateriaMeeting_December032018_BE485. 2018.
- 114. MetaMateria, et al., Information of MetaMateria Products. 2018: Columbus, OH.
- 115. Purolite, *Purolite FerrIX*TM*A33E Product Data Sheet*, in *Polystyrenic Macroporous, Chloride form.* 2020. p. 1.
- 116. Weinburg, E.H., Jessica; , "Hybrid Anion Exchanger with Dispersed Zirconium Oxide Nanoparticles: A Durable and Reusable Fluoride-Selective Sorbent" by Mike German, J. Hauda, Editor. 2020.
- 117. Shepsko, C., Advancement of the Hybrid Ion Exchange Nitrogen and Phosphate (HIX-NP) Recovery from Waste Water and a New Approach to Brine-Free Nitrate Removal, in Environmental Engineering. 2019, Leigh University.
- 118. Gustafsson, J.P., et al., *Phosphate removal by mineral-based sorbents used in filters for small-scale wastewater treatment.* Water Research, 2008. **42**(1): p. 189-197.
- 119. Sakadevan, K. and H.J. Bavor, *Phosphate adsorption characteristics of soils, slags and zeolite to be used as substrates in constructed wetland systems.* Water Research, 1998. **32**(2): p. 393-399.
- 120. National Slag Association. *Blast Furnace Slag*. 2013; Available from: http://www.nationalslag.org/blast-furnace-slag.
- 121. U.S. Geological Survey, *MINERAL COMMODITY SUMMARIES 2019 Iron and Steel Slag*, U.S.D.o.t. Interior, Editor. 2019. p. 86.
- 122. Yilmaz, D., et al., *Influence of Carbonation on the Microstructure and Hydraulic Properties of a Basic Oxygen Furnace Slag.* Vadose Zone Journal, 2013. **12**(2): p. 1-15.
- 123. Mann, R.A. and H.J. Bavor, *Phosphorus Removal in Constructed Wetlands Using Gravel and Industrial Waste Substrata.* Water Science and Technology, 1993. **27**(1): p. 107-113.
- 124. Hussain, S.I., et al., *Phosphorus Removal from Lake Water Using Basic Oxygen Furnace Slag:* System Performance and Characterization of Reaction Products. Environmental Engineering Science, 2014. **31**(11): p. 631-642.
- 125. National Slag Association. *Steel Furnace Slag*. 2013; Available from: http://www.nationalslag.org/steel-furnace-slag.
- 126. Gonzalez, J.M., C.J. Penn, and S.J. Livingston, *Utilization of Steel Slag in Blind Inlets for Dissolved Phosphorus Removal.* Water (Basel), 2020. **12**(6): p. 1593.

- 127. Penn, C., et al., *Performance of Field-Scale Phosphorus Removal Structures Utilizing Steel Slag for Treatment of Subsurface Drainage*. Water (Basel), 2020. **12**(2): p. 443.
- 128. Malasavage, N.E., et al., *Geotechnical Performance of Dredged Material—Steel Slag Fines Blends: Laboratory and Field Evaluation.* Journal of Geotechnical and Geoenvironmental Engineering, 2012. **138**(8): p. 981-991.
- 129. US FHA, User Guidelines for Waste and Byproduct Materials in Pavement Construction. 2016.
- 130. Biochar Engineering, 50kg/hr Mobile Unit, in Product Info Sheet. 2009: Golden, CO.
- 131. Langemeier, M.R., et al., 2020 Purdue Crop Cost & Return Guide. 2019, Purdue Extension.
- 132. Cole, E.J., et al., *Effects of Hardwood Biochar on Soil Acidity, Nutrient Dynamics, and Sweet Corn Productivity.* Communications in Soil Science and Plant Analysis, 2019. **50**(14): p. 1732-1742.
- 133. Mohan, D., et al., *Biochar production and applications in soil fertility and carbon sequestration a sustainable solution to crop-residue burning in India*. RSC Advances, 2018. **8**(1): p. 508-520.
- 134. Hardy, B., et al., *The Long-Term Effect of Biochar on Soil Microbial Abundance, Activity and Community Structure Is Overwritten by Land Management.* Frontiers in Environmental Science, 2019. **7**.
- 135. Erro, J., A. Ma Zamarreño, and J. Ma García-Mina, *Ability of various water-insoluble fertilizers to supply available phosphorus in hydroponics to plant species with diverse phosphorus-acquisition efficiency: Involvement of organic acid accumulation in plant tissues and root exudates.* Journal of Plant Nutrition and Soil Science, 2010. **173**(5): p. 772-777.
- Bawiec, A., *Efficiency of nitrogen and phosphorus compounds removal in hydroponic wastewater treatment plant.* Environmental Technology, 2019. **40**(16): p. 2062-2072.
- 137. Geng, Y., et al., Effect of plant diversity on phosphorus removal in hydroponic microcosms simulating floating constructed wetlands. Ecological Engineering, 2017. **107**: p. 110-119.
- 138. Hylander, L.D., et al., *Phosphorus retention in filter materials for wastewater treatment and its subsequent suitability for plant production.* Bioresource Technology, 2006. **97**(7): p. 914-921.
- 139. MetaMateria, *Instructions for PO4 Media Regeneration to extract P (Proprietary Information)*. n.d.: Columbus, OH.